SPACE RADIATION EFFECTS ON GRAPHITE-EPOXY COMPOSTIE MATERIALS

Virginia Polytechnic Institute and State University
Blacksburg, VA

Jun 84

DISCLAIMER NOTICE

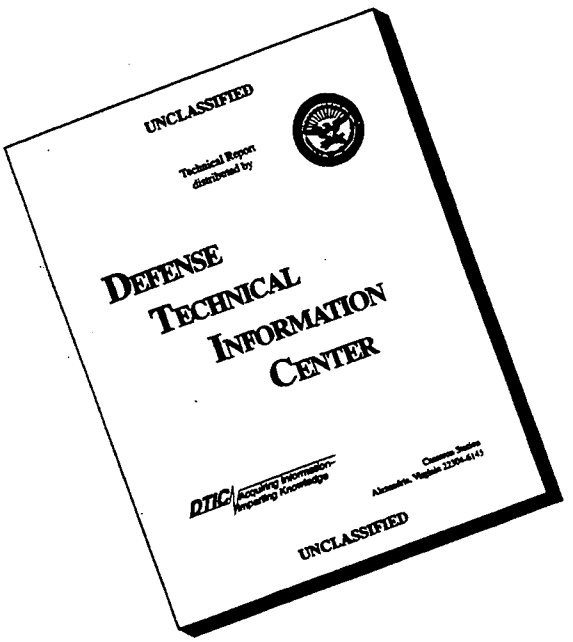

THIS DOCUMENT IS BEST QUALITY AVAILABLE. THE COPY FURNISHED TO DTIC CONTAINED A SIGNIFICANT NUMBER OF PAGES WHICH DO NOT REPRODUCE LEGIBLY.

CCMS-84-08
VPI-E-84-20

VIRGINIA TECH

CENTER FOR COMPOSITE MATERIALS AND STRUCTURES

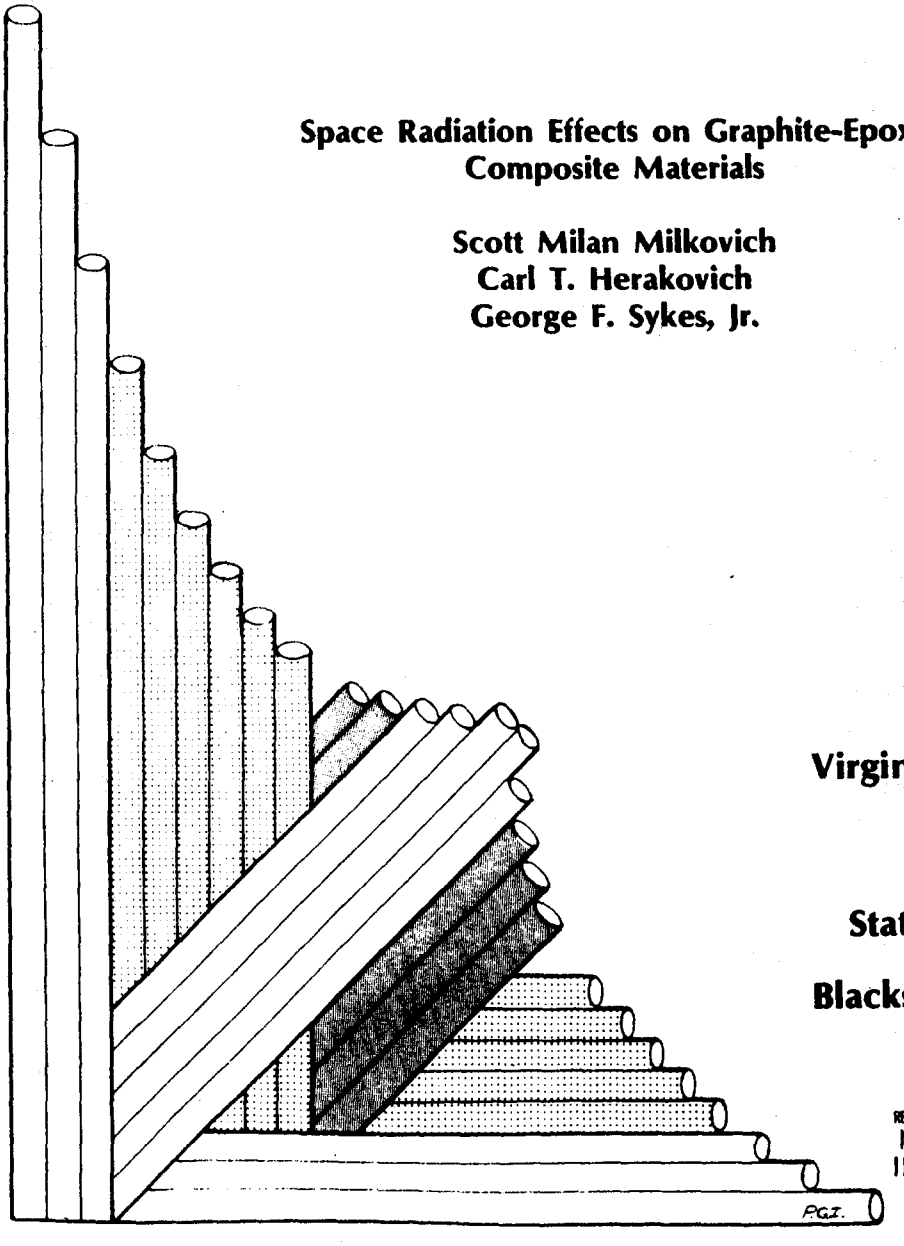

Space Radiation Effects on Graphite-Epoxy Composite Materials

Scott Milan Milkovich
Carl T. Herakovich
George F. Sykes, Jr.

Virginia Polytechnic Institute and State University

Blacksburg, Virginia 24061

BIBLIOGRAPHIC DATA SHEET	1. Report No. CCMS-84-08	2. VPI-E-84-20	3. Recipient's Accession No.

4. Title and Subtitle

SPACE RADIATION EFFECTS ON GRAPHITE-EPOXY COMPOSITE MATERIALS

5. Report Date: June, 1984

6.

7. Author(s)

S. M. Milkovich, C. T. Herakovich, G. F. Sykes, Jr.

8. Performing Organization Rept. No. VPI-E-84-20

9. Performing Organization Name and Address

Virginia Polytechnic Institute & State University
Engineering Science and Mechanics
Blacksburg, Virginia 24061

10. Project/Task/Work Unit No.

11. Contract/Grant No.

NAG-1-343

12. Sponsoring Organization Name and Address

National Aeronautics and Space Administration
Langley Research Center
Hampton, Virginia 23665

13. Type of Report & Period Covered

14.

15. Supplementary Notes

16. Abstracts

The objective of this study is to characterize radiation effects on engineering properties, dimensional stability, and chemistry on state-of-the-art composite systems. This investigation used T300/934 graphite-epoxy composite that was subjected to 1.0 MeV electron radiation for a total dose of 1.0×10^{10} rads at a rate of 5.0×10^{7} rads/hour. This simulates a worst-case exposure equivalent to 30 years in space.

Mechanical testing was performed on the 4-ply unidirectional laminates over the temperature range of -250°F (116K) to +250°F (394K). A complete set of in-plane tensile elastic and strength properties were obtained (E_1, E_2, ν_{12}, G_{12}, X_T, Y_T, and S). In addition electron microscopy was used to study and analyze the fracture surfaces of all specimens tested. Results indicate that little difference in properties is noted at room temperature, but significant differences are observed at both low and elevated temperatures.

Dynamic-mechanical analysis (DMA) showed that the glass-transition temperature of the epoxy matrix was lowered by over 100°F (56K) after being irradiated. Thermo-mechanical analysis (TMA) demonstrated that volatile products are produced upon heating the irradiated material. These degradation products were analyzed by infrared spectrophotometry and mass spectrometry, and found to be low molecular weight material produced by polymer chain scission and crosslink breakage.

In conclusion, electron radiation acts to produce low molecular weight material in the epoxy resin matrix. These degradation products plasticize the epoxy at elevated temperatures and embrittle it at low temperatures. Therefore, composite mechanical properties are altered.

17. Key Words and Document Analysis. 17a. Descriptors

composites, graphite-epoxy, in-plane tensile properties, electron radiation, temperature, dynamic-mechanical analysis (DMA), thermomechanical analysis (TMA), fracture surfaces, electron microscopy

17b. Identifiers/Open-Ended Terms

17c. COSATI Field/Group

18. Availability Statement

Distribution unlimited

19. Security Class (This Report) UNCLASSIFIED

21. No. of Pages 162

20. Security Class (This

22. Price

College of Engineering

Virginia Polytechnic Institute and State University

Blacksburg, VA 24061

VPI-E-84-20 June, 1984

Space Radiation Effects on Graphite-Epoxy Composite Materials

Scott Milan Milkovich[1]

Carl T. Herakovich[2] George F. Sykes, Jr.[3]

Department of Engineering Science & Mechanics

Interim Report 45
The NASA-Virginia Tech Composites Program

NASA Cooperative Agreement NAG-1-343

Prepared for: Applied Materials Branch
National Aeronautics & Space Administration
Langley Research Center
Hampton, VA 23665

[1] Graduate Student

[2] Professor of Engineering Science & Mechanics

[3] Research Scientist, NASA-Langley Research Center

ABSTRACT

The objective of this study is to characterize radiation effects on engineering properties, dimensional stability, and chemistry on state-of-the-art composite systems. This investigation used T300/934 graphite-epoxy composite that was subjected to 1.0 MeV electron radiation for a total dose of 1.0×10^{10} rads at a rate of 5.0×10^{7} rads/hour. This simulates a worst-case exposure equivalent to 30 years in space.

Mechanical testing was performed on the 4-ply unidirectional laminates over the temperature range of -250°F (116K) to +250°F (394K). A complete set of in-plane tensile elastic and strength properties were obtained (E_1, E_2, ν_{12}, G_{12}, X_T, Y_T, and S). In addition electron microscopy was used to study and analyze the fracture surfaces of all specimens tested. Results indicate that little difference in properties is noted at room temperature, but significant differences are observed at both low and elevated temperatures.

Dynamic-mechanical analysis (DMA) showed that the glass-transition temperature of the epoxy matrix was lowered by over 100°F (56K) after being irradiated. Thermomechanical analysis (TMA) demonstrated that volatile products are produced upon heating the irradiated material. These degradation products were analyzed by infrared spectrophotometry and mass spectrometry, and found to be low molecular weight material produced by polymer chain scission and crosslink breakage.

In conclusion, electron radiation acts to produce low molecular weight material in the epoxy resin matrix. These degradation products plasticize the epoxy at elevated temperatures and embrittle it at low temperatures. Therefore, composite mechanical properties are altered.

ACKNOWLEDGEMENTS

The authors wish to acknowledge that this research was supported by the NASA-Virginia Tech Composites Program and NASA Cooperative Agreement NAG-1-343. In addition, the authors wish to acknowledge Dr. M. W. Hyer, Dr. M. R. Louthan, Dr. K. L. Reifsnider, Dr. R. M. Jones, and Dr. D. R. Tenney for assistance concerning certain technical aspects of this research. We would also like to thank David Bowles and Steve Tompkins for their help with the thermal cycling portion of this work; and Mike Lightfoot for his help with the mechanical testing portion of this work. The authors would like to express their gratitude to Ms. Connie Callison for her time and effort spent in typing this manuscript.

TABLE OF CONTENTS

LIST OF FIGURES

LIST OF TABLES

I. INTRODUCTION

1.1 Space Applications for Composites

The use of fiber-reinforced composite materials as efficient high performance structural materials has greatly increased in recent years. The great advantage of these materials is their superior strength to weight and stiffness to weight ratios. This makes composites ideal for use in applications where high strength and light weight are important. Therefore, aerospace application has one of the largest potential uses of composite materials.

Use of composites in aircraft can provide weight reductions over metal designs. This saving can be put to work by increasing the range, payload, maneuverability, and speed of an aircraft or by simply reducing its fuel consumption. Another advantage of these materials is the ability to tailor fiber orientations to meet specific load and stiffness requirements, thus designing materials for individual applications. It is also possible to fabricate complex parts in one operation, reducing secondary assembly requirements.

Most emphasis of fiber-reinforced composites has been in aircraft. However, spacecraft are high on the list of weight-critical structures and can benefit greatly by their use. Nowhere else is weight, coupled with high performance, such a critical requirement. Advanced fiber-reinforced composites are ideal for use in space applications.

Currently, NASA's Space Shuttle Orbiter (Fig. 1) uses advanced composites in several areas [1]. The components include graphite-epoxy

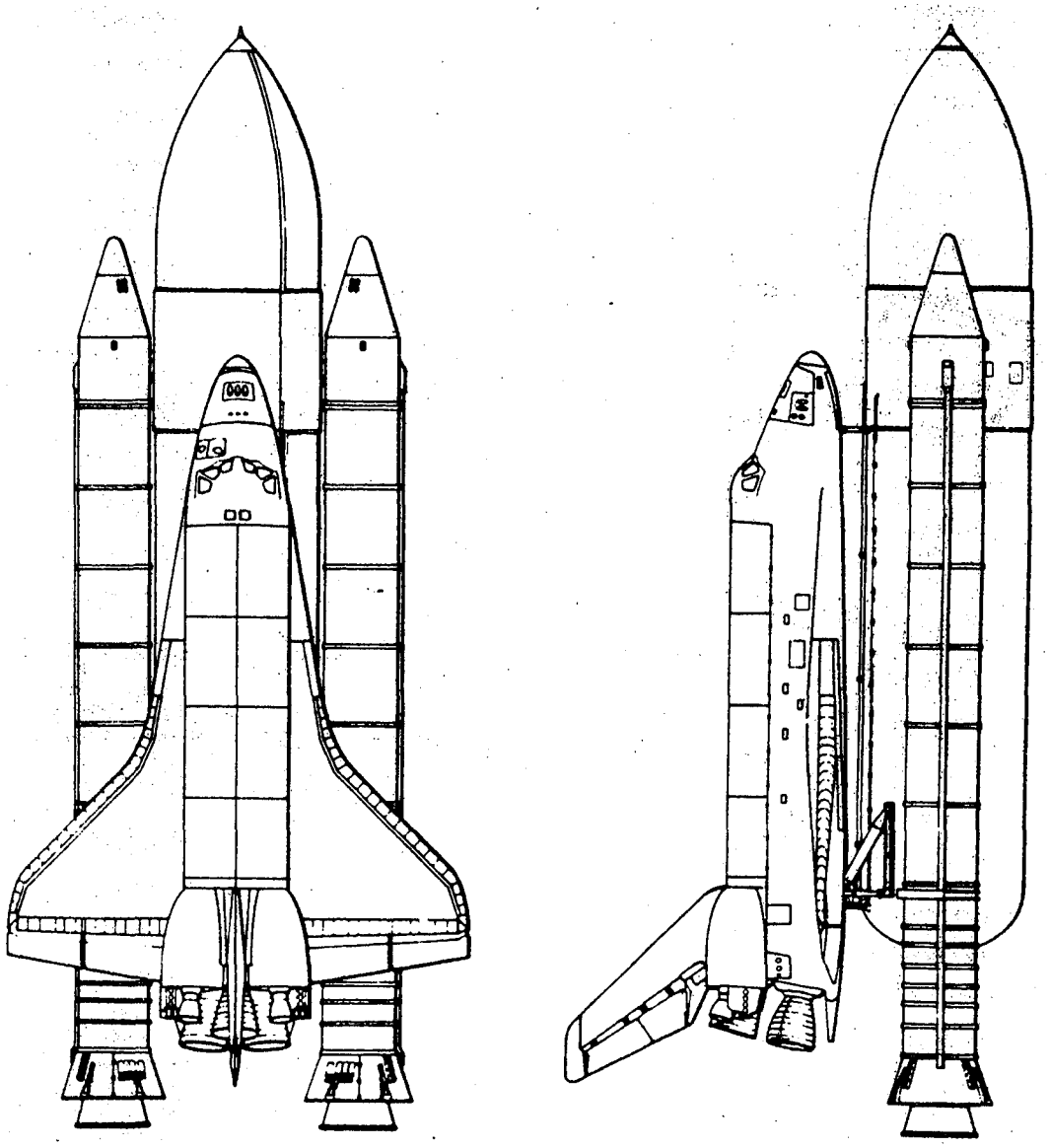

Fig. 1. NASA's Space Shuttle.

honeycomb sandwich skins on the orbital maneuvering system and titanium I-beams and tubes reinforced with boron-epoxy in the aft thrust structure. The other notable composite applications on the Shuttle are the payload bay doors. These are the largest graphite-epoxy structures ever built [2]. The doors are each 18.3 meters (60 feet) long with a transverse arc length of 4.6 meters (15 feet). Door panel skins are graphite-epoxy fabric and tape sheets over a honeycomb core.

Graphite-epoxy is also being used in the main support truss structure of NASA's Space Telescope (Fig. 2) [3]. This is a primary structure. The Space Telescope is due to be placed in orbit in 1986. Proposed large-scale space antennas and communications satellites as well as large-scale space platforms (up to 100 meters in diameter) will use graphite-epoxy composites [4,5]. Now that the Space Station is becoming a reality, graphite-epoxy support trusses are being considered in many of the proposed designs currently under review [6].

1.2 The Space Environment

The success of space exploration and exploitation, using composite materials, rests in their ability to withstand a hostile space environment. In an almost perfect vacuum, the cold of space coupled with radiant solar heating effects can lead to a wide range of operating temperatures. Temperature cycling will occur every time the space structure orbits the earth.

In addition, a space structure will be subjected to ultraviolet, electron, and proton irradiation. Ultraviolet is electromagnetic radiation produced by the sun. Electron and proton radiation are present

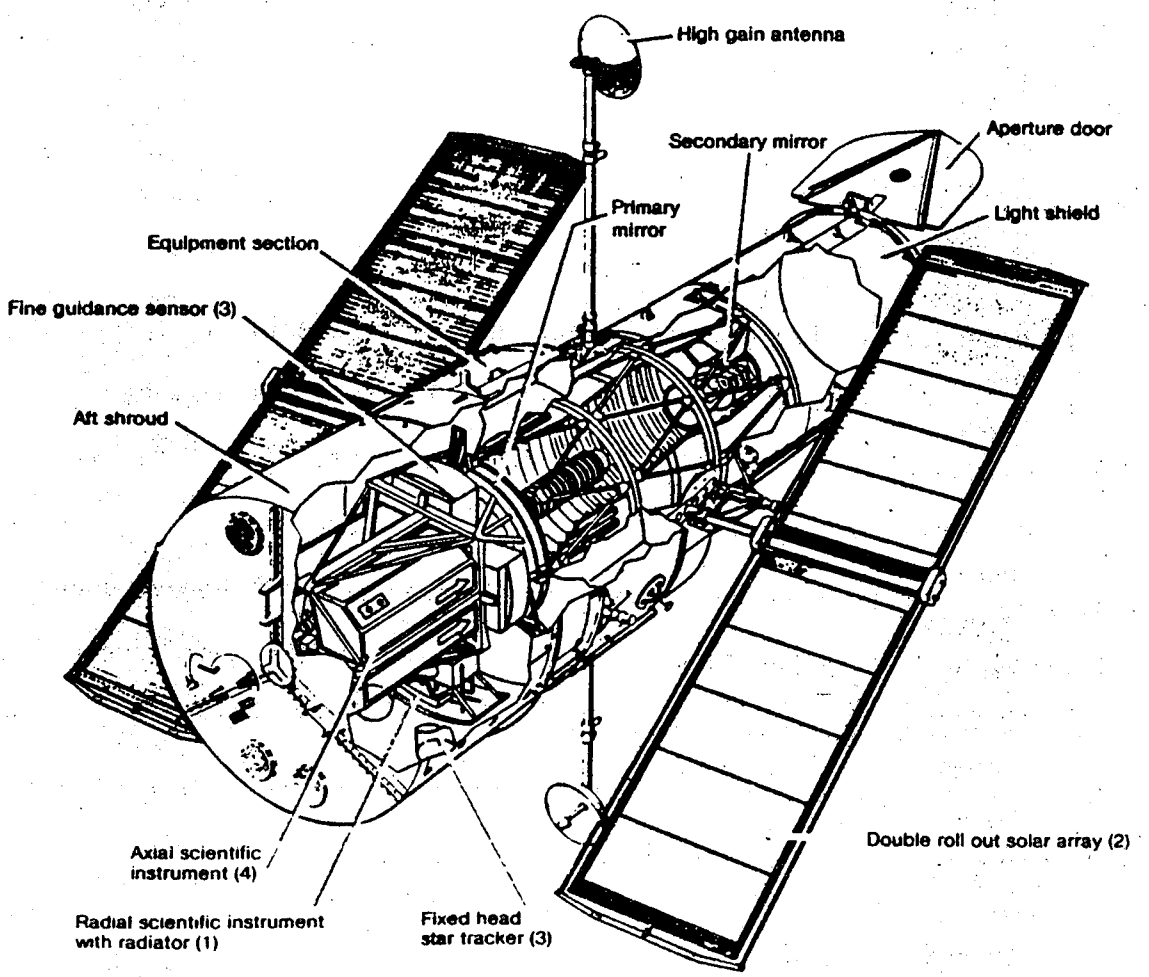

Fig. 2. NASA's Space Telescope.

from trapped particles in the earth's Van Allen radiation belts. Ultraviolet and proton radiation will only affect the surface of a spacecraft, but electron radiation will be highly penetrating. A summary of these conditions is presented in Tables 1 and 2 [7,8]. The column headed GEO (Table 1) is a listing of conditions that a spacecraft in geosynchronous earth orbit would have to withstand. The heading LEO designates low earth orbit conditions.

In order to utilize graphite-epoxy composite material in space, the effect of the above conditions on its material properties must be investigated. Composites will be used in future space structures with life-times of 10-20 years [9]. A key materials technology need is the ability to understand how fiber-reinforced materials will behave under such harsh conditions for long periods of time. The two most severe parameters of the space environment are its temperature extremes coupled with the highly penetrating electron radiation. Therefore, these two conditions will be the primary thrust of this study.

1.3 Objective of Present Study

It is the objective of this study to characterize radiation effects on engineering properties, dimensional stability, and chemistry of state-of-the-art composite systems.

The material chosen for this study is T300/934 graphite-epoxy fiber-reinforced composite material. This composite system is one of the few designated as "space-approved" by NASA. The designation T300/934 indicates that the graphite fibers are Thornel (Union Carbide) T300 fibers in a matrix consisting of Fiberite 934 epoxy resin. These

Table 1

Parameters of the Space Environment.

Environmental parameter	GEO Composite structure	LEO Manned habitat
Optical properties	α/ε - selectible with $\varepsilon \leq 0.3$	α/ε - selectible with $\varepsilon \geq 0.8$
Temperature	$-148^{o}F$ to $176^{o}F$ 173K to 353K	$-148^{o}F$ to $104^{o}F$ 173K to 313K
Environment	UV, e^{-}, p^{+}, VAC., ΔT	UV, VAC., ΔT
Electrical conductivity	$< 10^{-3}$ $(ohm^{-1}\text{-}cm^{-1})$	10^{-8} - 10^{-17} $(ohm^{-1}\text{-}cm^{-1}$
Lifetime	10 to 20 years	10 years

Table 2

Ranges of the Parameters of the Space Environment.

Environmental parameter	Nominal range of parameter	Reason for interest in parameter
Vacuum	Pressure: 10^{-11} - 10^{-19} Pa	Vacuum outgassing results in loss of moisture and solvents resulting in dimensional and mechanical property changes
Ultraviolet	Wavelength: 0.1 - 0.4 μm Intensity: 1.4 Kw/m^2	Degradation of coatings
Protons	Energy: 0.1 - 4.0 MeV Flux: 10^8 p^+/cm^2 - sec	Degradation of coatings and surface plies of composites
Electrons	Energy: 0.1 - 4.0 MeV Flux: 10^8 e^-/cm^2 - sec	Surface and bulk damage; spacecraft charging
Temperature cycling	Material temperature: 80K to 420K	Microcracking, thermal warping, deterioration of critical surfaces

graphite fibers are produced by carbonizing high modulus organic precursors (Poly-Acrylonitrile, PAN) at high temperatures in an inert atmosphere [10]. The epoxy resin is a thermosetting polymer binder that cures at 350°F. Cured epoxy resins are very highly crosslinked structures [10].

The radiation exposure used in this investigation is 1.0×10^{10} rads of electron irradiation with energies of 1.0 MeV and a dose rate of 5.0×10^{7} rads per hour. This will simulate a "worst-case" exposure of 30 years in space [7]. Great care has been taken to assure that the test specimens did not overheat during their accelerated irradiation exposure. Testing and characterization covers the temperature range of -250°F (116K) to +250°F (394K). This range represents the temperature extremes that may be encountered in a space environment [7].

A complete tensile set of engineering constants has been obtained to fully characterize the in-plane elastic and strength properties of the graphite-epoxy composite. These in-plane tensile properties have been collected over the above temperature range for both the non-irradiated and irradiated laminates. Most importantly, tests have been conducted to understand how electron radiation, in combination with temperature has affected and changed the composite's properties. In addition, a mechanism has been proposed to describe the degrading effect of the ionizing electrons on the graphite-epoxy composite. This approach is diagramed in greater detail in Fig. 3.

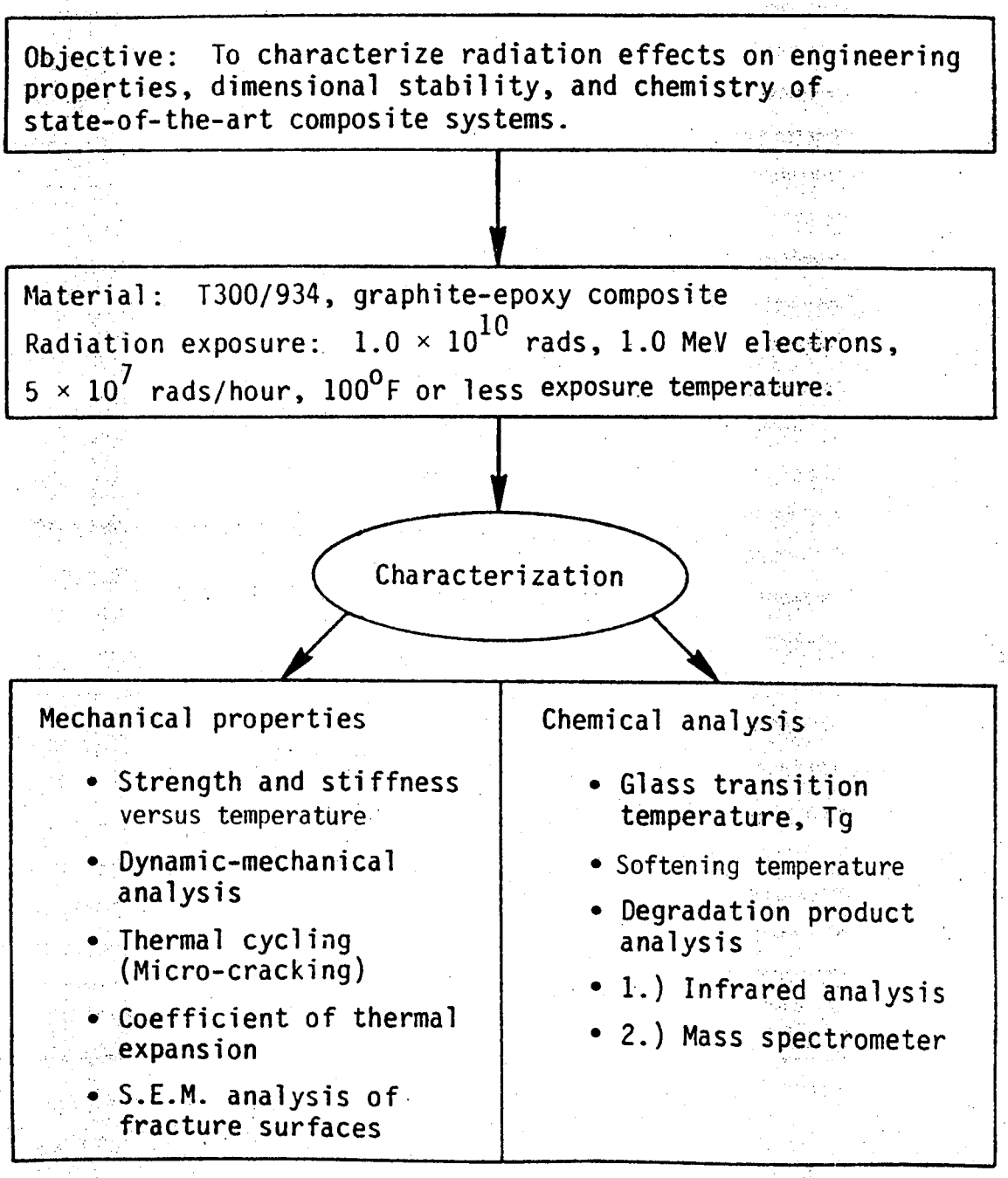

Fig. 3. Outline of Testing Program for this Study.

II. LITERATURE REVIEW AND ANALYTICAL CONSIDERATIONS

A survey of the literature dealing with radiation effects on various composite systems was conducted and is presented in section 2.1. The composite materials used in these studies are listed along with the testing techniques employed. Special attention was given to noting the radiation facilities used, and a summary is given. The conclusions stated are the opinions of the author, unless otherwise stated.

A discussion of the testing methods used in this investigation is presented in section 2.2. This includes mechanical and dynamic-mechanical characterization. Special detail is given in describing the 10° and 45° off-axis mechanical tension tests (section 2.2.1). The theory of dynamic-mechanical analysis (DMA) is also discussed (section 2.2.2).

The final section of the literature review deals with the effect of residual stresses and fiber waviness on the modulus of elasticity (section 2.3). The role of residual stress is very important in any discussion of mechanical characterization. Residual stresses affect the degree of fiber waviness within a composite which in turn has an effect on the modulus of elasticity of that composite material.

2.1 Radiation Effects on Composites

A study entitled, "Advanced Composite Design Data for Spacecraft Structural Applications" was prepared and presented in 1980 by J. F. Haskins and R. D. Holmes, at General Dynamic's Convair Division, for the U.S. Air Force [11,12]. The two composite systems chosen for this study were T300/934 and GY70/X30. They state that the T300/934 system was

selected because it is the most widely used material for high-strength applications. GY70/X30 is the most widely used material for high-stiffness and thermally stable applications. Both of these materials use 350°F-cure epoxies.

Haskins and Holmes reported on specimens cut from 12-ply unidirectional panels for tension tests and 24-ply panels for compression tests. In addition, 16-ply $[0/45/90/135]_{2s}$ laminate specimens and 20-ply $[0/45/0/135/0]_{2s}$ laminate specimens, as well as short-beam shear and rail-shear specimens, were produced. Some of these samples were exposed to various amounts of electron radiation. Four radiation dose levels were used for this study (3×10^7 rads, 3×10^8 rads, 3×10^9 rads, and 6×10^8 rads). The authors do not site the energy level or dose rate of the electrons, only that they were high-energy electrons and that a cooling plate was required for the specimens during irradiation. After irradiation, mechanical tests were performed over the temperature range of -300°F (89K) to +250°F (394K). The unidirectional and laminate specimens were subjected to both tension and compression tests. No unidirectional off-axis tests were performed.

Haskins and Holmes conclude that changes in mechanical properties due to electron radiation were small, except at high temperatures. They attribute the difference, at high temperatures, for both tensile and shear tests, to lowered glass-transition temperatures in the epoxy resin (which were also measured). They go on to say that there may be some indication that the lower radiation levels may even improve mechanical properties, but were at a loss to explain why. The authors summarize by stating that the effects of cross-linking, load transfer between fiber

and resin, and flexibility of the resin were not investigated and further studies could provide ways of improving properties.

In 1982, V. T. Mazzio et al., from General Electric, generated a study entitled, "Composite Data for Spacecraft," [13,14] to follow-up the work done by Haskins and Holmes. This program was also supported by the U.S. Air Force. They state that the program was designed to generate an advanced composite materials data base to support the design and application of lightweight structures for spacecraft. Five new materials were selected for study: C3000/CE339, P75/CE339, C6000/PMR-15, T300/1700, and Kevlar 49/5209. T300/934 and GY70/X30 were not selected because they had been studied by Haskins and Holmes.

Tensile samples were cut from composite panels with the following orientations: unidirectional, $[0/90]_S$, $[0/45/90/135]_S$, $[\pm 45]_S$, and $[0/45/0/135/0]_S$. Three levels of electron beam radiation were used to expose the composite specimens to the space environment (3×10^8 rads at 22°C, 3×10^8 rads at 100°C, and 3×10^9 rads at 22°C). The electron beam was generated with a Van de Graaff accelerator with a nominal electron energy of 2.0 MeV. Specimens were exposed to a high dose rate of 1.0×10^7 rads/hr and a low dose rate of 5.0×10^6 rads/hr. A key feature of their exposure facility was its test specimen rotating drum. This "carousel" provided an even radiation exposure while also allowing for excellent heat dissipation. Mechanical data were obtained from axial and transverse mechanical tests in both tension and compression. In-plane shear (±45) specimens (ASTM-D 3518-76) were also tested [15,16]. Tests were performed over the temperature range of -300°F (89K) to +250°F (394K).

Mazzio et al. observed that tensile and compression strengths increase as a result of low and high dose rate exposure. They attribute this result to a post-curing effect of the resin, but do not substantiate their conclusion. It is stated that modulus values appear to vary as a function of fiber volume fraction. They observe and conclude that, from in-plane shear properties behavior, a flexible epoxy resin system such as CE399 has potentially a better chance of survival in the space environment over a long life period. Long exposures would not rigidize the resin systems to the extent of causing microcracks and subsequent property degradation.

A large amount of work has been done at North Carolina State University in the area of high energy electron effects on graphite fiber composites [17,18,19,20,21,22]. Graphite fibers in both an epoxy matrix and a polyimide matrix were irradiated with 0.5 MeV electrons. The composite systems investigated were T300/5208 and C6000/PMR-15.

Samples were irradiated using an electron accelerator producing 0.5 MeV electrons. The specimens were mounted on a moving conveyor for an even exposure and to prevent sample heating induced by the radiation. The composite samples received a total dose of up to 5.0×10^9 rads. A dose rate is not stated. Mechanical properties (strength and flexural modulus) were measured by using a three-point flexure test, ASTM method D-790 [23]. Samples used in this test were unidirectional (axial and transverse), $[0/\pm45/0]_T$, and $[90/\pm45/90]_T$. Interlaminar shear strength test specimens were fabricated according to ASTM method D-3846 [24]. These unidirectional samples were, however, pulled in tension which does not follow the ASTM standard. ASTM-D-3846-79 recommends that these

samples be tested in compression. All tests, both flexural and interlaminar, were run at room temperature.

The North Carolina State group points out that interlaminar shear strength decreases significantly with radiation dosage, while little change was observed in the flexural strength and modulus. Interlaminar shear measurements exhibit an initial increase in shear strength with a maximum value occurring between 1.0×10^9 and 2.0×10^9 rads. This is followed by a decrease with further radiation exposure. They conclude that the initial increase in strength with radiation exposure is probably due to relaxation, by chain cleavage, of internal stresses created at the interface during composite fabrication. After the internal stresses are relieved, further radiation exposure leads to bond degradation near the interface due to chain scisson, and thus the decrease in interlaminar shear strength. Flexural strength and modulus, measured by the three-point bend test, however, do not exhibit any characteristics of this behavior.

It is important to note here that unpublished work performed at the NASA-Langley Research Center by G. F. Sykes indicates that the interlaminar shear specimen (ASTM-D-3846-79) under tensile load produces a "peeling" moment at the specimen's notches. This would adversely affect the test by producing a non-pure shear stress state. Interlaminar tests on composite specimens, run at NASA-Langley in the compression mode, did not exhibit significant changes with irradiation.

L. B. Fogdall and P. H. Lindenmeyer are working with graphite-epoxy at Boeing in Seattle, Washington [25]. The materials being investigated are C3000/1634A (350°F-cure epoxy), C3000/1648A (250°F-cure epoxy), and

C3000/PMR-15 (polyimide). They are using 1.0 MeV electrons, generated with a Van de Graaff accelerator, with a total dose of up to 1.0×10^{10} rads. The composite samples receive 1.0×10^{8} rads/hr and are cooled with a baseplate.

Mechanical testing is being performed using a 45°-off axis compression test and dynamic-mechanical analysis (DMA) equipment manufactured by DuPont. Dynamic-mechanical analysis is the measurement of the mechanical properties of materials as they are deformed under periodic stress [26,27]. DMA measures the changes in the resonant-frequency of the test material over a very large temperature range (-300°F to +500°F). From this information the material's modulus of elasticity, over that temperature range, is calculated, as well as the glass-transition temperature of the polymer matrix (from the damping characteristics of the test material).

Boeing reports that the 45°-off axis compression test can detect the influence of electron radiation at the 1.0×10^{10} rad dose level with a 95% confidence level. Compressive strength is lowered by irradiation. In addition, DMA measurements show that a 1.0×10^{10} rad dosage of 1.0 MeV electron radiation has the effect of decreasing the glass-transition temperature of the epoxy matrix material. No mechanism is stated to explain this phenomenon.

At the Lockheed Research Laboratory in Palo Alto, California, R. E. Mauri and F. W. Crossman are working with T50(PAN)/F263 (350°F-cure epoxy), 75S(PITCH)/948 (250°F-cure epoxy), and Kevlar-49/E719 [28]. They are producing 1.5 MeV electrons at the rate of 1.5×10^{6} rads/hr. The composite samples receive a total-dose of between 3.0×10^{9} to $1.0 \times$

10^{10} rads. Mechanical properties are measured using the flexure strength test, inplane shear test, and short-beam shear test over the temperature range of -200°F (143K) to +250°F (394K).

Their results indicate that the 250°F and 350°F curing graphite/epoxies are not significantly altered except at the highest test temperature (+250°F), where the 350°F curing epoxy systems experienced a degradation of matrix-dependent properties of up to 20 percent. Mauri and Crossman attribute this degradation to the reduction in glass-transition temperature of the matrix because of chain scisson of the epoxy by the penetrating radiation.

A study was conducted at the Argonne National Laboratory in Argonne, Illinois, by S. Egusa, M. A. Kirk, R. C. Birtcher, M. Hagiwara, and S. Kawanishi, on cloth-filled organic composites [29]. Four types of cloth-filled organic composites (filler: glass or carbon fibers; matrix: epoxy or polyimide resin) were irradiated with 2.0 MeV electrons, at room temperature, and were mechanically examined using the three-point bend test.

They summarize by stating that following irradiation, the modulus of elasticity of these composites remains practically unchanged, even after irradiation of up to 1.5×10^{10} rads. The shear modulus and ultimate strength, on the other hand, begin to decrease after the absorbed dose reaches about 2.0×10^{9} rads for the glass/epoxy composite and about 5.0×10^{9} to 1.0×10^{10} rads for the other composites. They attribute this change to the decrease in the capacity of load transfer from the matrix to the fiber due to the radiation-induced debonding at the interface.

Work done by C. Giori, T. Yamauchi, K. Rajan, and R. Mell, at the IIT Research Institute in Chicago, Illinois, is concerned with the degradation mechanisms for graphite/polysulfone and graphite/epoxy laminates exposed to high-energy electron radiation [30]. The graphite/polysulfone system used was C6000/P1700 and the graphite/epoxy systems were T300/934 and T300/5208. 12.0 MeV electrons, at the rate of 3.9×10^7 rads/hr, were used to give total doses of 5.0×10^7 rads up to 1.0×10^9 rads. Composite degradation was investigated with the aid of gas-chromatograph (GC) and mass-spectometer (MS) analysis.

Giori et al. state that all the composite materials evaluated have shown high electron stability up to the dose levels used. Hydrogen and methane have been identified as the main by-products of irradiation, along with unexpectedly high levels of carbon monoxide and carbon dioxide. They go on to state that gas formation in irradiated polymers reflects the occurrence of chain scission and crosslinking reactions. And conclude that, although the primary process of electron irradiation damage involves ionization, subsequent steps lead to chain scission and crosslinking, with concurrent gas formation.

Summary of Current Literature on Radiation Effects on Composites

Many of the studies noted in the previous section do not use a large enough total radiation dose to adequately simulate a long space exposure. The two major works, that performed by Haskins and Holmes and that performed by Mazzio et al., have a largest total dose of only 3.0×10^9 rads [11,12,13,14]. This is equivalent to less than 10 years in space. The largest dose obtained by the North Carolina group translates

into 15 years exposure (5.0×10^9 rads) [17,18,19,20,21,22]. If space structures are meant to have useful lifes of 10 to 20 years, clearly this is not enough. If we are to design a structure for use in a space environment, data is needed past the useful life of that structure.

Most researchers used electron energies that are equivalent to those found in the Van Allen radiation belts, although some were on the high side. In some cases, samples were not continuously irradiated under the electron beam, but nothing is mentioned as to whether the temperature cycling that must have been taking place would have any effect. All investigators agreed that temperature control during irradiation is very important, and all made attempts to control it.

Accelerated exposure is a controversial subject that almost all the researchers did not address. However, the study performed by Mazzio et al. used a high dose rate of 1.0×10^7 rads/hr and a low dose rate of 5.0×10^6 rads/hr [13,14]. No differences were noted.

Very few of these studies made an attempt to obtain a complete set of inplane tensile properties. If design considerations are to be made with the space environment in mind, a complete set of properties must be available. Many researchers used a large temperature range, -300°F (88K) to +250°F (394K), when performing mechanical tests.

The most disturbing development that can be drawn from this literature review is that many researchers make conclusions to describe the degradation noted, but do not support these conclusions with experimental measurements. Therefore, many conflicting statements are made about radiation effects and what can be done to compensate for them.

2.2 Testing Methods

2.2.1 Mechanical Testing

All researchers in the field of composites testing generally agree that lamina properties in the fiber direction (ultimate stress: X_T, elastic modulus: E_1, and Poisson's ratio: ν_{12}) and transverse to the fiber direction (ultimate stress: Y_T, elastic modulus: E_2, and Poisson's ratio: ν_{21}) can be measured using unidirectional laminates in the 0° and 90° orientations (Fig. 4). However, much less agreement is found in determining shear properties (ultimate shear strength: S, and shear modulus: G_{12}), due to the difficulty of producing a state of pure shear in practical laboratory test specimens.

One method for measuring shear properties was proposed by C. C. Chamis and J. H. Sinclair of the NASA-Lewis Research Center in Cleveland, Ohio, in 1977 [31]. Their combined theoretical and experimental investigation proposed using the 10°-off axis tensile-test laminate for intralaminar-shear characterization of unidirectional composites. The theoretical approach included classical lamination theory (CLT), a combined-stress failure criterion, and a finite element analysis of the problem. Several 10°-specimens of Mod-I/epoxy, T300/epoxy, and S-glass/epoxy were fitted with strain gage rosettes to experimentally verify their findings. They conclude that the procedure is suitable for shear characterization and recommend that it should be considered as a possible standard test specimen.

Further work by Pindera and Herakovich has shown that shear-coupling at low fiber orientations leads to less than satisfactory results [33]. Thus, the 10°-specimen is suitable for shear strength (S) deter-

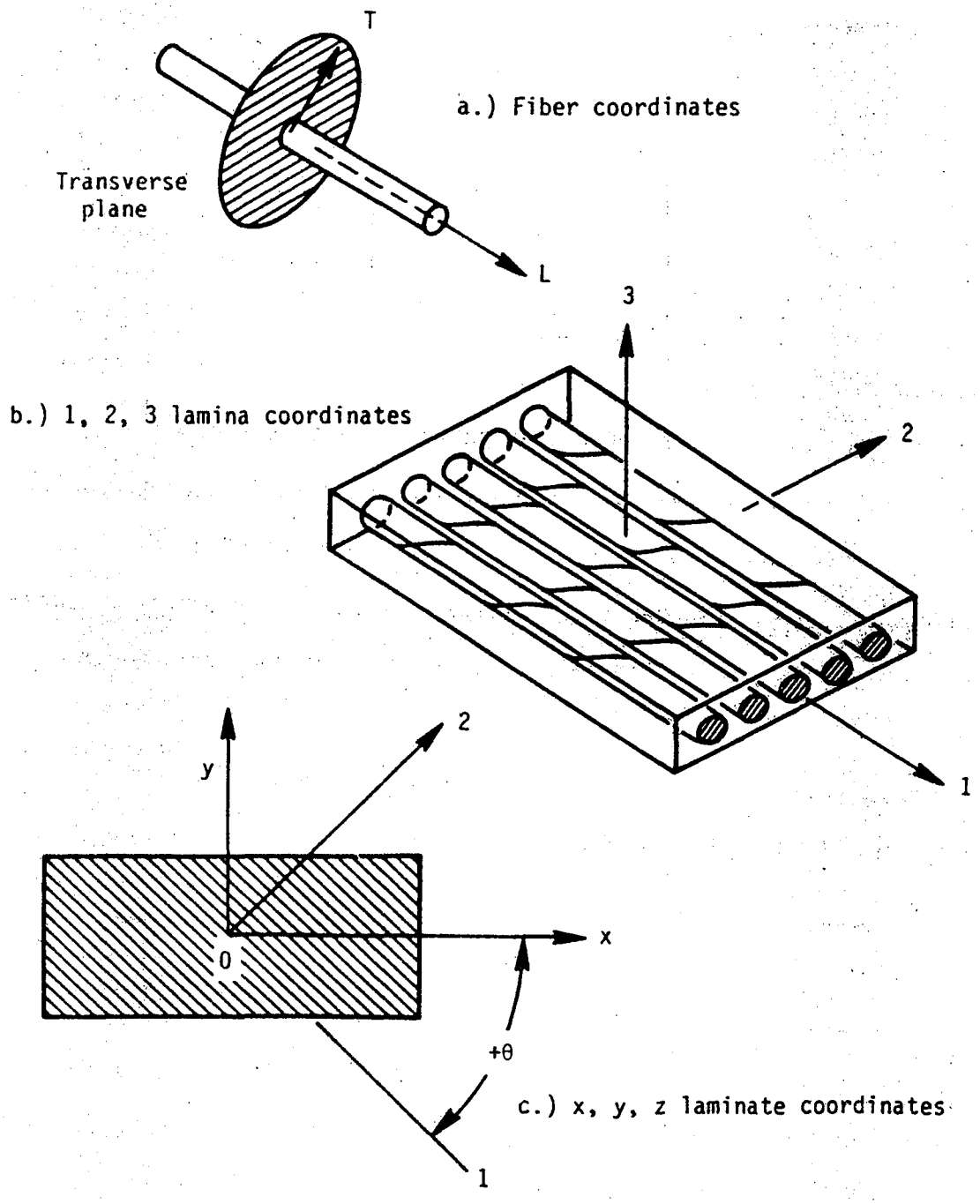

Fig. 4. Coordinate Systems Used in this Study.

mination, but the 45°-specimen is preferred for determination of the shear modulus (G_{12}). Therefore, it was decided to use the 10°-laminate for shear strength and the 45°-laminate for shear modulus.

The basic theory of this test utilizes the biaxial stress-state that is present when a 10°-off axis laminate is subjected to an axial load. The induced stress-state has three stress components; longitudinal $\sigma_{\ell 11}(\sigma_1)$, transverse $\sigma_{\ell 22}(\sigma_2)$, and intralaminar $\sigma_{\ell 12}(\sigma_{12})$ as indicated in Fig. 5. In order for this specimen to serve as a useful means of intralaminar-shear characterization, the stress component $\sigma_{\ell 12}(\sigma_{12})$ must be the only stress component that is near its critical value. Fracture must occur at the 10° orientation when the intralaminar shear, σ_{12}, reaches this critical value. Experimental measurements, made by Chamis and Sinclair, have determined that this is the case [31].

The stresses in a lamina with a fiber orientation of θ are determined from the following standard stress transformation equation [32].

$$\{\sigma\}_x = [T]^{-1}\{\sigma\}_1 \tag{1}$$

Where $\{\sigma\}_x$ are the stresses in laminate coordinates and $\{\sigma\}_1$ are the stresses in lamina coordinates. [T] is the transformation matrix listed below in which θ is the fiber orientation within a given lamina [32].

$$[T] = \begin{bmatrix} \cos^2(\theta) & \sin^2(\theta) & -2\sin(\theta)\cos(\theta) \\ \sin^2(\theta) & \cos^2(\theta) & 2\sin(\theta)\cos(\theta) \\ \sin(\theta)\cos(\theta) & -\sin(\theta)\cos(\theta) & \cos^2(\theta)-\sin^2(\theta) \end{bmatrix} \tag{2}$$

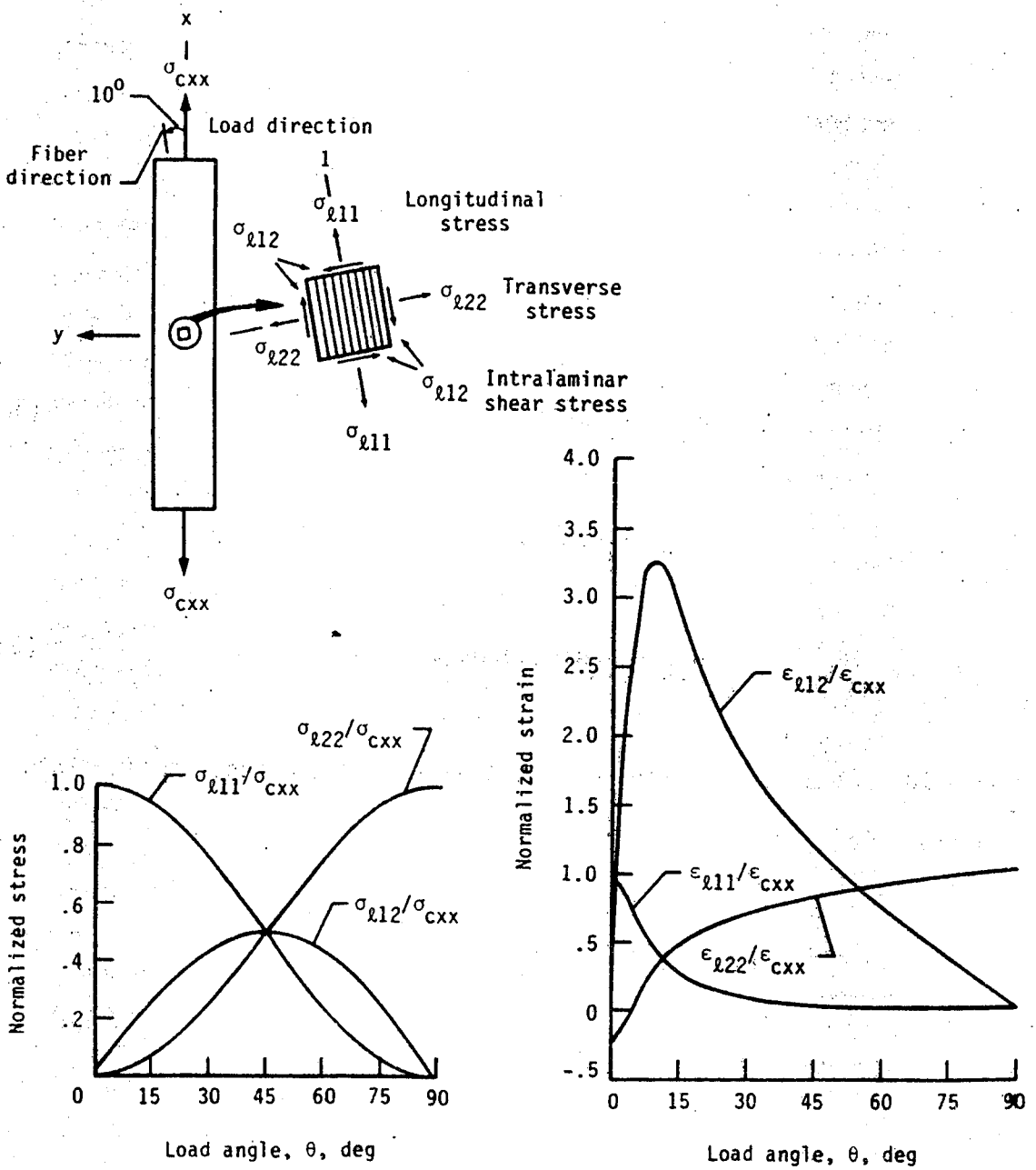

Fig. 5. The 10°-Off Axis Tensile Test for Determining Shear Properties.

Chamis states that, for a uniaxial load along the x-axis of a laminate, σ_x has a measurable value, but σ_y and σ_{xy} are equal to zero. Note that Pindera and Herakovich have shown that σ_{xy} can only be taken to be zero for very large aspect ratios [33]. Therefore, from equations (1) and (2), the following equations can be written.

$$\sigma_1 = \sigma_x \cos^2(\theta) \tag{3a}$$

$$\sigma_2 = \sigma_x \sin^2(\theta) \tag{3b}$$

$$\sigma_{12} = \sigma_x \sin(\theta)\cos(\theta) \tag{3c}$$

For a 10°-off axis laminate, θ is equal to 10° and substituting into equations (3) gives:

$$\sigma_1 = \sigma_x 0.970 \tag{4a}$$

$$\sigma_2 = \sigma_x 0.030 \tag{4b}$$

$$\sigma_{12} = \sigma_x 0.171 \tag{4c}$$

In this investigation, the 10°-off axis specimen was used to measure shear strength only, due to work done by M. J. Pindera and Herakovich that indicates that this is not a good test for the measurement of shear modulus [33]. Therefore, from equation (4c), an equation

can be written for the ultimate shear strength, S.

$$S = \sigma_{ult}(10°)\ 0.171 \tag{5}$$

Where $\sigma_{ult}(10°)$ is the ultimate stress of the 10°-laminate.

Pindera and Herakovich go on to state that the 45°-off axis test is more suited for the measurement of shear modulus, G_{12}. Shear coupling is small in the 45°-laminate, thus permiting its use to measure shear modulus. In addition, since the 45°-laminate fails in a mixed mode of inplane shear and transverse tension, it is not a good specimen for measuring shear strength. In this investigation, the 45°-off axis laminate was used to measure shear modulus, G_{12}.

The basis of this test method begins with the generalized Hooke's law [32].

$$\{\sigma\} = [C]\{\varepsilon\} \tag{6}$$

where σ and ε are stress and strain, and [C] is the stiffness matrix. By rewriting this equation in terms of strain and in lamina coordinates, the following relationship is obtained:

$$\{\varepsilon\}_1 = [S]\{\sigma\}_1 \tag{7}$$

where [S] is the compliance matrix, which when expanded gives the following relations (in lamina coordinates).

$$S_{11} = \frac{1}{E_1} \tag{8a}$$

$$S_{12} = -\frac{\nu_{12}}{E_1} = -\frac{\nu_{21}}{E_2} \tag{8b}$$

$$S_{22} = \frac{1}{E_2} \tag{8c}$$

$$S_{66} = \frac{1}{G_{12}} \tag{8d}$$

where E_1, E_2, ν_{12}, ν_{21}, and G_{12} are engineering constants in lamina coordinates.

Hooke's law can also be written in terms of the laminate coordinate system [32].

$$\{\varepsilon\}_x = [\bar{S}]\{\sigma\}_x \tag{9}$$

where $\{\varepsilon\}_x$ are the strain components and $\{\sigma\}_x$ are the stress components. $[\bar{S}]$ is the transformed compliance matrix and its first element is found to be equal to

$$\bar{S}_{11} = S_{11}\cos^4(\theta) + (2S_{12} + S_{66})\sin^2(\theta)\cos^2(\theta) + S_{22}\sin^4(\theta) \tag{10}$$

A substitution can now be made from equations (8) and noting that in laminate coordinates, the relation shown in equation (11) is true.

$$\bar{S}_{11} = \frac{1}{Ex} \tag{11}$$

$$\frac{1}{E_x} = \frac{1}{E_1}\cos^4(\theta) + \left(\frac{1}{G_{12}} - \frac{2\nu_{12}}{E_1}\right)\sin^2(\theta)\cos^2(\theta) + \frac{1}{E_2}\sin^4(\theta) \tag{12}$$

For a 45°-off axis laminate, θ is equal to 45° and substituting into equation (12) gives

$$\frac{1}{E_x} = \frac{1}{4}\left[\frac{1}{E_1} - \frac{2\nu_{12}}{E_1} + \frac{1}{G_{12}} + \frac{1}{E_2}\right] \tag{13}$$

By rearranging

$$G_{12} = \left[\frac{4}{E_x} - \frac{1}{E_1} - \frac{1}{E_2} + \frac{2\nu_{12}}{E_1}\right]^{-1} \tag{14}$$

In this equation, E_x is the axial modulus of the 45°-specimen and E_1, E_2, and ν_{12} are determined from other tests.

2.2.2 Dynamic-Mechanical Analysis

Dynamic-mechanical analysis (DMA) is being used increasingly for polymer and composite materials characterization. Properties measured by this technique include the dynamic modulus of the material, its damping characteristics, and glass-transition temperature. The glass-transition temperature of a polymer is defined as the temperature at which the polymer loses its "crystallinity" and becomes more plastic, soft, and pliable.

DMA is the measurement of the mechanical properties of materials as they are deformed under periodic stress [26,27]. In a typical test arrangement, Fig. 6, a sample is clamped between the arms of a compound resonance system in which the resonant frequency is dependent almost entirely on the configuration and modulus of the sample [25]. The

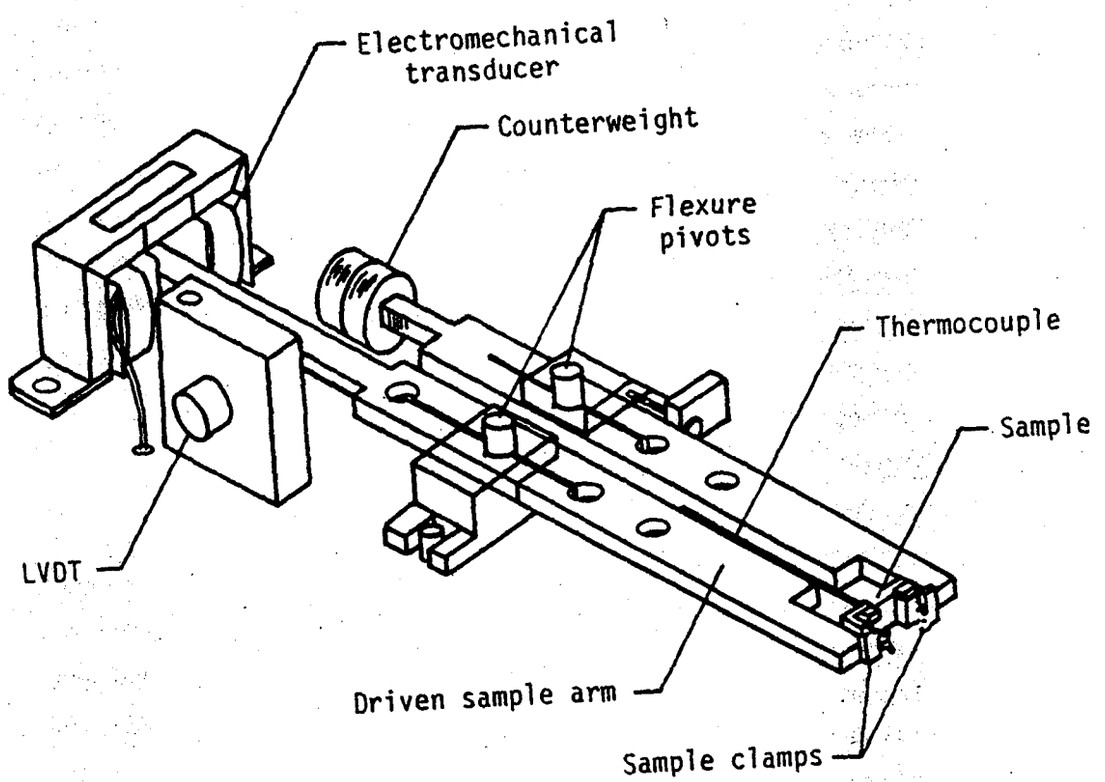

Fig. 6. Illustration of Dynamic Mechanical Analysis (DMA) Test Equipment.

sample-arm-pivot system is oscillated at its resonant frequency by an electromechanical transducer. The frequency and amplitude of this oscillation are detected by an LVDT positioned at the oscillated end of the active arm. The LVDT provides a signal to the electromechanical transducer, which in turn keeps the sample oscillating at constant amplitude.

During each cycle, the test specimen is subjected to an alternating flexural deformation. The ability of this test specimen to store and dissipate energy upon deformation is monitored by the DMA system. When the test specimen is deformed and then relaxed, a portion of the energy required to deform the sample is dissipated as heat that is released at a rate that is characteristic of the test material. This dissipation energy, the damping, is characteristic of the molecular structure and mechanical properties of the viscoelastic material being tested [27].

By monitoring damping energy as a function of temperature, the glass-transition temperature of the polymeric material can be determined. Due to molecular chain movement at the glass-transition temperature, a huge increase in damping energy will be noted.

The solution for the dynamic equation of motion for the system gives the following relationship between the dynamic modulus of elasticity and DMA frequency [25]:

$$E = \frac{(4^2 f^2 J - K)}{2W(\frac{L}{2} + D)^2} \cdot (\frac{L}{T})^3 \qquad (15)$$

where

E = Dynamic modulus of elasticity (Pa)

f = DMA frequency (Hz)

J = Moment of inertia of arm ($kg \cdot m^2$)

K = Spring constant of pivot ($N \cdot m/rad$)

D = Clamping distance (m)

W = Sample width (m)

T = Sample thickness (m)

L = Sample length (m)

By monitoring the dynamic modulus as a function of temperature, the temperature at which the polymer softens can be determined. At this temperature the modulus decreases greatly.

By comparing outputs of damping and/or modulus versus temperature for various polymers, conclusions can be drawn about the effect of molecular structure on DMA data. Fig. 7 is a typical plot of damping versus temperature for three polymeric materials [26]. The large peak at the high temperature is the glass-transition temperature of the polymer. If the average molecular weight of the material could be decreased, the height of this peak would be increased. In addition, the peak would shift slightly toward lower temperatures. It is readily observable that differences in the molecular weights of different materials can be easily compared with the DMA technique. It should also be noted here that a large distribution of molecular weights would produce a broader glass-transition temperature peak than would a tight distribution of molecular weights.

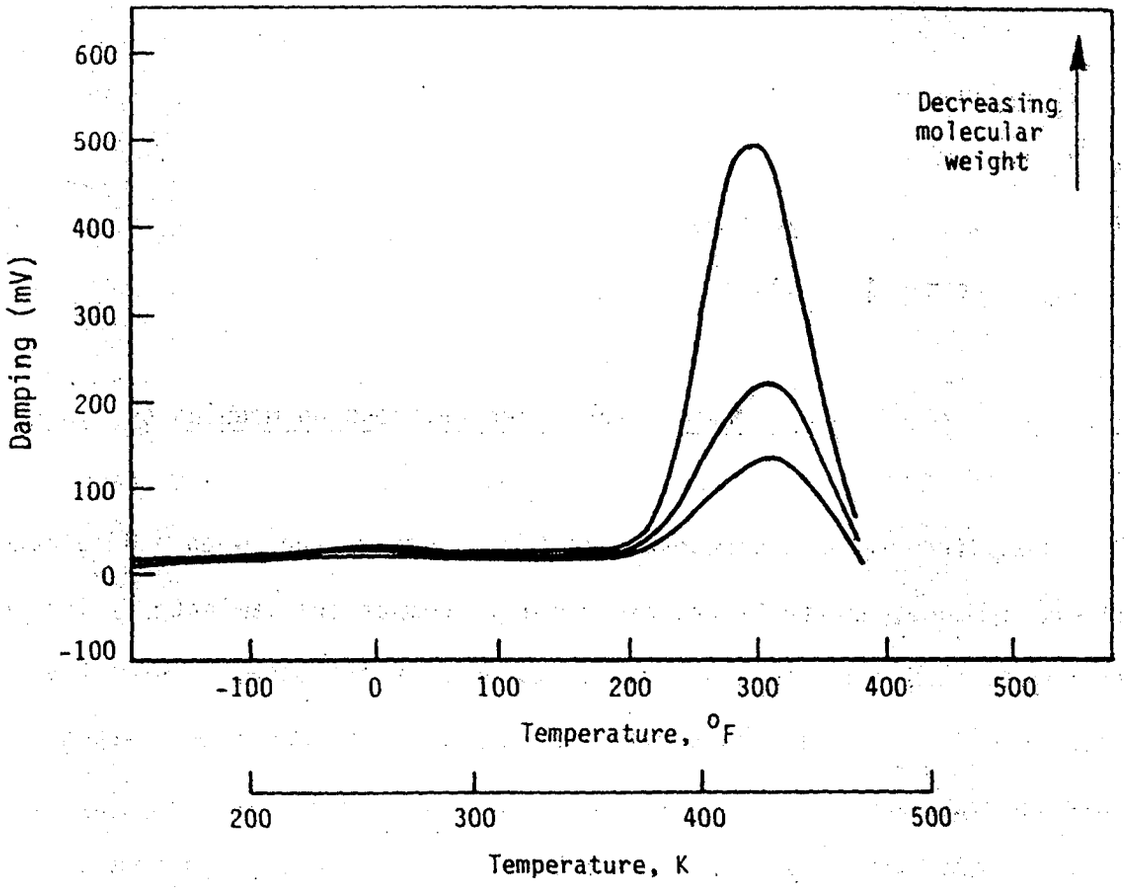

Fig. 7. Effect of Molecular Weight of a Polymeric Material on DMA Output.

Dynamic-mechanical analysis can be used to measure the effect of a change in crosslink density on the damping characteristics of a polymeric material. A plot of damping versus temperature as a function of crosslinking is illustrated in Fig. 8 [26]. The glass-transition temperature peak would be shifted toward lower temperatures as well as be slightly increased in height if crosslink density were decreased. Again, changes in polymers due to changes in molecular arrangement are easily detected with DMA techniques.

2.3 Effect of Residual-Stresses and Fiber Waviness on Modulus of Elasticity

Composite materials researchers have observed that when a 0° graphite-epoxy (or graphite-fiber, resin-matrix composite) laminate is loaded in tension, it exhibits nonlinear stress-strain response; the stiffness increases with increasing stress. In addition, the nonlinear response observed is reversible over almost the entire range of allowable stress. Reversibility is no longer possible only after significant damage has occurred within the laminate. Significant damage is usually evident only when the specimen has obtained ninety percent of its ultimate stress [34]. The increase in modulus of elasticity can be as much as thirty percent [35].

Poisson's ratio of transverse strain compared to axial strain also exhibits nonlinearity in 0°-specimens under tension. In this case, Poisson's ratio decreases with increasing applied load [34]. The response is reversible until significant damage has been induced in the specimen.

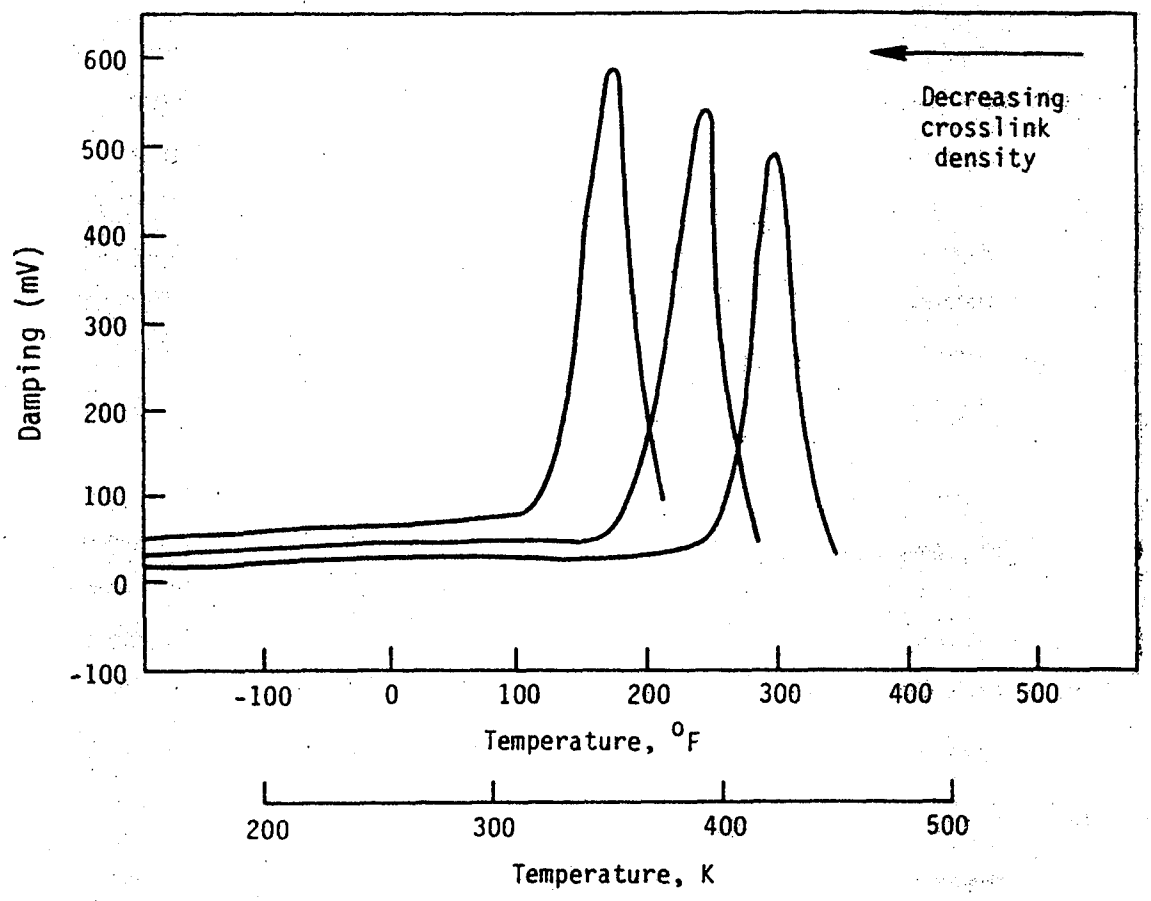

Fig. 8. Effect of Crosslinking Density of a Polymeric Material on DMA Output.

The above observations and laminate responses are noted only in specimens tested in the fiber direction. Off-axis laminates and shear specimens do not exhibit similar behavior.

Several investigators have performed studies aimed at citing causes to explain the nonlinear behavior. The two most common explanations involve the effect of graphite fiber waviness and nonlinear response of the graphite fiber itself.

Curtis, Milne, and Reynolds identified two modes of fiber behavior which are altered by applied load [35]. Initially, the increase in the modulus of elasticity of carbon fibers is attributed to movement and subsequent pinning of basal dislocations within the crystalline structure of the fibers. This change in crystalline orientation with applied load is reversible. In the second mode, load applied to the fiber causes straightening of the cellular structure of the fiber itself.

Beetz performed a similar study and made the same observations [36]. He summarizes by stating that the observed fiber stiffening can be explained by a strain-induced increase in the fiber preferred orientation and modeled by either a uniform stress or elastic unwrinkling model. Conclusions drawn by both Curtis et al. and Beetz point to both changes in crystalline orientations within the fibers and straightening of the fibers themselves.

With this information in mind, analytical and experimental investigations were performed by Mansfield and Purslow, Bazant, Comninou and Yannas, Bert, VanDremel and Kemp, and Pindera and Herakovich to determine the influence of fiber waviness on composite material properties [34, 37, 38, 39, 40, 41]. In these studies, unidirectional lamina with

varying degrees of fiber waviness were modeled, observed, and characterized. Results reveal that fiber waviness has negligible effect on the modulus of elasticity and shear properties when composite matrices are stiff and brittle. However, in those systems where matrices are ductile and flexible, significant influence is predicted and measured. Fiber waviness can significantly increase the modulus of elasticity of a 0°-laminate provided the matrix of that composite is flexible.

Essentially straight fibers in a ductile matrix produce a greater composite modulus than wavy fibers in the same matrix. For a composite material, stiffness in the fiber direction is directly influenced by the degree of fiber waviness.

The amount of residual stress present in a composite laminate can directly influence the degree of fiber waviness within that laminate [42,43]. Composite laminates are manufactured at high temperatures (250°F to 350°F) to allow the epoxy resin matrix material to cure. Upon cooling, the matrix will contract and the fibers will expand slightly, due to differences in thermal expansion. Equilibrium is obtained when compressive forces in the fibers equal the tensile forces in the matrix. This state of equilibrium of internal forces is termed the residual stress state. Since the thin, slender fibers are in compression, they may tend to buckle slightly. The larger the residual stresses, the larger the degree of waviness of the fibers.

The amount of residual stress present in a composite laminate will directly influence the degree of fiber waviness in that laminate. This influence is also affected by the degree of ductility of the matrix material. Fibers with a high degree of waviness will produce a com-

posite material that is less stiff in the fiber direction as compared to a composite containing straighter fibers. Reducing residual stresses within a laminate will result in straighter fibers and therefore higher values for the modulus of elasticity of that laminate.

III. METHODS AND MATERIALS

The experiments described here focused on two main objectives:

a) To determine the effects of a space environment on the mechanical properties of a graphite-epoxy composite, and

b) To characterize the changes in the epoxy matrix of this composite due to its exposure.

The material tested in this study and the radiation facility used to expose it are described in sections 3.1 and 3.2. Subsequent mechanical testing is discussed in section 3.3. The methods used to characterize the epoxy resin matrix are presented in sections 3.4 through 3.8.

3.1 Material

The material chosen to be investigated in this study is T300/934 graphite-epoxy advanced composite. Panels were produced following the manufacturer's curing procedures. Two 18-inch (45.72 centimeters) by 24-inch (60.96 centimeters) panels of 4-ply unidirectional material were cured and used in the mechanical tests. One panel of similar size with a $[0/90]_S$ lay-up was used in the thermal-cycling tests. The laminates were limited to a thickness of 4 plies (0.0242 inches, 0.615 millimeters) in order to ensure uniform radiation exposure through the thickness of the composite. Prior to use, these panels were ultrasonically C-scanned to ensure integrity.

Samples of the graphite-epoxy panels were tested for fiber volume, volatile content, and density; these results are tabulated in Table 3. These measurements were conducted for both the non-irradiated and the

Table 3

Fiber Volume and Density of T300/934 Graphite-Epoxy Composite.

T300/934, Graphite-epoxy 4-ply, unidirectional material
Fiber volume: 68%
Volatile content: < 1%
Density: 1.568 g/cm^3

irradiated material and no differences could be detected. Dimensional measurements were also made before and after radiation exposure, and no dimensional changes were discovered. A visual examination of the irradiated material detected a slight darkening in color when compared to non-irradiated material.

Prior to testing, all test specimens were placed in a vacuum drying oven (1.0×10^{-3} torr, 110°F) for a minimum period of two weeks. A plot of weight loss due to moisture for this material is presented in Fig. 9.

3.2 Radiation Facility

A radiation exposure of 1.0×10^{10} rads was used in this investigation to simulate a "worst case" of 30 years in space [7]. Electrons with energies of 1.0 MeV were used which are characteristic of those found in the Van Allen radiation belts surrounding the earth [8]. A dose rate of 5.0×10^{7} rads per hour accelerated exposure times to 200 hours. This translates into actual facility use times of 14 to 21 days.

The facility that was used to produce radiation exposures for this investigation is the Space Materials Durability Laboratory located at the NASA-Langley Research Center in Hampton, Virginia (Fig. 10). This installation uses an electron accelerator to produce a 10-inch (25.4-centimeter) electron beam capable of producing exposures of the type described above. A water-cooled backplate is used to keep the composite samples from overheating during their radiation exposure. This system insures that the specimens will not experience temperatures greater than 100°F, and experience has shown that lower temperatures are more probable. Using this configuration, a change in temperature (ΔT) from the

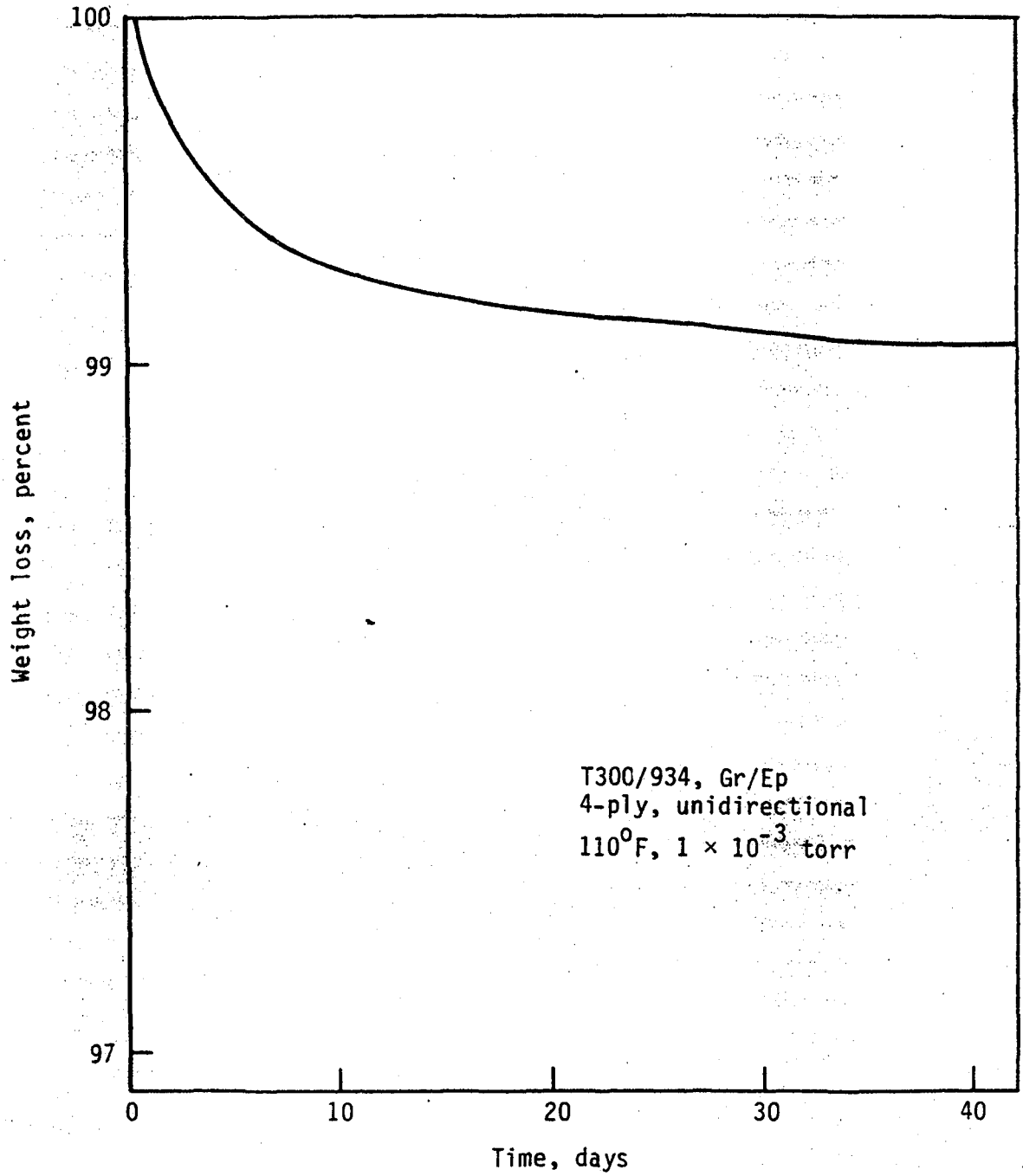

Fig. 9. Weight Loss Due to Moisture for T300/934 Graphite-Epoxy Composite.

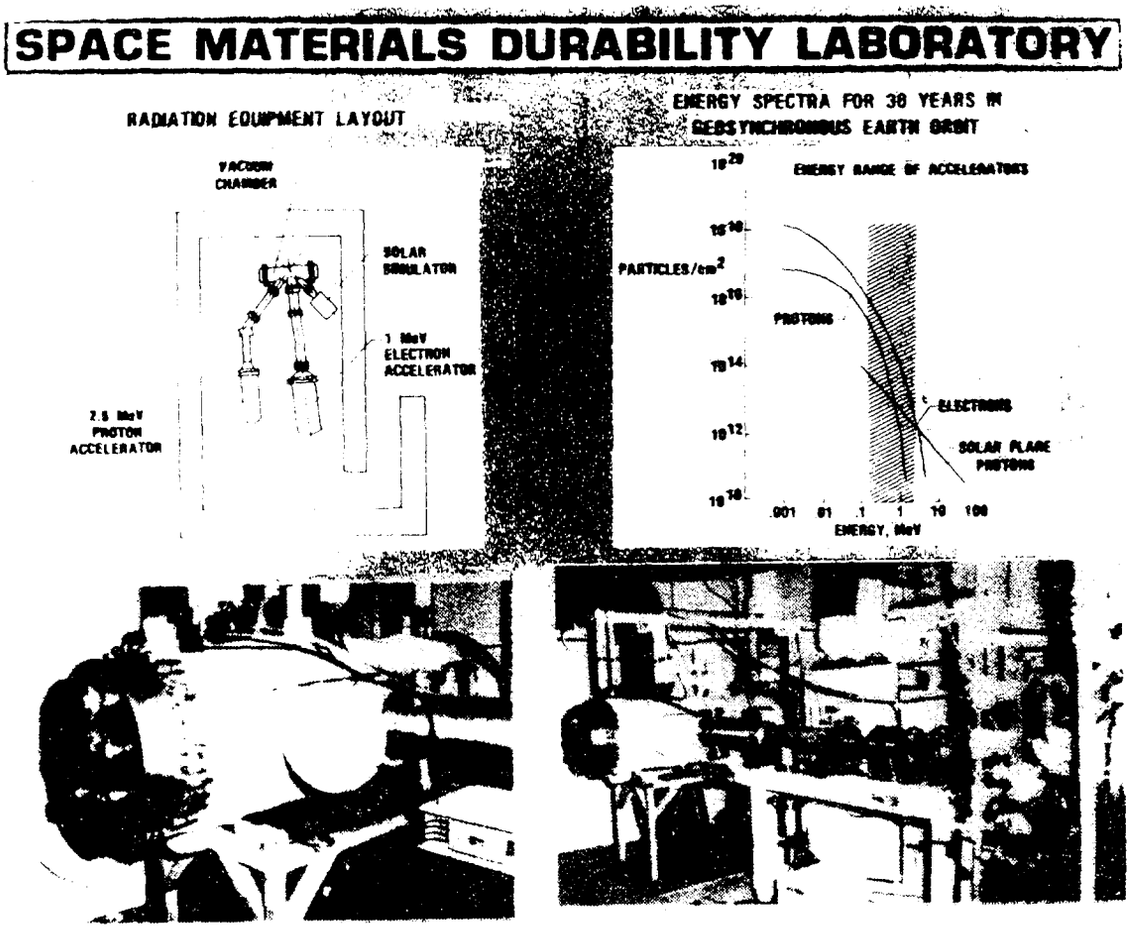

Fig. 10. Space Materials Durability Laboratory Located at NASA-Langley Research Center, Hampton, Virginia.

front surface to the back surface of the samples, during irradiation, is not present [44].

In preparation for a radiation exposure, composite samples are first attached to an aluminum plate (Fig. 11). The 10-inch (25.4-centimeter) circle inscribed on the plate is a guide to indicate where the electron beam will strike the plate. The aluminum plate is then attached to the water-cooled backplate of the exposure facility (Fig. 12). As seen in the photograph, a thermocouple is connected to the plate to monitor temperature and a Faraday cup is used to measure electron dose and dose rate. This entire assembly is positioned in the vacuum chamber of the facility and exposured to the electron radiation (Fig. 13).

3.3 Mechanical testing

In order to characterize the inplane tensile behavior of the graphite/epoxy system being tested in this study, the following properties have been measured or calculated: E_1, E_2, G_{12}, ν_{12}, ν_{21}, X_T, Y_T, and S. A 0°-laminate was used to measure X_T, E_1, and ν_{12} which are properties in the fiber direction. A 90°-laminate was used to measure the transverse properties Y_T and E_2. As stated earlier, the shear strength, S, was calculated from the 10°-off axis specimen and the shear modulus, G_{12}, from the 45°-off axis specimen. Poisson's ratio, ν_{21}, was calculated from the following well known equation [32].

$$\nu_{21} = \frac{E_2}{E_1} \cdot \nu_{12} \qquad (16)$$

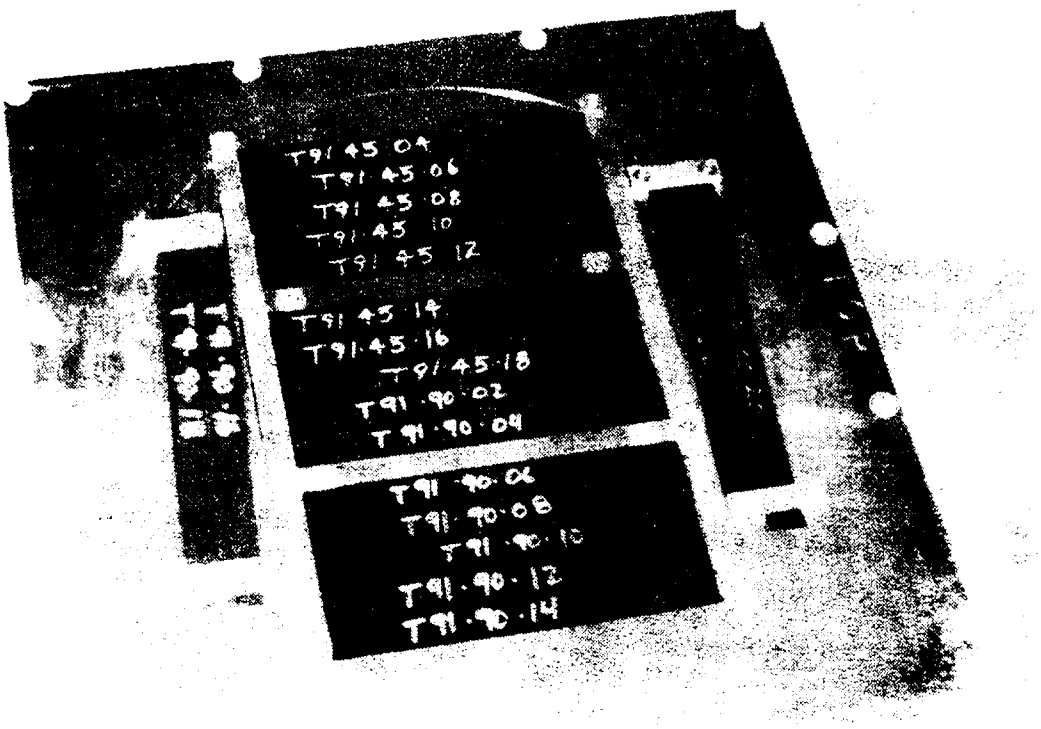

Fig. 11. Photograph of Graphite-Epoxy Specimens Attached to Aluminum Backplate.

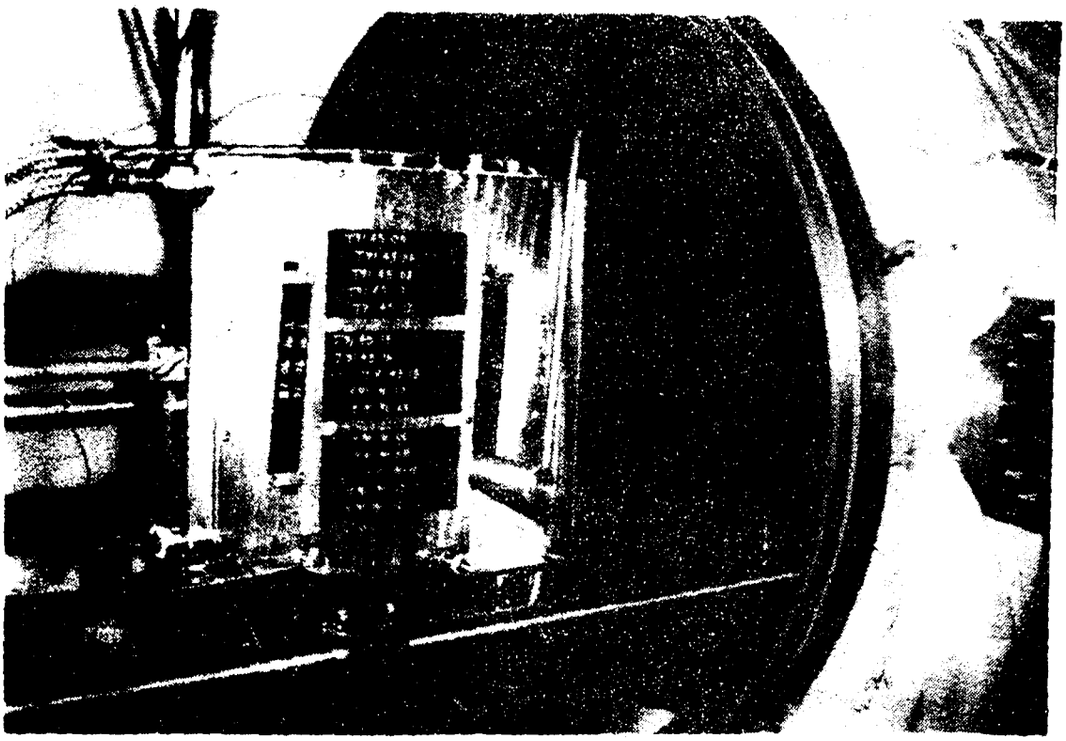

Fig. 12. Photograph of Aluminum Backplate Attached to Cooling Plate in Irradiation Facility.

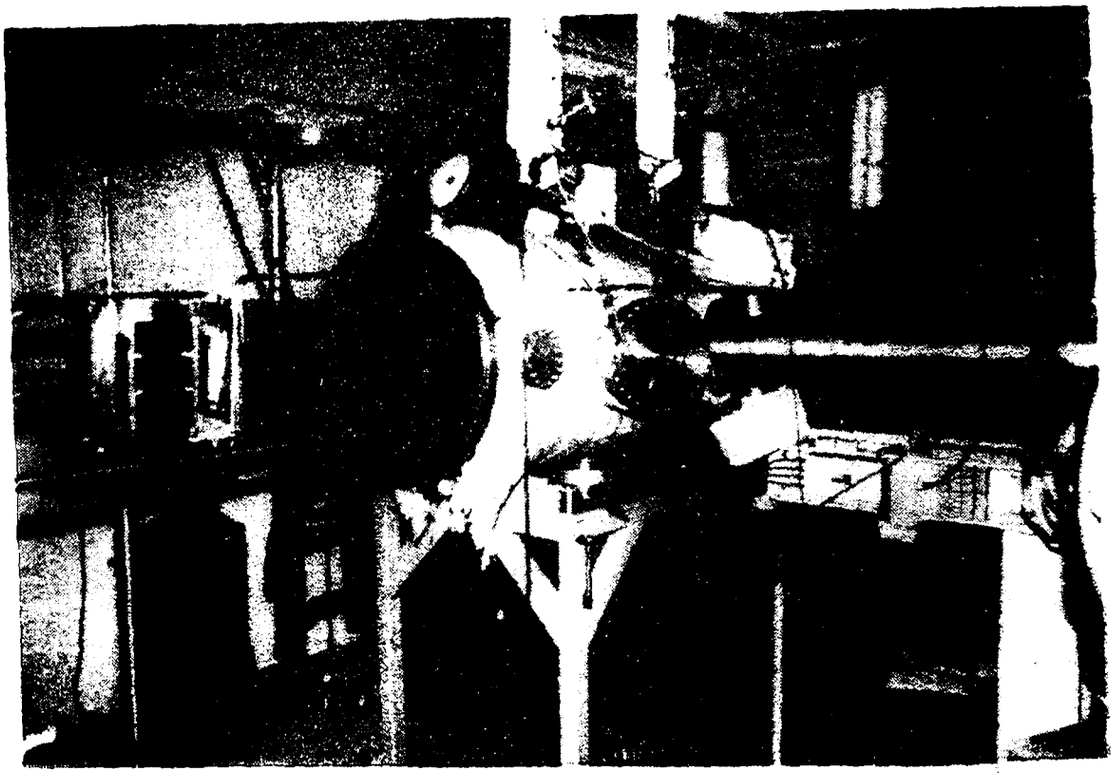

Fig. 13. Photograph of Graphite-Epoxy Specimens in Irradiation Facility.

A table of the laminates utilized and the properties obtained is presented in Table 4.

Mechanical tests were performed for both the non-irradiated and irradiated material over the temperature range of -250°F (116K) to +250°F (394K). Table 5 is the testing matrix that was used.

Test specimens were cut from the unidirectional panels of T300/934 graphite-epoxy. The laminate was limited to a thickness of 4 plies in order to insure uniform radiation exposure through the thickness of the composite. A length and width of 6 inches (15.24 centimeters) by 0.5 inches (1.27 centimeters) was chosen to optimize the number of specimens that could be placed under the 10 inch (25.4 centimeter) electron beam, without overly compromising on the aspect ratio (length to width) of the test specimen. Fiberglass tabs were used for load introduction to prevent the mechanical grips from biting into the test coupon and damaging the composite. Strain was measured with wide-temperature range strain-gages (SK-06-125AD-350, Micro-Measurements). The $[0]_4$ laminates were fitted with both axial and transverse gages (for measurement of Poisson's ratio, ν_{12}), while all others were mounted with axial gages only. A schematic of the test coupon used in this investigation is presented in Fig. 14, while Fig. 15 is a photograph of an instrumented specimen.

All tests were performed in an environmental chamber that uses resistance elements for heating and liquid nitrogen for cooling. The heat from the resistance elements is circulated by an internal fan. The liquid nitrogen evaporates as it enters the chamber and is circulated by a slight overpressure from the nitrogen source. Temperature is moni-

Table 4

Properties Measured from the Laminate Lay-Ups Used.

Laminate lay-up	Properties measured
$[0^o]_4$	X_T, E_1, ν_{12}
$[10^o]_4$	S
$[45^o]_4$	G_{12}
$[90^o]_4$	Y_T, E_2

Table 5

Test Matrix.

Test condition	Temperature	Laminate lay-up $[0^o]_4$	$[10^o]_4$	$[45^o]_4$	$[90^o]_4$
non-irradiated	-250°F (116K)	3	3	3	3
	Room temperature	3	3	3	3
	+250°F (394K)	3	3	3	3
1.0×10^{10} rads	-250°F (116K)	3	3	3	3
	Room temperature	3	3	3	3
	+250°F (394K)	3	3	3	3

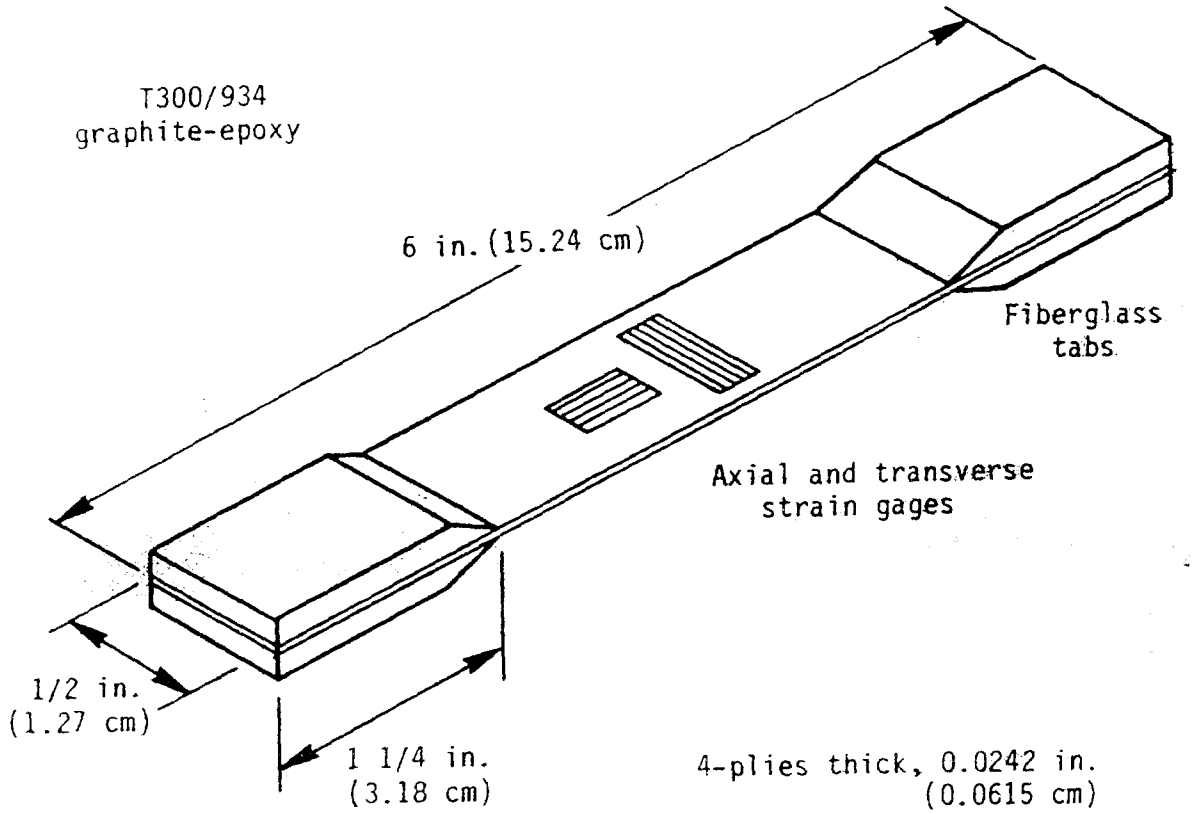

Fig. 14. Diagram of Mechanical Test Specimen.

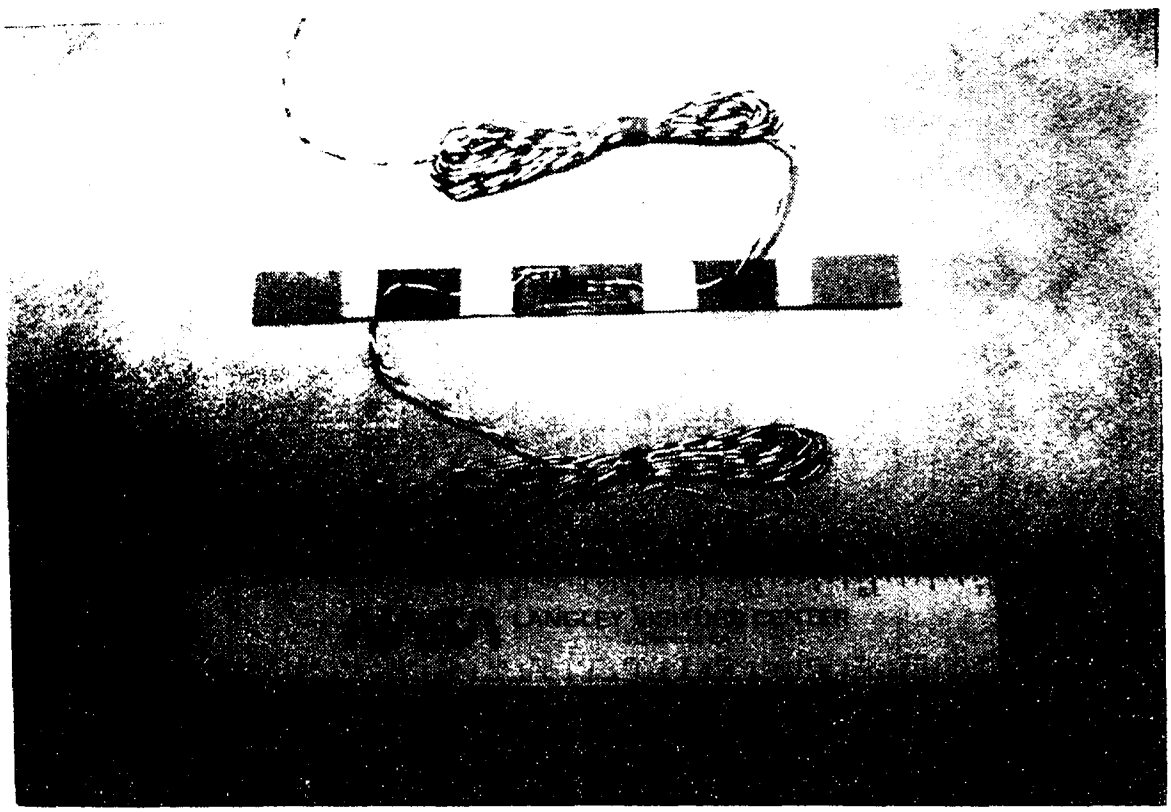

Fig. 15. Photograph of Mechanical Test Specimen.

tored throughout the chamber by thermocouples placed at various locations within the chamber, including one thermocouple attached directly to the test specimen. Tests were conducted at three different temperatures: -250°F (116K), room temperature (304K), and +250°F (394K). Approximately one hour was required to reach both the low and high test temperatures. Soak times of fifteen minutes were used to attain stable conditions.

The environmental chamber is mounted on an Instron testing machine. The mechanical grips, used to pull the composite coupons in tension, fit entirely within the chamber. Load was measured by a resistance load cell located outside of the chamber and isolated from temperature fluctuations. During a test, stress and strain data were automatically and periodically sampled and recorded by a computerized data acquisition system. After each test had been performed, all test data were graphed, tabulated, analyzed, and stored by the computer.

In preparation for a mechanical test, the graphite-epoxy specimens are placed in the mechanical test grips (Fig. 16). These grips are held rigidly in place with C-clamps for alignment purposes. When the mechanical grips are positioned in the Instron test machine, a spacing bar with two C-clamps is used to prevent flexing of the specimen during placement. One C-clamp is removed immediately before a test is to be conducted (Fig. 17). An overall view of the mechanical measurement facility showing the Instron machine fitted with an environmental chamber is shown in Fig. 18. The temperature controls are located on the right-hand side of the tensile machine. The data acquisition equipment is located on the left-hand side.

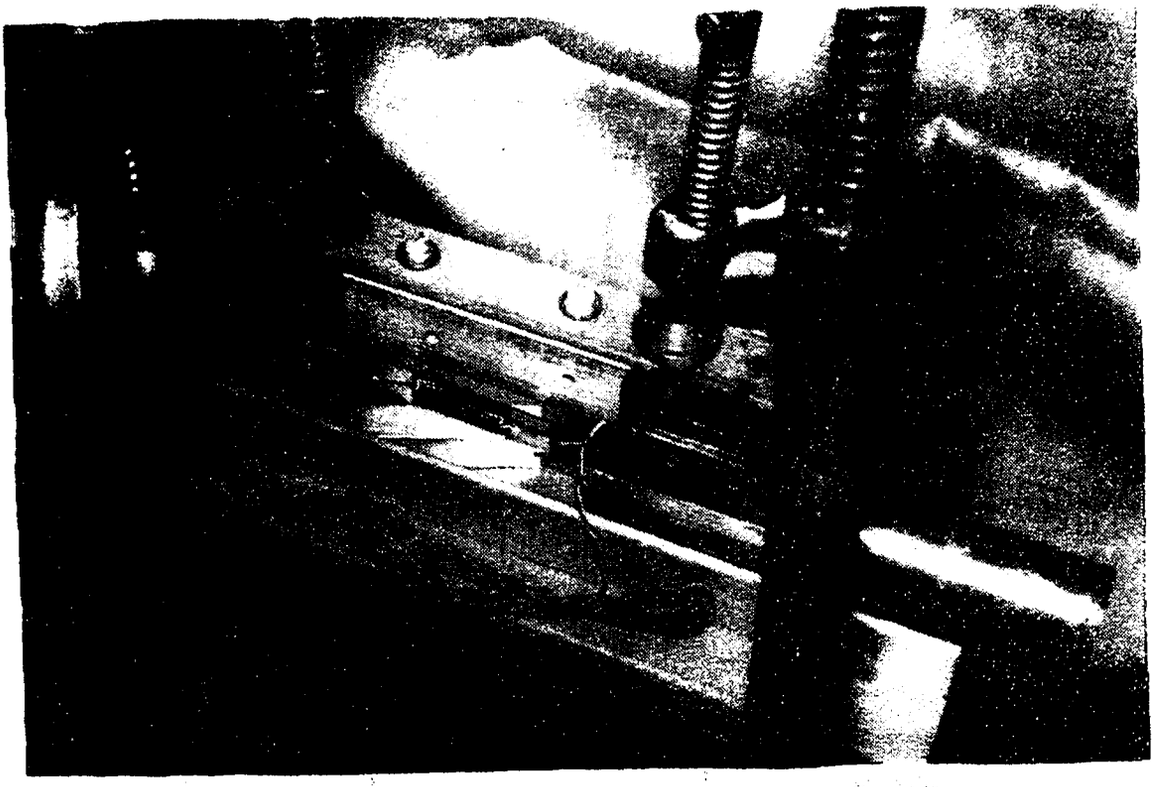

Fig. 16. Photograph of Specimen Mounted in Mechanical Test Grips Showing Alignment Precautions.

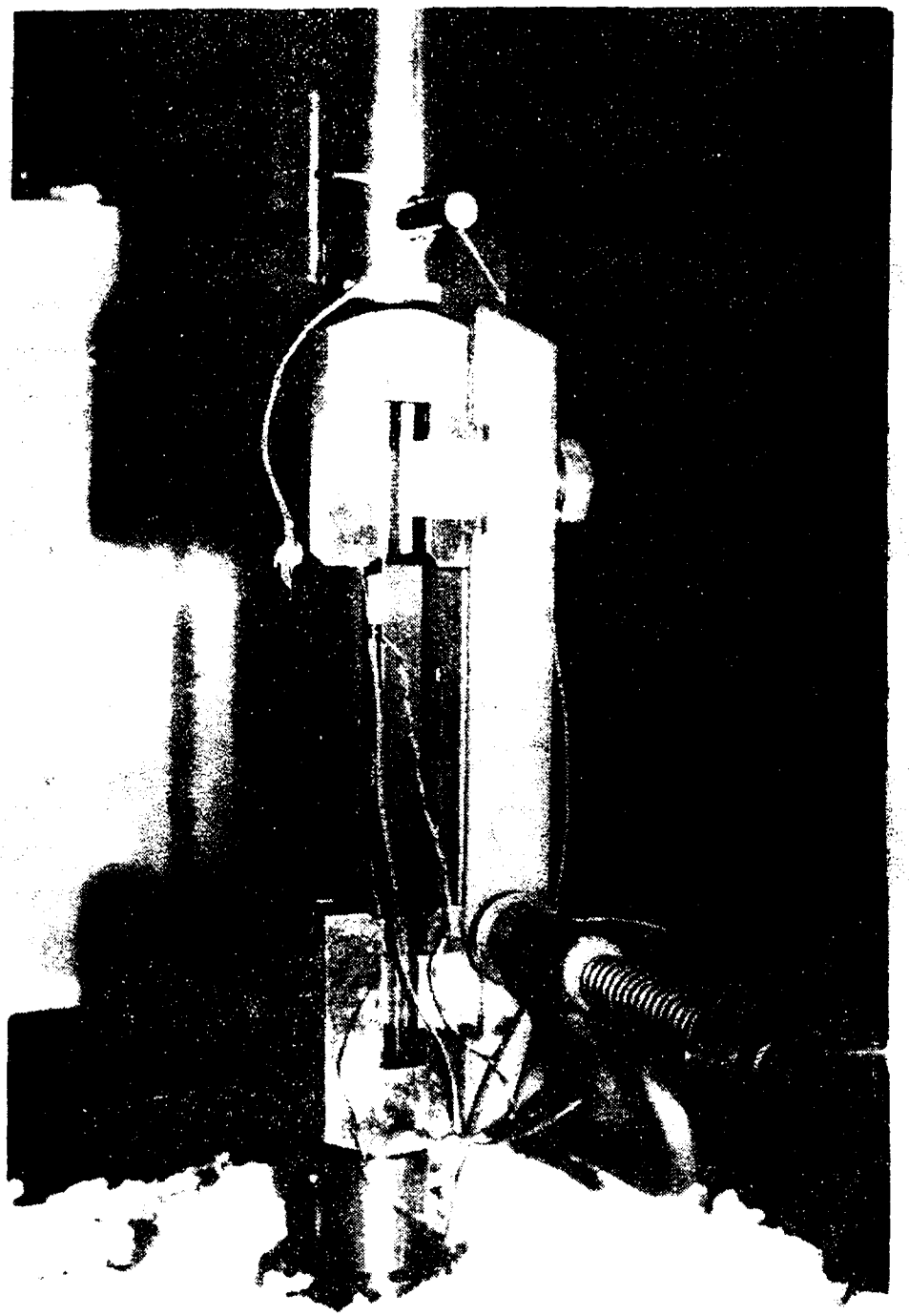

Fig. 17. Photograph of Mechanical Grips Positioned in Tensile Testing Machine.

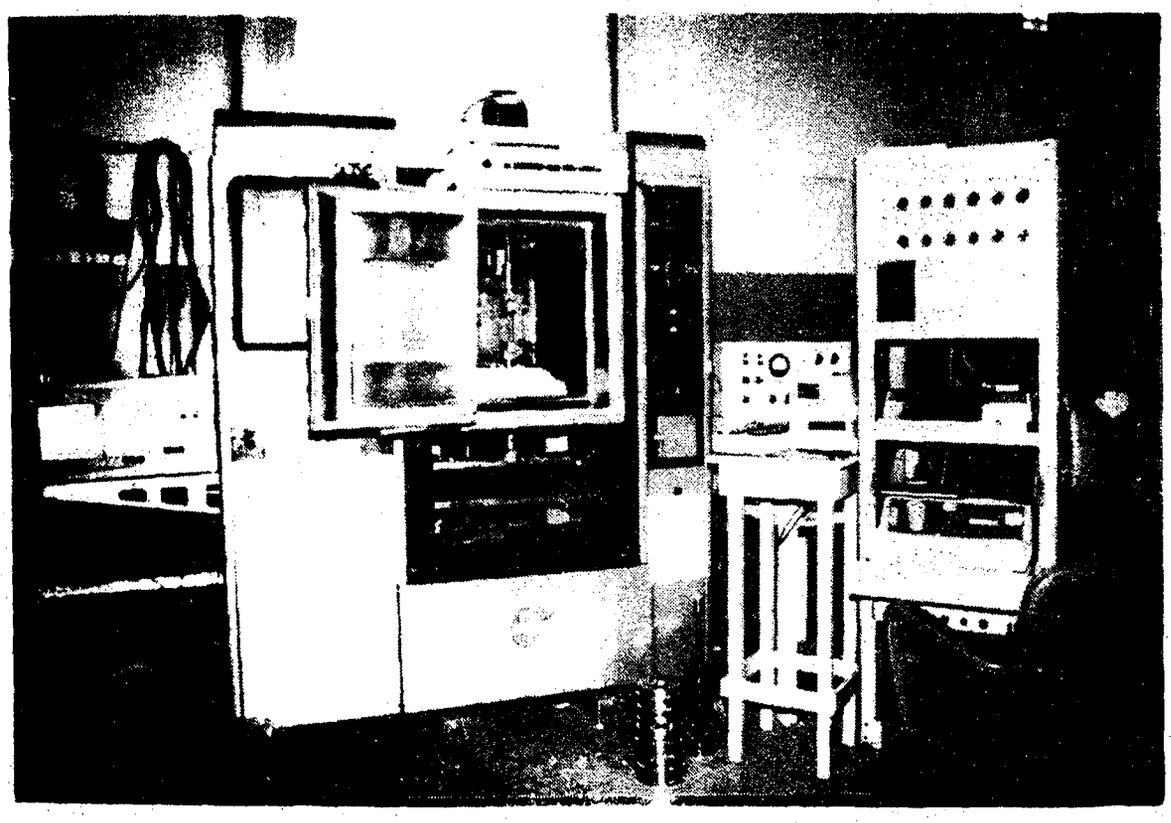

Fig. 18. Photograph of Mechanical Testing Equipment.

3.4 Dynamic-Mechanical Analysis

Although the dynamic-mechanical analysis (DMA) technique has been used for several decades, its recent acceptance has come from the DuPont 981 dynamic-mechanical analyzer [45,46]. With this instrument, a 1.0-inch (2.54 centimeter) by 0.5-inch (1.27 centimeter) sample is clamped between two arms (Fig. 19). One arm is fixed, and the other arm is moveable (Fig. 20). The test specimen and the arms are displaced and set into oscillation by an electromechanical transducer through the moveable arm. By means of a feed-back loop, the sample is made to vibrate at its own natural frequency with a constant amplitude. Then, by comparing the amount of energy required by the moveable arm to maintain the resonant frequency of the sample, the tendency of the sample to convert mechanical energy into heat when stressed is measured. This defines the inherent stiffness of a material as well as its damping characteristics.

With the 981 DMA analyzer, changes in the resonant-frequency of the test material over a very large selectable temperature range (-300°F to +500°F) can be monitored. An overall view of the dynamic-mechanical analyzer is shown in Fig. 21. Damping and the dynamic modulus of elasticity (Eq. 15) are recorded as a function of temperature. From this data, the glass-transition temperature of the polymeric matrix can be calculated. In addition, modulus and damping are plotted as a function of temperature.

The DMA technique is very useful for comparing the temperature dependent characteristics of one polymer with another. In this study, material that has not been irradiated has been characterized in both the

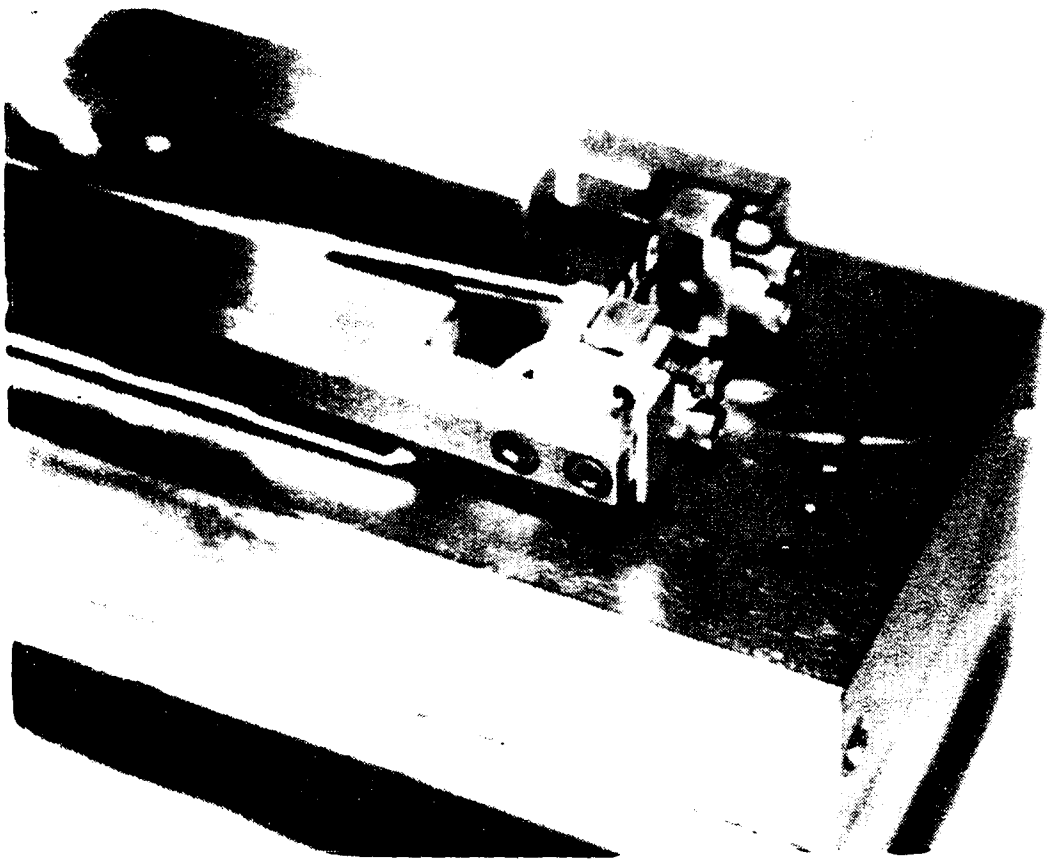

Fig. 19. Photograph of Dynamic-Mechanical Analysis (DMA) Equipment Showing Composite Sample Clamped Between Two Arms.

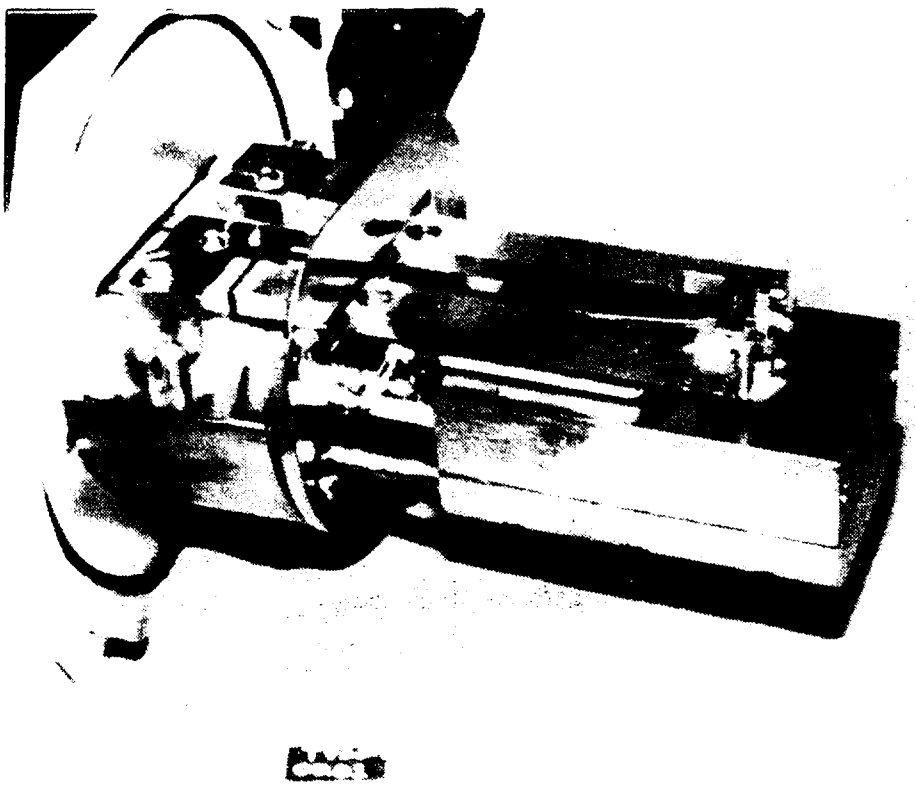

Fig. 20. Photograph of DMA Equipment Showing Moveable and Fixed Arms.

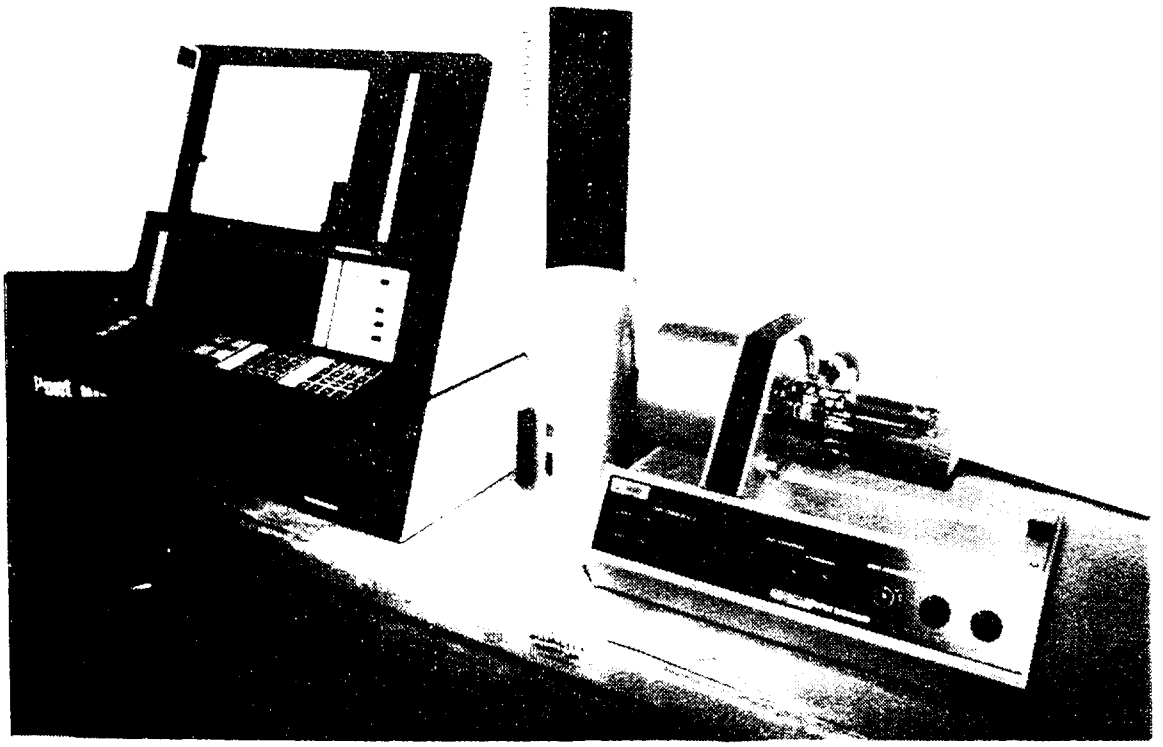

Fig. 21. Overall Photograph of DMA Equipment.

fiber direction and transverse to the fibers. This was accomplished by using both a 0° and a 90° specimen. This data was then compared to data from irradiated material. Radiation induced temperature dependent changes of the graphite-epoxy composite system can be noted.

3.5 Thermomechanical Analysis

Thermomechanical analysis (TMA) can also be used to measure the glass-transition temperature of a polymer or a polymer within a composite. This test will yield information about the softening points, phase transitions, modulus changes, and creep properties of the test specimen. DuPont manufacturers the 942 thermomechanical analyzer to make these measurements [47]. With this instrument, a probe is positioned on the composite sample and loaded with a given load (diagram, Fig. 22 and photograph, Fig. 23). A small 0.25-inch (0.64 centimeter) square sample is placed under a probe with a steel ball of 0.125-inch (0.3175 centimeter) diameter attached to its end. The stress is applied by means of a 15 gram weight positioned at the top of the probe. A record of the penetration of the probe into the sample, by means of a moveable-core linear variable differential transformer (LVDT), is obtained as a function of temperature. Penetration into the sample as well as expansion of the specimen can be recorded with this equipment. From the plot of the displacement of the probe versus temperature, conclusions can be drawn about the softening temperatures of the test material.

In this investigation, both nonirradiated and irradiated graphite-epoxy composites were characterized by this technique. From these data, radiation-induced temperature dependent changes can be noted.

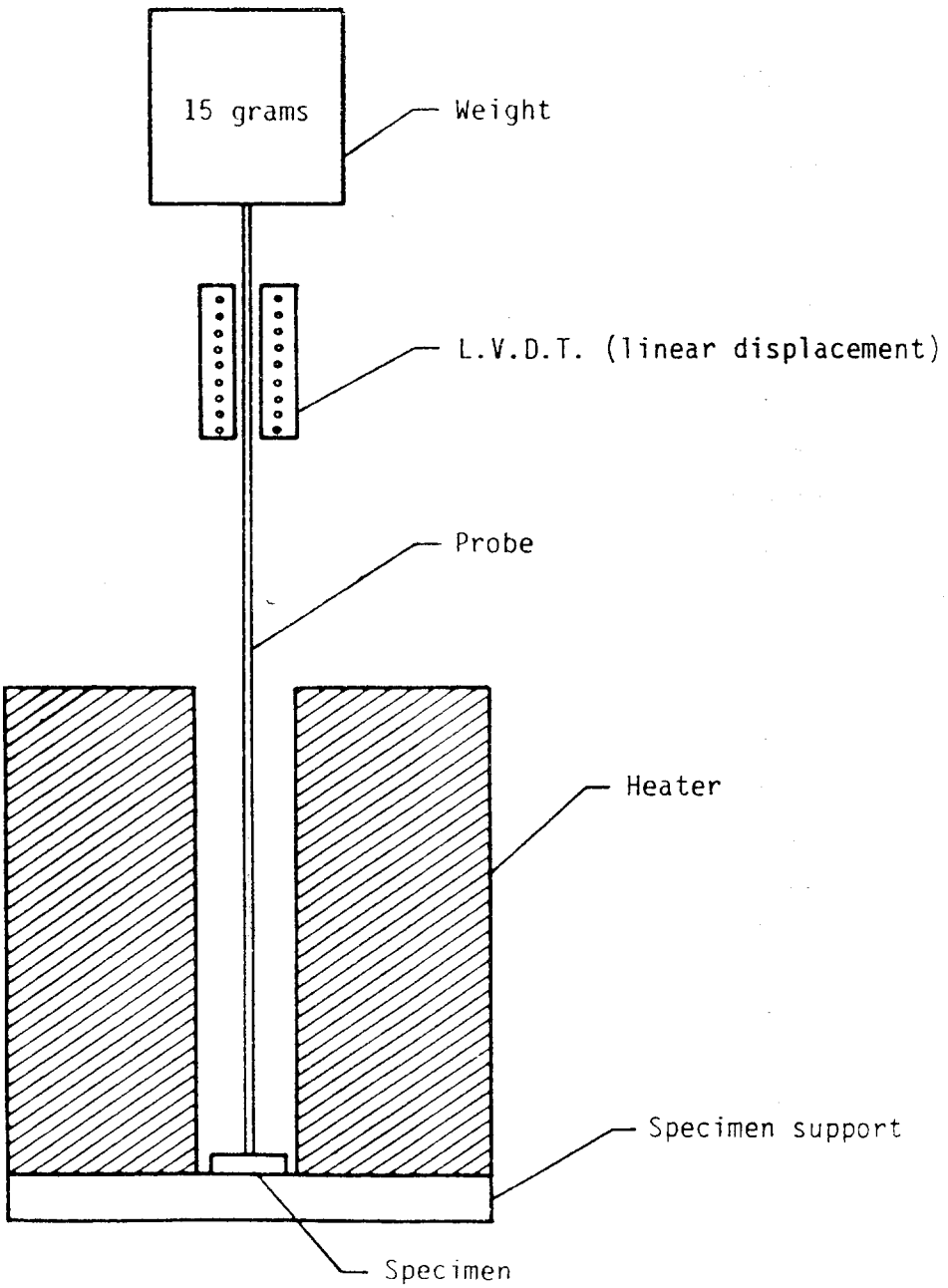

Fig. 22. Illustration of Thermomechanical Analysis (TMA) Test Equipment.

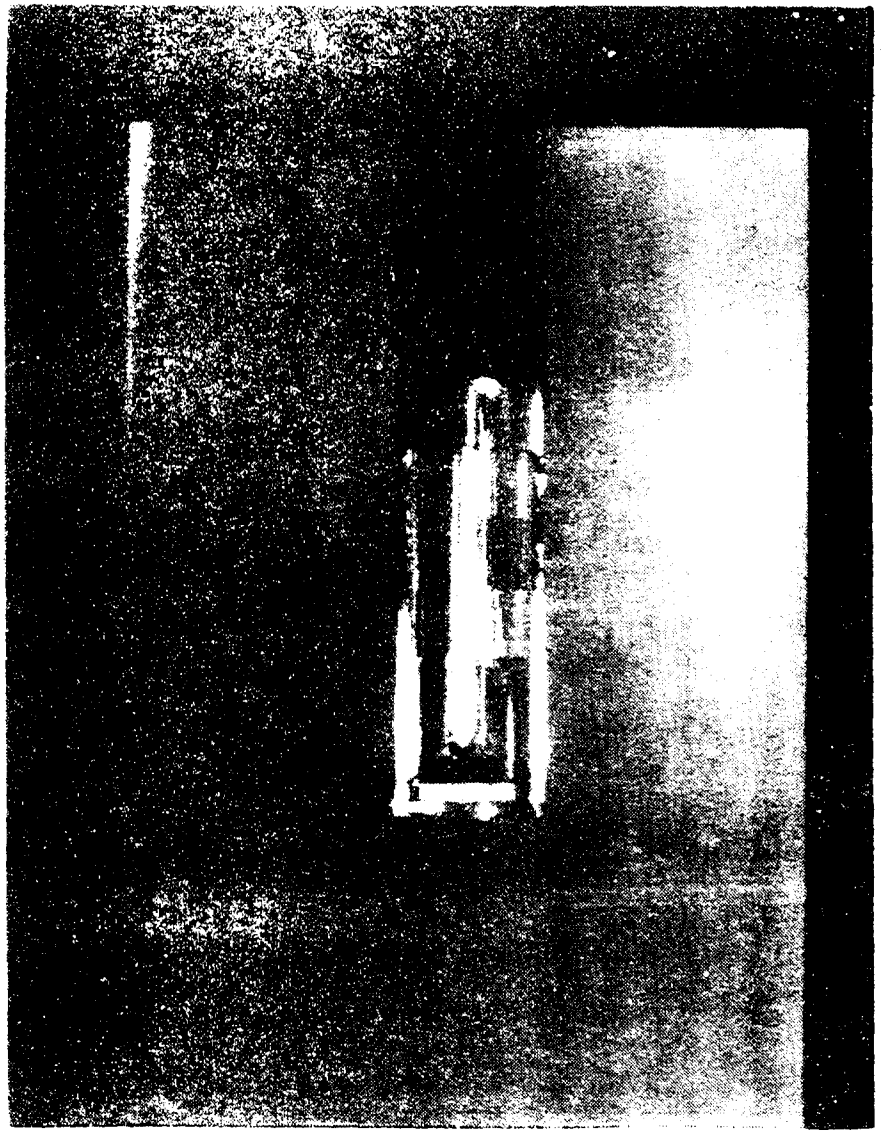

Fig. 23. Photograph of IMA Equipment.

3.6 Degradation Product Chemical Analysis

Results from the dynamic-mechanical analyzer and thermomechanical analyzer (to be presented in a later section), indicate that by irradiating a graphite-epoxy composite, degradation products will be generated due to chain scissioning and crosslink breaking. These degradation products can be identified by using Infrared Analysis and Mass Spectroscopy.

Once degradation products are identified, and by knowing the chemical structure of the original material, the parts of the epoxy macromolecules which are susceptible to electron radiation can be discovered. From this information, it may be possible to predict a degradation mechanism and possibly explain the observed changes in mechanical properties of this graphite-epoxy system.

Degradation products are extracted from the irradiated composite material by boiling a sample of the laminate in acetone. The next step is to let the acetone evaporate, leaving behind a residue consisting of the radiation-induced degradation products. This residue can be placed in an infrared analyzer and/or mass spectrometer to chemically identify its constituents and characterize these irradiation-induced byproducts.

3.7 Thermal Cycling

In an extremely cold environment, large thermal stresses may develop within a composite laminate due to the mismatch in the coefficient of thermal expansion (CTE) of adjacent plies at different orientations [48]. If the inplane normal stress becomes sufficiently large, transverse cracks (microcracking) will result.

Since the graphite-epoxy material used in this study becomes very brittle at low temperatures and very plastic at high temperatures when irradiated (from results to be presented in a later section), its thermally induced microcracking behavior may be altered. Since the transverse modulus of elasticity is significantly increased when irradiated, the inplane normal stresses will be increased and microcracking may occur.

Test specimens, used in this part of the study, were cut from the $[0/90]_S$ panel of T300/934 graphite-epoxy. Samples had a length of 6 inches (15.24 centimeters) and a width of 0.5 inches (1.27) centimeters). Test specimens were ultrasonically C-scanned and examined by optical microscopy, prior to use, to insure no microcracking or delamination was present. The edges of the laminates were polished to aid in optical examination. Prior to thermal cycling, all test laminates were placed in a vacuum drying oven (1.0×10^{-3} torr, 110°F) for a minimum period of two weeks.

The $[0/90]_S$ composite laminates were exposed to each of the following conditions, and checked for microcracking.

1) Baseline (as is)
2) Irradiated (1.0×10^{10} rads).
3) 500 thermal cycles (±250°F).
4) First irradiated then thermally cycled.
5) First thermally cycled then irradiated.

The thermal cycling equipment used for this study was built at the NASA-Langley Research Center and is illustrated in Fig. 24. The apparatus has a hot chamber that is kept at +250°F (394K) and a cold chamber that is kept at -250°F (116K). Specimens are placed in a sliding tray that slides from one chamber to the next and back again. Thermocouples attached to the samples regulate soak times.

In preparation for thermal cycling, the prepolished composite specimens are placed in a stainless steel "bag" as shown in Fig. 25. The "bag" is then welded shut and a vacuum is pumped within the "bag". A stainless steel screen "box" keeps the "bag" from collapsing on the composite laminates. The stainless steel "bag", containing the test specimens, with the vacuum pulled, is shown in Fig. 26. The "bag" is then placed in the sliding tray of the thermal cycling equipment, Fig. 27.

Once the composite laminates have received their appropriate exposure, the polished edges are inspected with the aid of an optical microscope for microcracks. The laminates were also inspected with x-ray equipment.

3.8 Fracture Surface Analysis

A scanning electron microscope (SEM) was used to examine the fracture surfaces of the laminates broken during the mechanical testing phase of this study. Mechanical tests were performed over the temperature range of -250°F (116K) to +250°F (394K) for both the non-irradiated and irradiated conditions. By greatly magnifying the fracture surfaces of these laminates, differences in failure modes were observed. Obser-

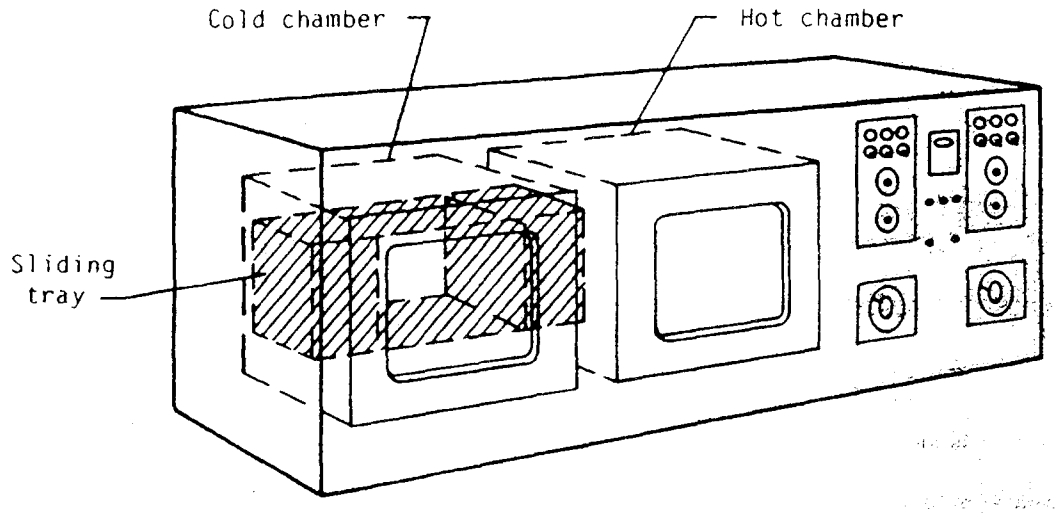

a.) Thermal cycling apparatus

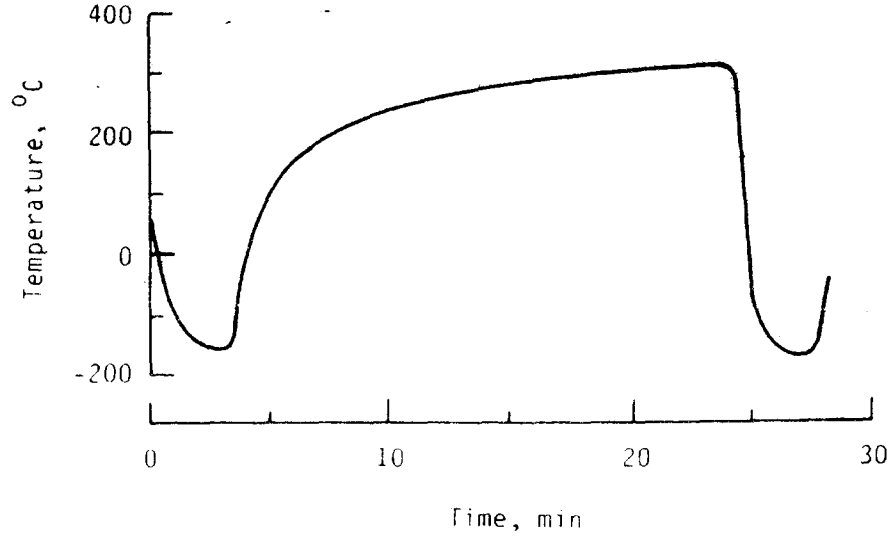

b.) Typical specimen temperature history for one cycle

Fig. 24. Illustration of Thermal Cycling Equipment.

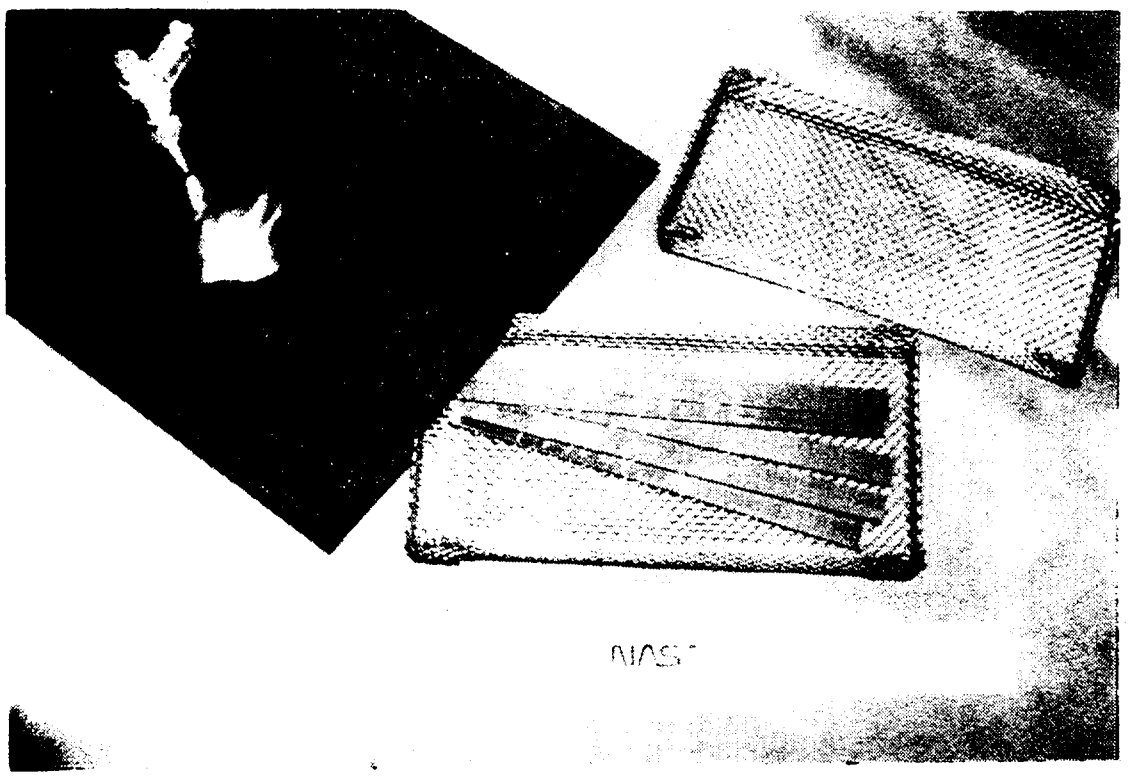

Fig. 25. Photograph of Thermal Cycling Specimens Being Placed in Stainless Steel "Bag".

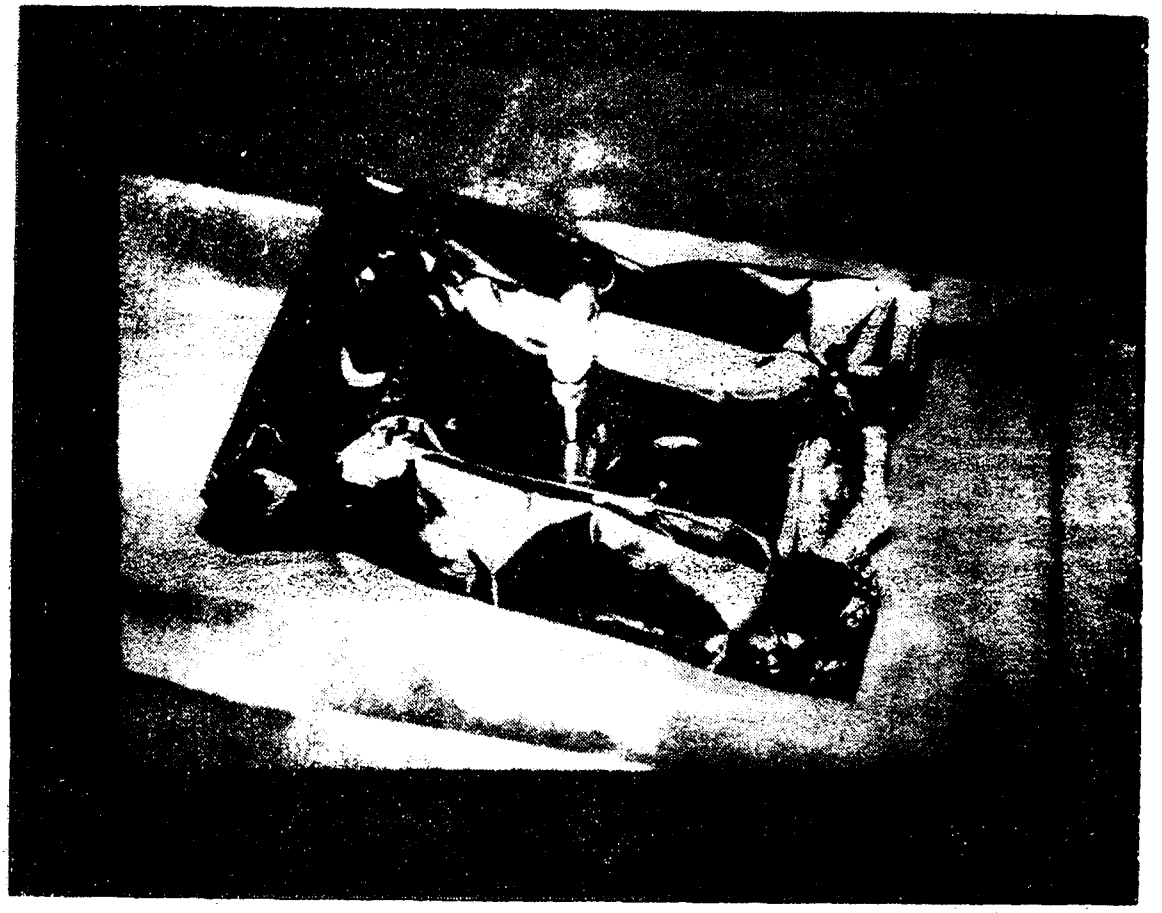

Fig. 26. Photograph of Stainless Steel "Bag" after Vacuum Has Been Pumped.

Fig. 27. Photograph of Thermal Cycling Equipment.

vations of the temperature-dependent behavior of the non-irradiated laminate failures were compared to the irradiated laminate failures. (Note: these laminates cannot actually be observed at the test temperature used.)

SEM inspection was made on the matrix-dominated fracture surfaces of the $[90]_4$ laminate. This laminate fails in pure tension. Observations were also made on the $[10]_4$ laminate which should fail mostly by shear [31]. Inspection of the $[0]_4$ laminates was impossible, since these laminates are almost completely destroyed at failure. Inspection of the $[45]_4$ fracture surface was not deemed appropriate since this laminate fails in a mixed tension and shear mode.

Photographs of the fracture surfaces were taken for both the non-irradiated and irradiated $[90]_4$ and $[10]_4$ laminates at all three test temperatures (-250°F (116K), room temperature, and +250°F (394K)) at magnifications of 375x and 3,400x. All fracture surfaces were coated with gold-palladium prior to SEM inspection.

IV. RESULTS

The results obtained in this investigation into the effects of a space environment on graphite-epoxy composite can be divided into the following three topics:

1) The effect of electron radiation on inplane mechanical properties of the composite as a function of temperature (section 4.1).

2) Characterization of the degrading effect of radiation on the epoxy resin matrix material of the composite (section 4.2).

3) Inspection of the fracture surfaces produced by failure of both non-irradiated and irradiated graphite-epoxy laminates (section 4.3).

4.1 Effect of Radiation on Mechanical Properties

The elastic and strength properties of T300/934 graphite-epoxy are presented first with the non-irradiated laminate data, and then secondly by adding the irradiated data. Figures 28 through 31 are the stress-strain curves (as a function of temperature) for non-irradiated T300/934. The data in Figs. 32 through 35 are the stress-strain curves with the irradiated data added. Results for the non-irradiated elastic properties as a function of temperature are illustrated in Figs. 36 through 42 and with the irradiated data added, Figs. 43 through 49. Non-irradiated strength data is presented in Figs. 50 through 54 and with the irradiated data added, Figs. 55 through 59. All test data are tabulated in Tables 6 through 8. Bar charts of temperature-dependent

changes (compared to room temperature) in mechanical properties for both non-irradiated and irradiated laminates is shown in Figs. 60 and 61. A bar chart of radiation-induced changes in mechanical properties as a function of temperature is shown in Fig. 62. Polynomial regression coefficients are listed in Tables 9 through 11. Individual test results are tabulated in the appendix (Tables A1 through A4).

4.1.1 Stress-Strain Curves

The data presented in Figs. 28 and 32 show that the stress-strain behavior is nearly linear for both the non-irradiated and irradiated 0°-material at all test temperatures. The 0°-material does exhibit a stiffening behavior at high strains, as expected, for all temperatures [34]. Very little temperature dependence is noted (Fig. 28). Electron irradiation tends to increase slightly the modulus at all test temperatures (Fig. 32).

Axial stress-strain behavior for the other laminates is roughly linear at low and room temperatures for both the non-irradiated and irradiated cases (Figs. 29-31, 33-35). At -250°F (116K), the stress-strain curves are essentially linear. As the test temperature is increased, the elastic modulus decreases and the degree of nonlinearity increases. Significant nonlinearity is noted in the behavior of the non-irradiated laminates at the elevated temperature (Figs. 29-31). This behavior is as expected in view of the known influence of temperature on the response of the epoxy matrix material. Extreme nonlinearity is noted for the irradiated material at +250°F (394K) (Figs. 33-35). This behavior is largest for the $[10]_4$ and $[45]_4$ laminates.

Radiation greatly increases the plasticity of the epoxy matrix material at elevated tempertures, but not significantly at lower temperatures. This plasticity is attributed to the epoxy because it is known that the fibers exhibit linear behavior and further because the nonlinearity is more pronounced in matrix dominated behavior with high shear. Furthermore, graphite fibers are thought by most researchers to be inert under radiation because of studies performed on carbon control rods that are used in nuclear reactors.

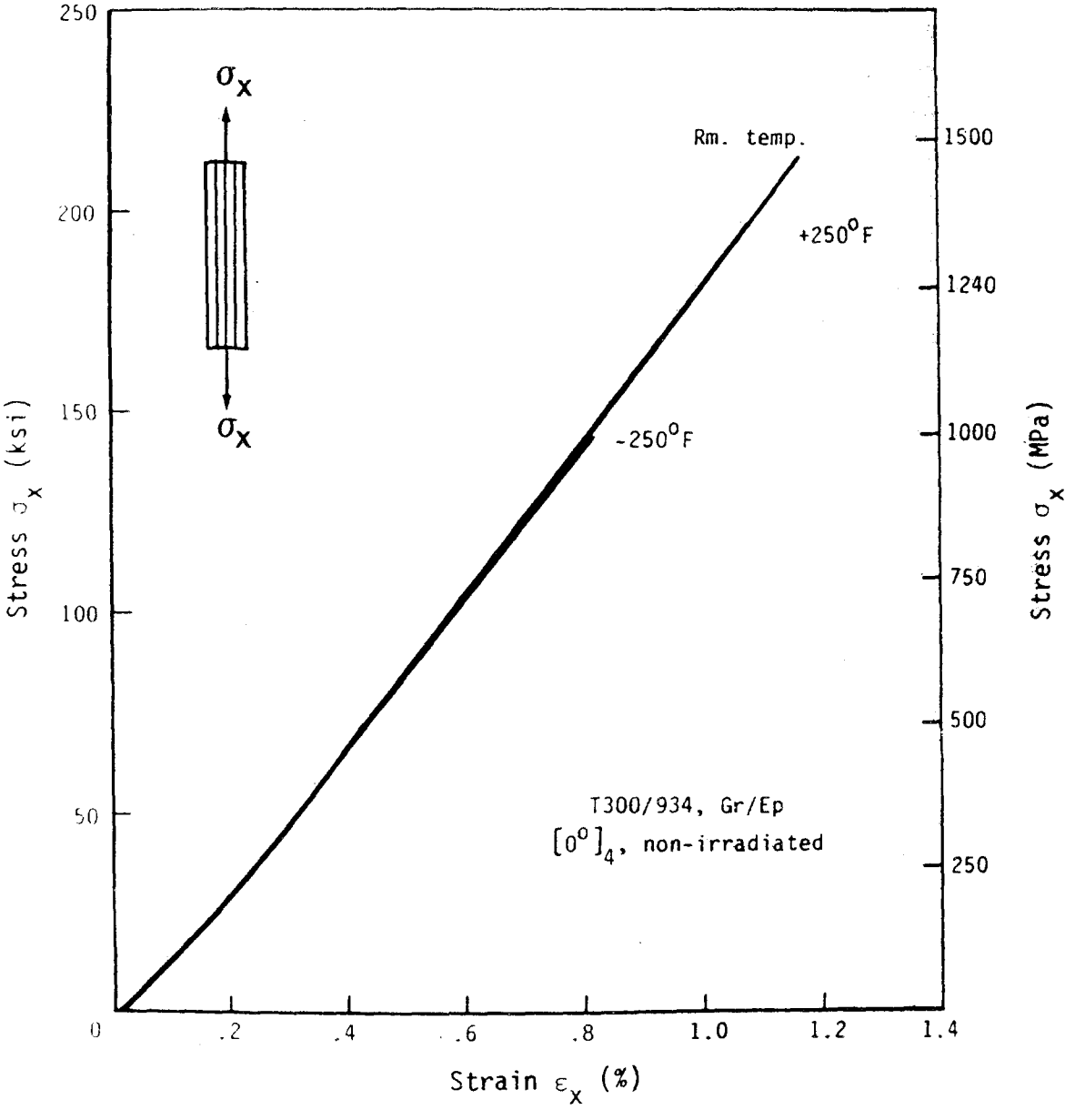

Fig. 28. **Non-Irradiated Stress-Strain Curves for the $[0]_4$ Laminate as a Function of Temperature.**

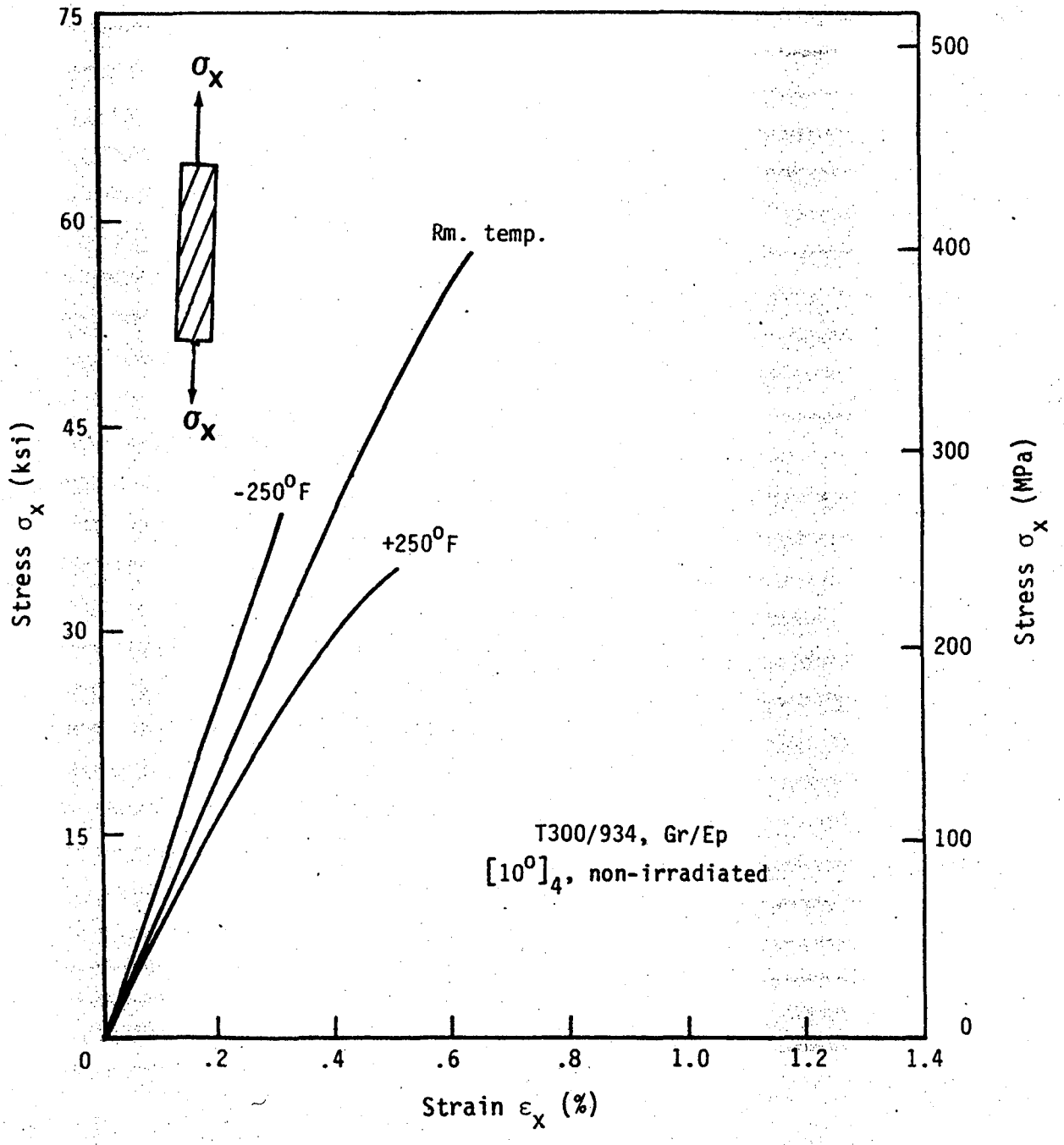

Fig. 29. Non-Irradiated Stress-Strain Curves for the $[10]_4$ Laminate as a Function of Temperature.

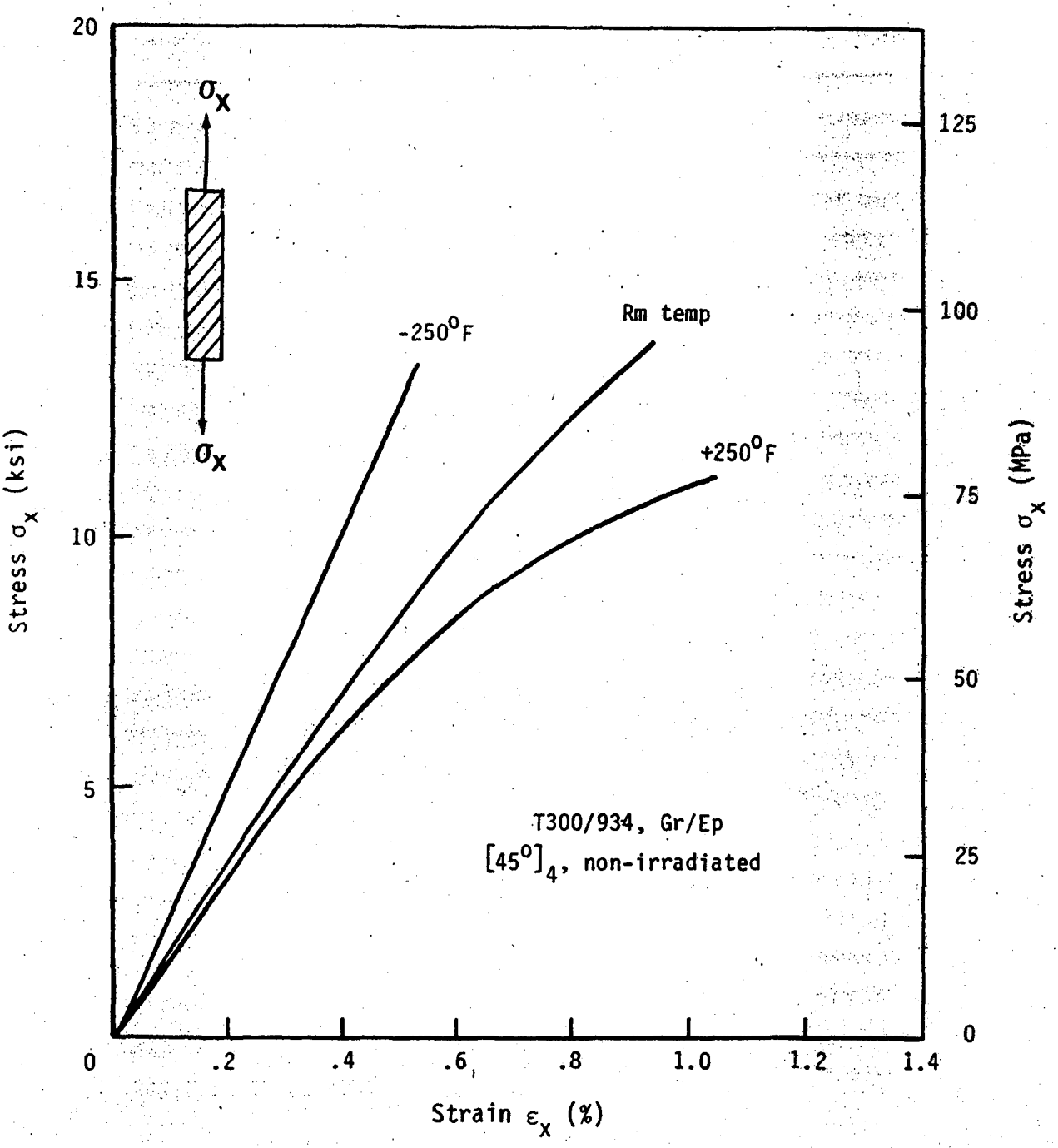

Fig. 30. Non-Irradiated Stress-Strain Curves for the $[45]_4$ Laminate as a Function of Temperature.

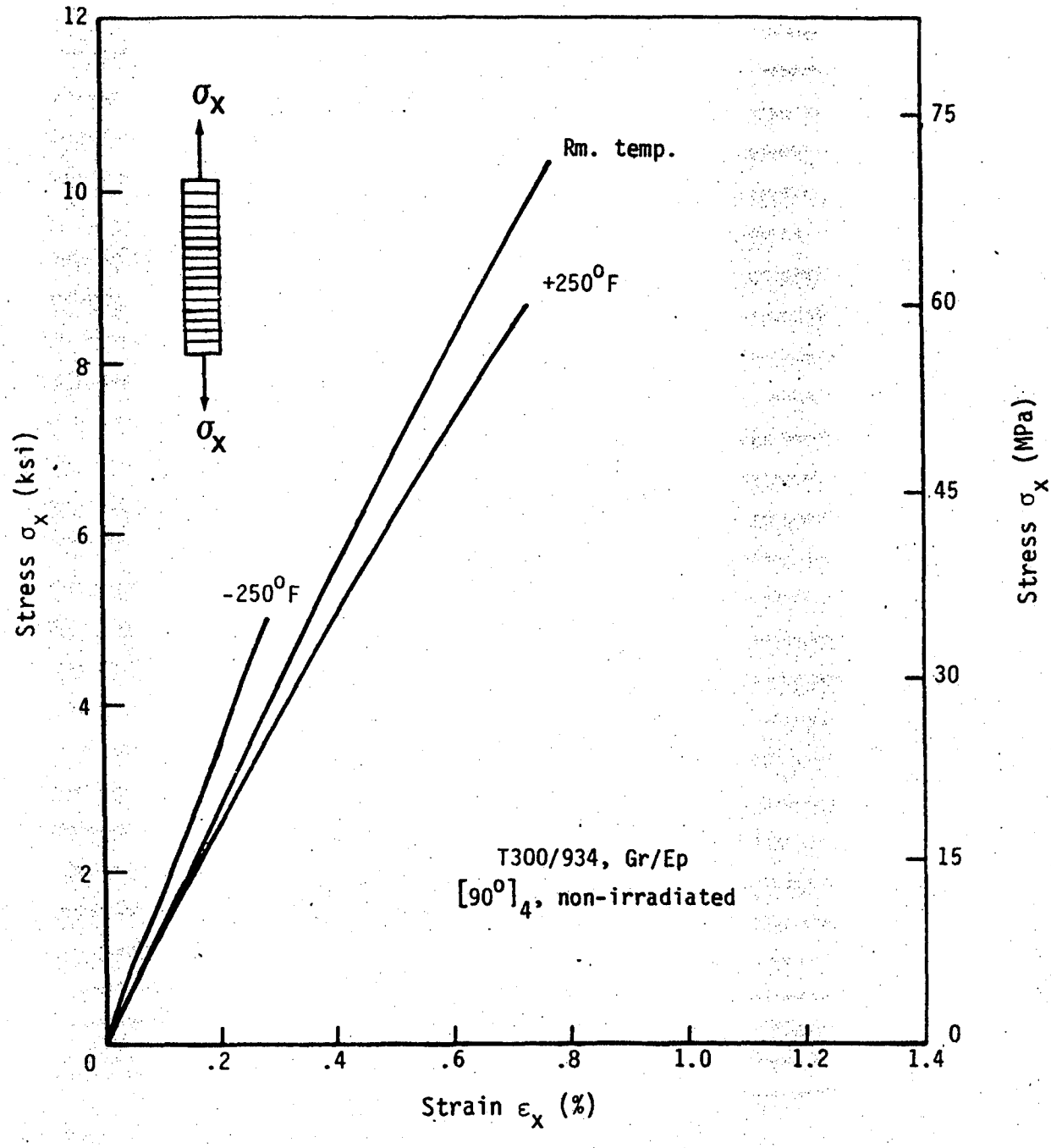

Fig. 31. Non-Irradiated Stress-Strain Curves for the $[90]_4$ Laminate as a Function of Temperature.

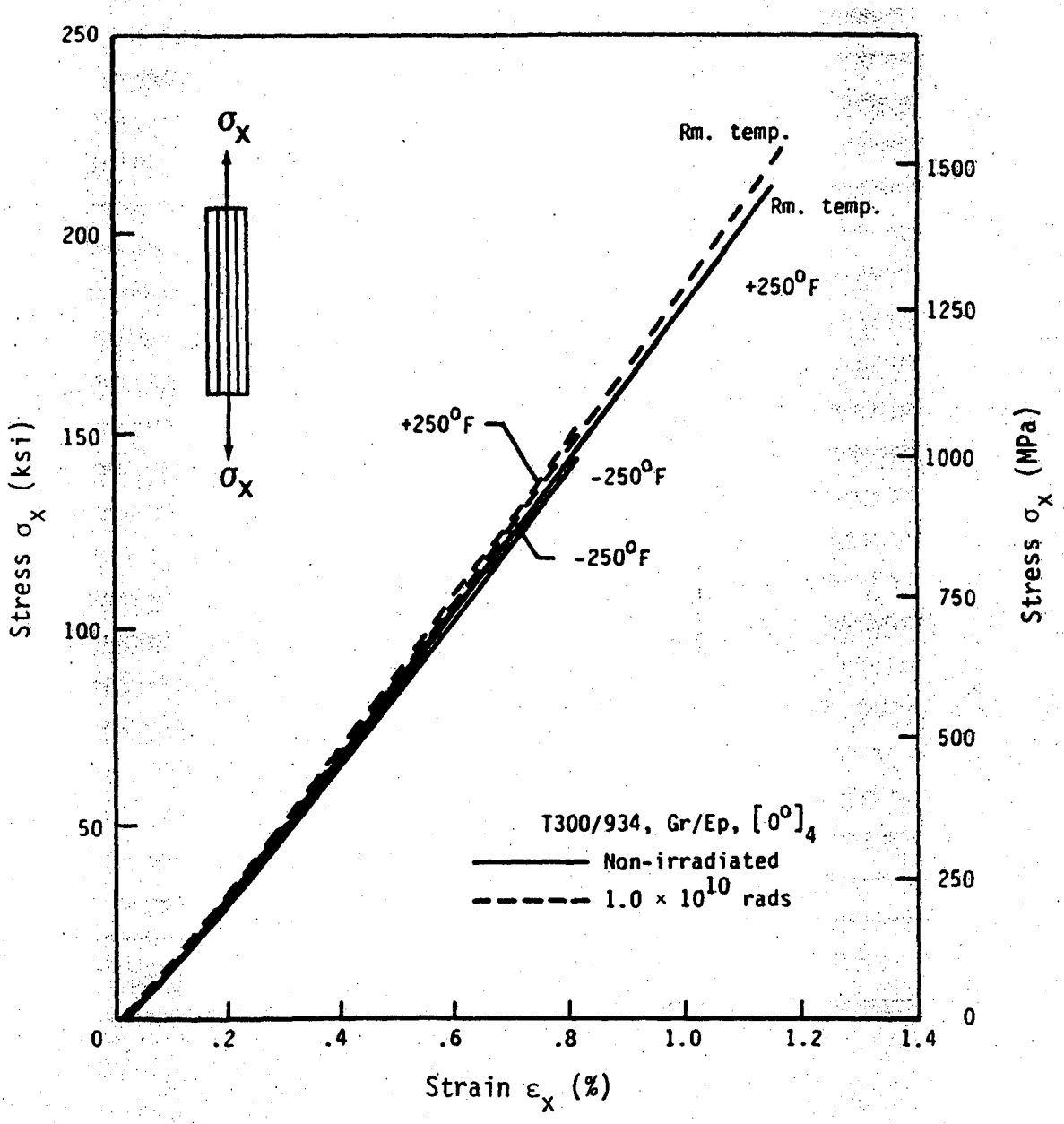

Fig. 32. Non-Irradiated Stress-Strain Curves Compared to Irradiated Stress-Strain Curves for the $[0]_4$ Laminate as a Function of Temperature.

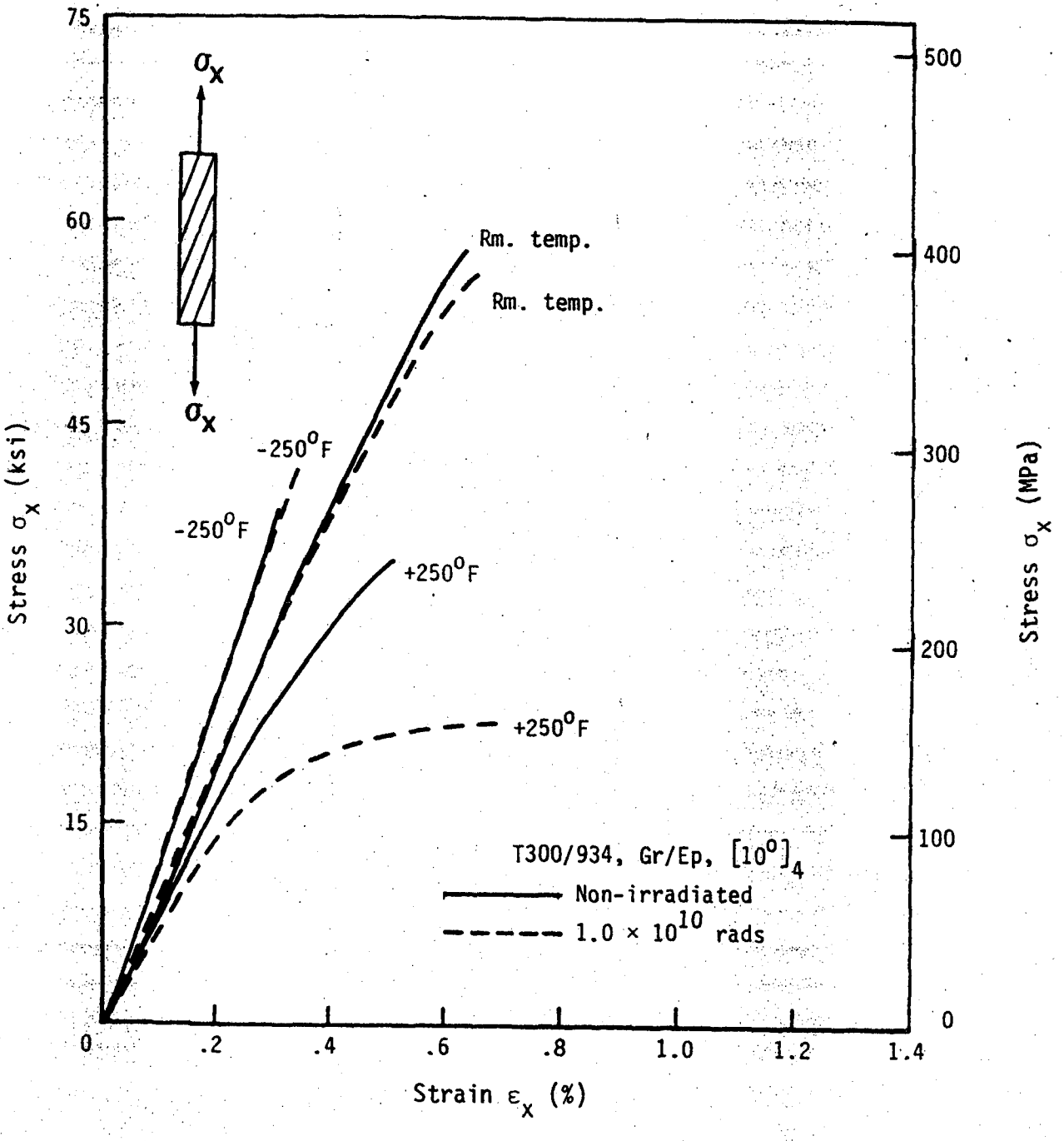

Fig. 33. Non-Irradiated Stress-Strain Curves Compared to Irradiated Stress-Strain Curves for the $[10]_4$ Laminate as a Function of Temperature.

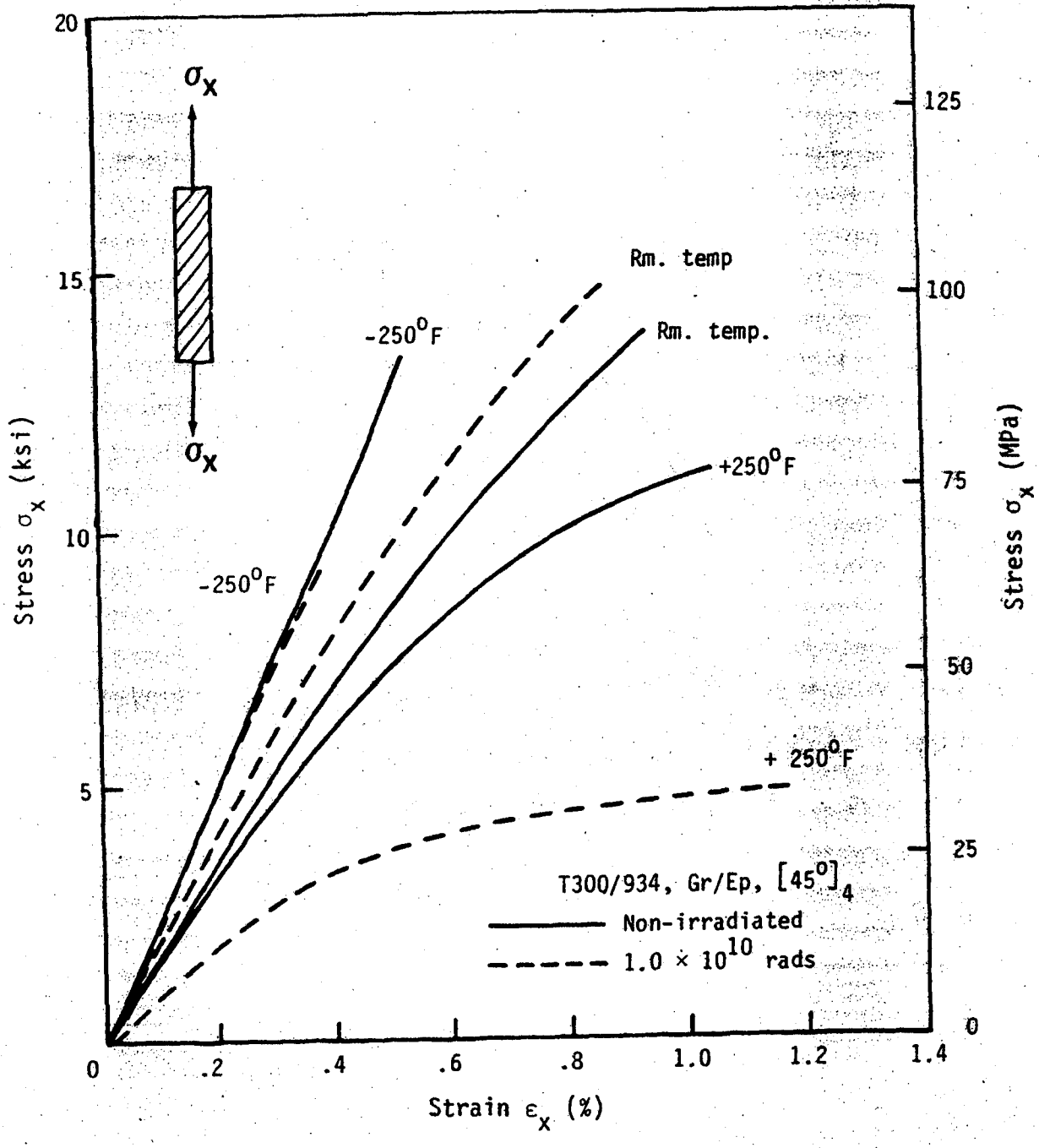

Fig. 34. Non-Irradiated Stress-Strain Curves Compared to Irradiated Stress-Strain Curves for the $[45]_4$ Laminate as a Function of Temperature.

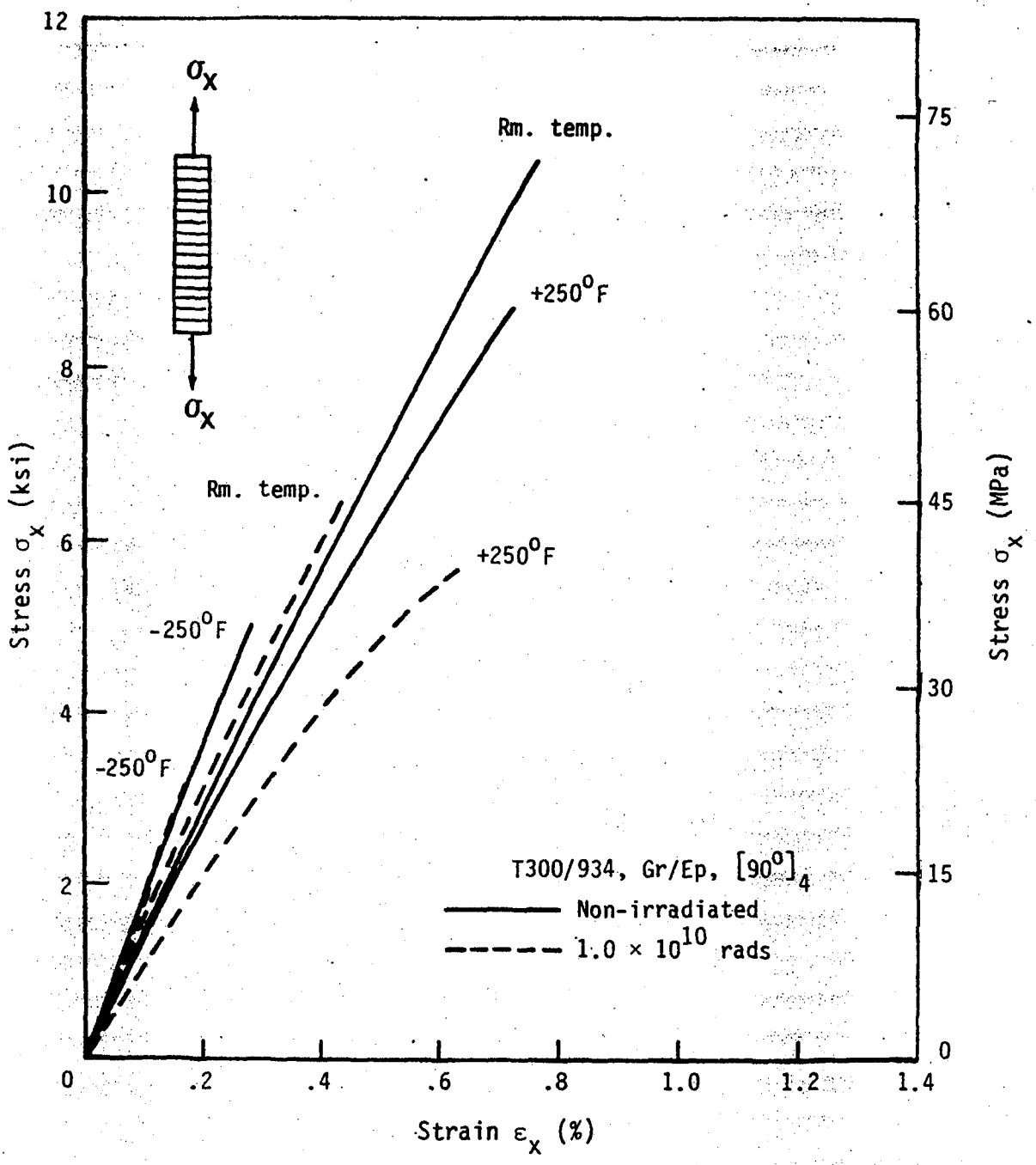

Fig. 35. Non-Irradiated Stress-Strain Curves Compared to Irradiated Stress-Strain Curves for the $[90]_4$ Laminate as a Function of Temperature.

4.1.2 Elastic Properties

0°-Laminate: E_1. The experimental results for the elastic modulus, E_1, are plotted as a function of temperature for the non-irradiated material in Fig. 36 and for the irradiated material in Fig. 43. For the non-irradiated material, the modulus is 2 to 3 percent higher at the elevated temperature and roughly unchanged at the low temperature, as compared to that measured at room temperature (Fig. 36). For the irradiated material, the modulus is only 4 to 5 percent higher at the elevated temperature, and again almost unchanged at the lower temperature (Fig. 43). There is more scatter in the data for the irradiated material. Over the entire temperature range, the irradiated material has a higher modulus of elasticity than the non-irradiated material (Fig. 43). This increase is from 2 to 4 percent.

Since fiber properties are independent of temperature (over this range), the temperature dependence observed here is a function of the changing matrix properties, fiber waviness, and residual stresses [42, 43]. The higher modulus at the elevated temperature is believed to be due primarily to reduced residual stresses which result in lower matrix stresses. Lower stresses in the matrix results in a higher modulus of the composite due to the absence of nonlinear matrix behavior and fiber waviness [35-41].

Since, in all cases, the modulus of the irradiated material is higher than that of the non-irradiated material, it appears that the irradiated material has lower residual stresses and, consequently, straighter fibers than the non-irradiated material. We can conclude

here that electron irradiation acts to reduce residual stresses in the epoxy matrix resulting in somewhat higher modulus.

10°-Laminate. Results for the axial modulus of the $[10]_4$ laminate are shown in Fig. 37. The modulus of this laminate exhibits a linear temperature dependence, with larger values of stiffness at lower temperatures. Modulus values are 22 percent higher at -250°F (116K) and 22 percent lower at +250°F (394K), when compared to room temperature.

Data taken from irradiated laminates are added in Fig. 44. At all temperatures, the moduli from the irradiated material are lower than those taken from the non-irradiated material. These values range from 7 percent lower at the low test temperature to 26 percent lower at the high test temperature.

Note that the 10°-off axis specimen was chosen to measure shear strength only, these results have been included for the sake of completeness.

45°-Laminate. Fig. 38 presents the axial modulus of the $[45]_4$ laminate as a function of temperature. A linear dependence is noted, with larger values of modulus occurring at lower temperatures. Stiffness values are 55 percent higher at -250°F (116K) and 15 percent lower at +250°F (394K), when compared to room temperature.

Data for the irradiated laminates are added in Fig. 45. At low temperatures, the moduli from the irradiated material are larger than those from the non-irradiated material. At high temperatures, these values are smaller. A three-percent increase over non-irradiated data is noted at the low test temperature, and a 25-percent decrease is noted at high test temperatures.

Again, note that the 45°-off axis specimen was chosen primarily for shear modulus measurements. These results have been included for the sake of completeness.

90°-Laminate: E_2. The results for the transverse modulus, E_2, for the non-irradiated material, indicate that there is a 33 percent increase at the low temperature and a 10-percent decrease at the high temperature (as compared to room temperature, Fig. 39). The epoxy matrix material is stiffer at the low temperatures and softer at high temperatures. Epoxies are known to exhibit this type of behavior. The irradiated case shows a 40-percent increase at the low test temperature and a 30-percent decrease at the high temperature (Fig. 46). Also, at room temperature, the irradiated modulus is already 10 percent higher than the non-irradiated modulus. This places the irradiated material data higher than the non-irradiated data at the low test temperatures, but lower than the non-irradiated material at the elevated temperature (Fig. 46).

A lower transverse modulus at the elevated temperature for the irradiated case as compared with the non-irradiated material is consistent with the increased plasticity noted in the stress-strain curves. Upon irradiation, the elastic modulus decreases and the degree of nonlinearity increases at the elevated temperature. The behavior of the transverse modulus at the low test temperature is not as easily explained (irradiated compared to non-irradiated). Some other effect must be occurring that can not be identified at this time. Also note here that residual stresses do not play as large a role in affect-

ing transverse modulus as compared to their influence in the fiber direction.

Shear Modulus, G_{12}. Figure 40 shows that the shear modulus of the non-irradiated material is 70 percent higher at the low temperature and 18 percent lower at high temperature, as compared to room temperature. This is consistent with the epoxy's behavior as shown in previous results. For the irradiated material, the shear modulus is 45 percent higher at the low test temperature and 49 percent lower at the elevated temperature (as compared to room temperature, Fig. 47). Over the entire temperature range, the shear modulus for the irradiated case is equal to or lower than that measured for the non-irradiated material (Fig. 47). The data range from roughly equal at the lower temperature to 30 percent lower at the higher temperature (irradiated compared to non-irradiated).

These data indicate that shear behavior of a laminate is mainly influenced by the plastic behavior of that laminate. At high temperatures, where the irradiated material becomes much more plastic than the non-irradiated material, the shear modulus decreases. At lower temperatures, where no plastic behavior is observed in either the non-irradiated or irradiated laminates, the shear modulus is the same for both non-irradiated and irradiated materials.

Poisson's Ratio: ν_{12}. Poisson's ratio ν_{12} was measured during the 0°-material test by taking the ratio of the strain measured by the transverse strain-gage to that measured by the axial gage. These results for the non-irradiated case show that Poisson's ratio remains roughly the same at low temperatures, as compared to room temperature, but increases by about 10 percent at the elevated test temperature

(Fig. 41). This increase at higher temperatures is consistent with the increase in plasticity at higher temperatures noted in the stress-strain behavior. The irradiated data exhibits a 40-percent increase in Poisson's ratio at the elevated temperature, but also a 30-percent increase at the low temperature as well (as compared to room temperature, Fig. 48). Poisson's ratio for the irradiated material is higher than the non-irradiated material at both high and low temperatures, but lower at room temperature (Fig. 48).

The large increase in Poisson's ratio for the irradiated data at elevated temperatures is consistent with the extreme amounts of plasticity noted at this temperature in the stress-strain curves. However, the reason for the increase in Poisson's ratio at the low temperature for this material is not immediately apparent.

The fact that Poisson's ratio for the irradiated material is lower than that for the non-irradiated material at room temperature may be attributed to reduced residual stresses in the irradiated 0° laminate. Lower residual stresses result in straighter fibers. Straighter fibers give rise to a decreased Poisson's ratio, ν_{12} [34].

Poisson's Ratio: ν_{21}. Poisson's ratio ν_{21} was calculated from E_1, E_2, and ν_{12} using eq. 16. The calculated values for the non-irradiated data are plotted in Fig. 42. There is no change between room and elevated temperatures, but a 34-percent increase is noted at the low temperature. The modulus ratio, E_2/E_1, is larger at the low temperature compared to the room temperature ratio and ν_{12} is constant. Thus, a higher ν_{21} at the low temperature would be expected. The modulus ratio,

E_2/E_1, is smaller at high temperature compared to the room temperature value, and ν_{12} is larger. Thus, ν_{21} does not significantly change.

The calculated values for the irradiated data are shown in Fig. 49. There is no change between room and elevated temperatures, but an 84-percent increase is noted at the low temperature. No difference is seen between irradiated and non-irradiated material at room and elevated temperatures. Poisson's ratio, ν_{21}, is calculated to be larger at the low temperature for the irradiated data as compared to the non-irradiated data.

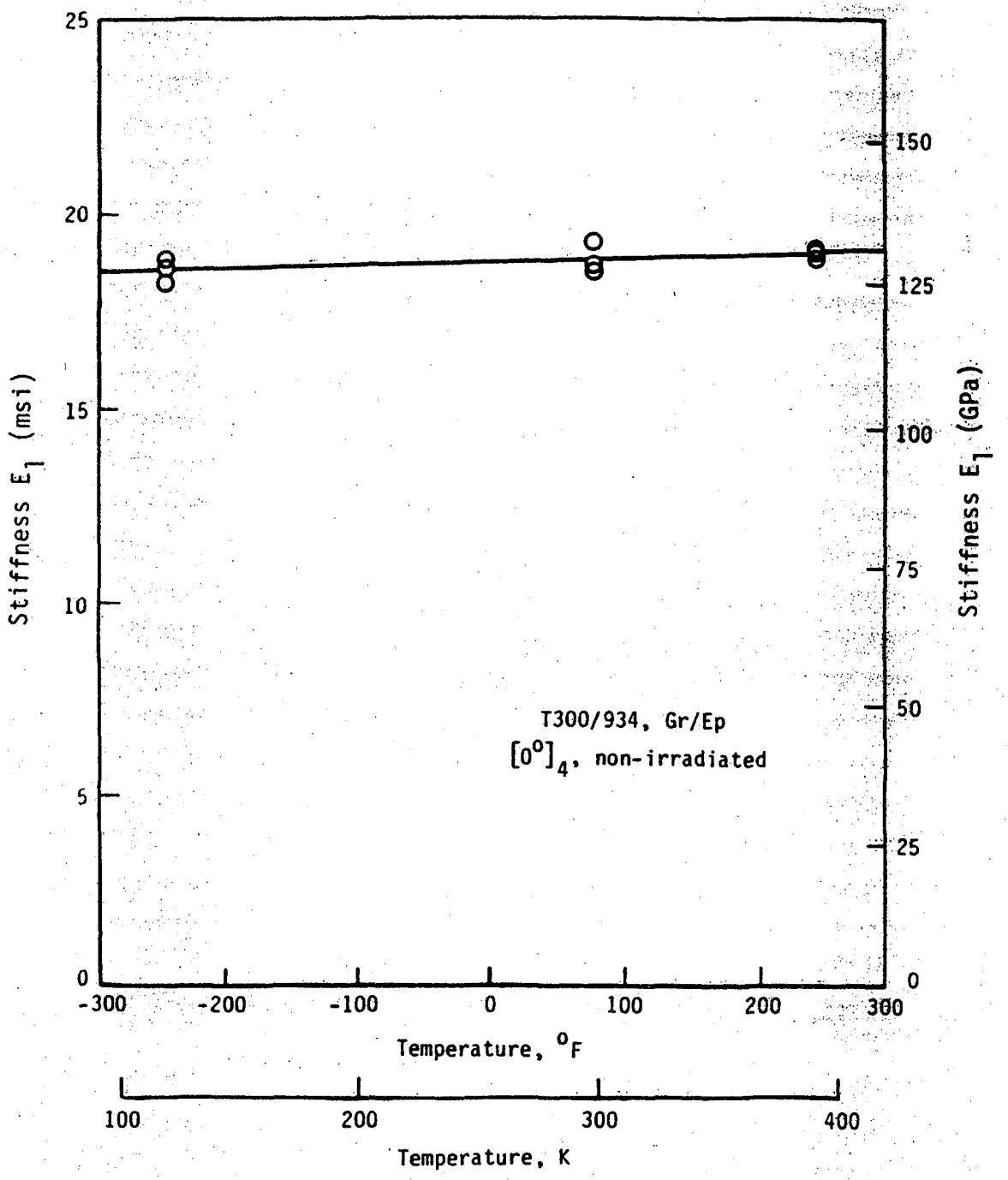

Fig. 36. Non-Irradiated Modulus of Elasticity, E_1, as a Function of Temperature.

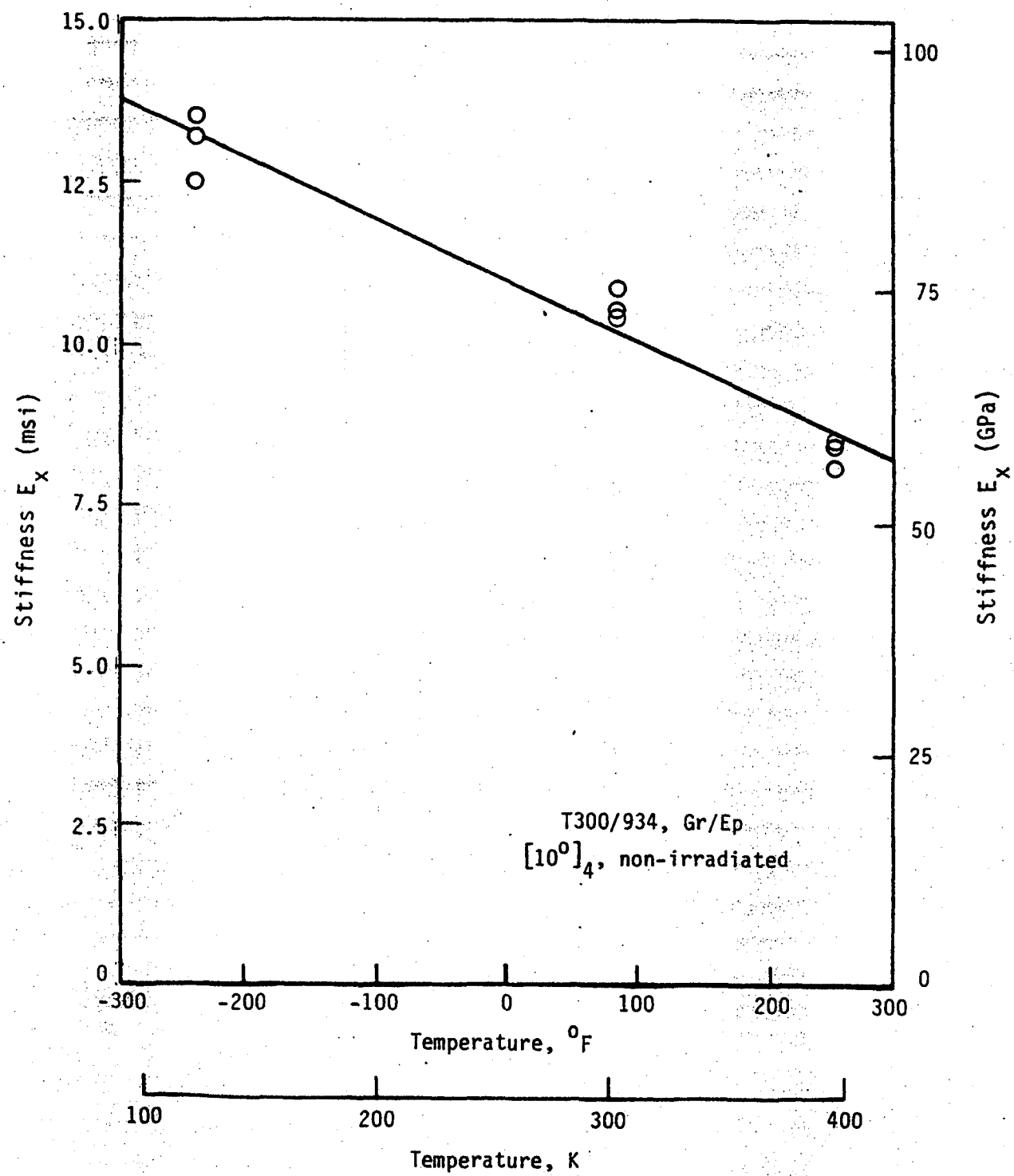

Fig. 37. Non-Irradiated Axial Modulus of the $[10]_4$ Laminate as a Function of Temperature.

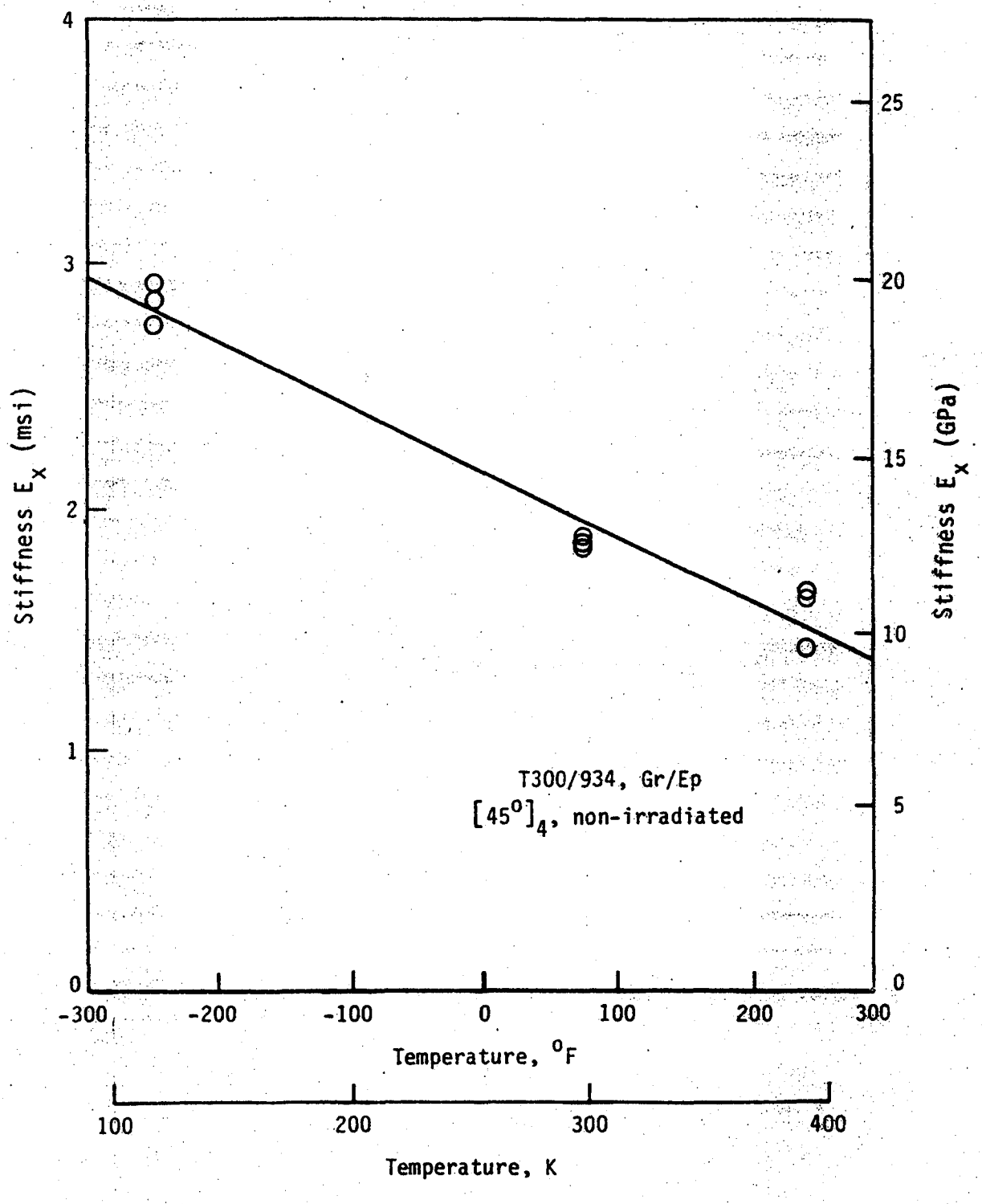

Fig. 38. **Non-Irradiated Axial Modulus of the $[45]_4$ Laminate as a Function of Temperature.**

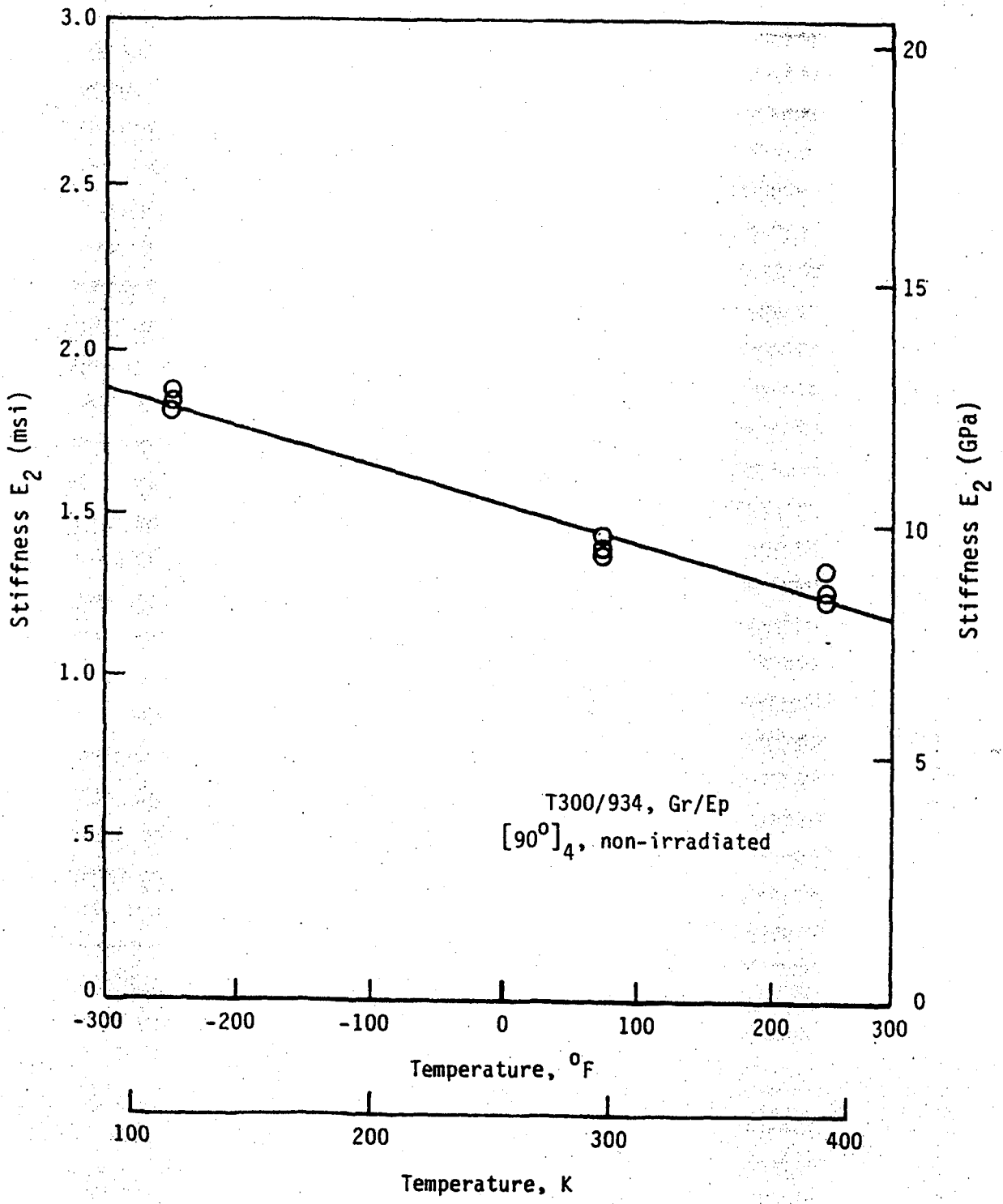

Fig. 39. Non-Irradiated Modulus of Elasticity, E_2, as a Function of Temperature.

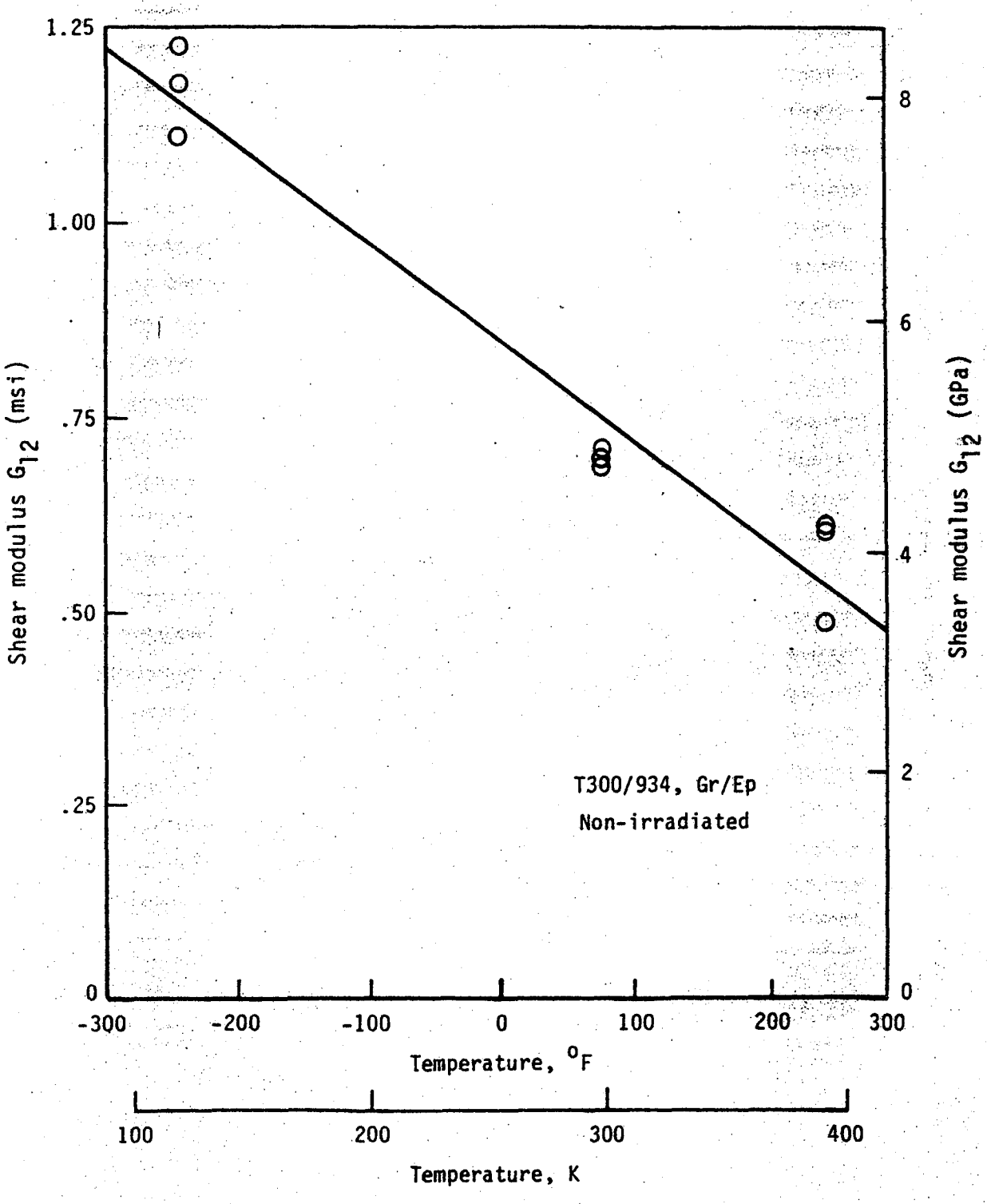

Fig. 40. Non-Irradiated Shear Modulus, G_{12}, as a Function of Temperature.

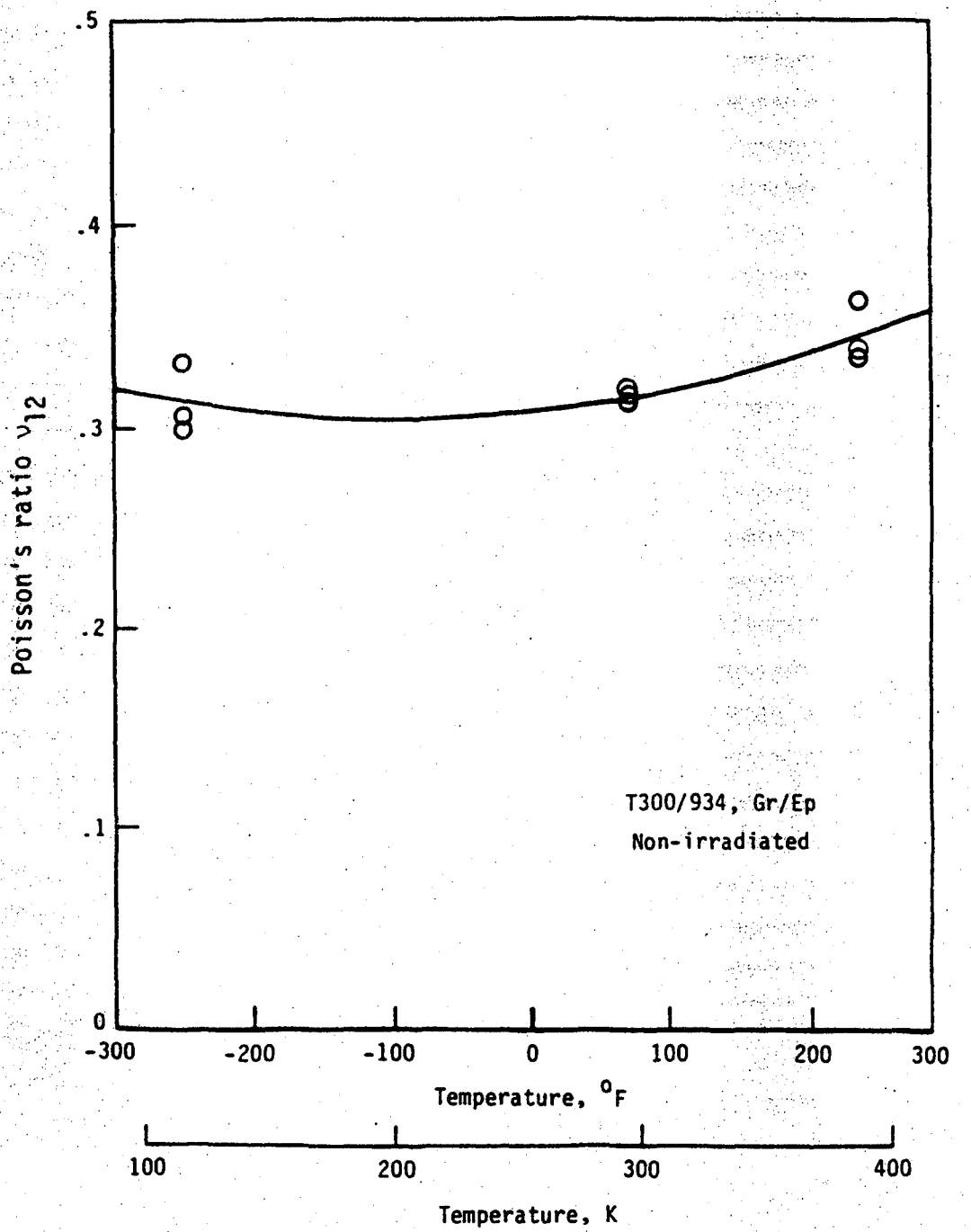

Fig. 41. Non-Irradiated Poisson's Ratio, ν_{12}, as a Function of Temperature.

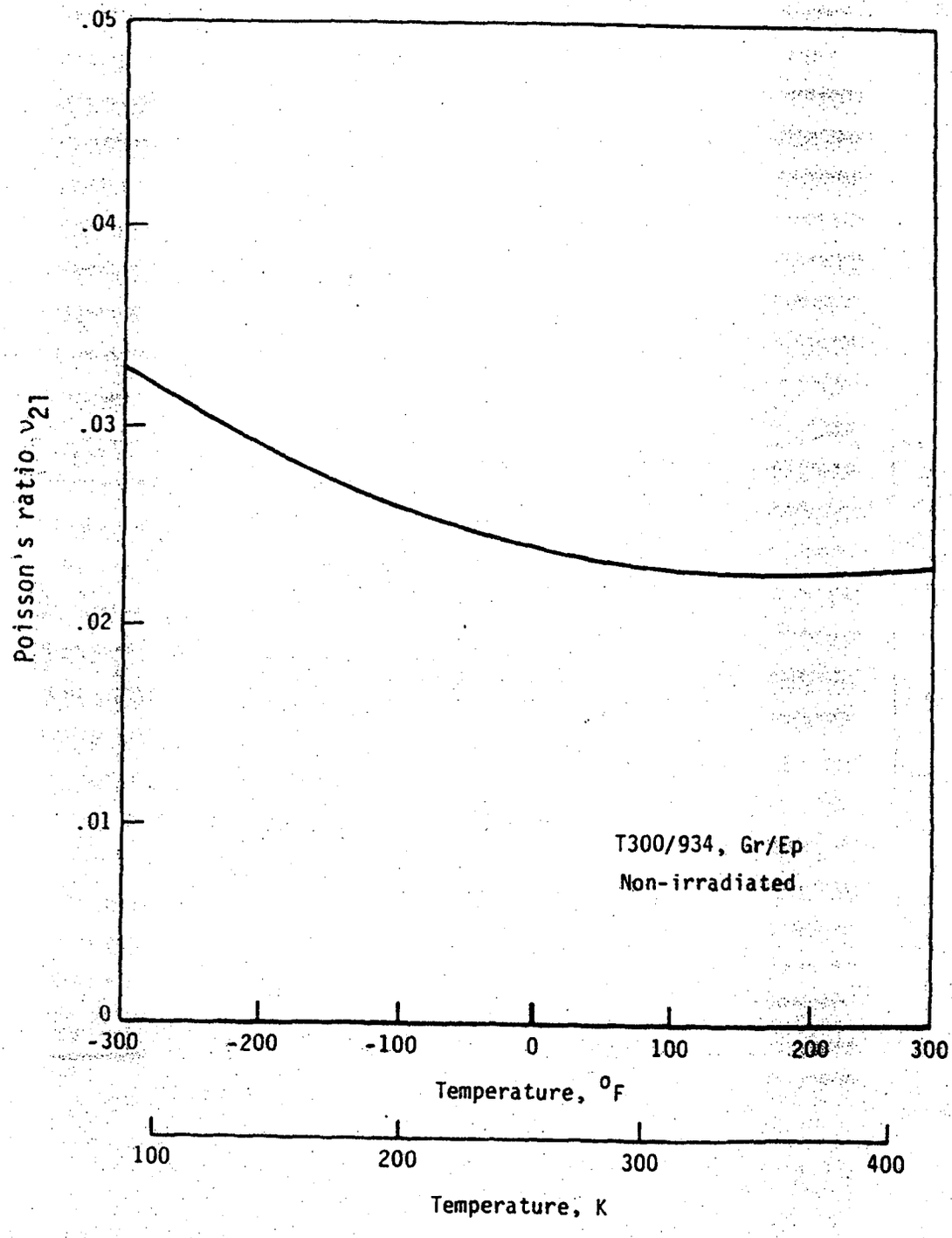

Fig. 42. Calculated, Non-Irradiated Poisson's Ratio, ν_{21}, as a Function of Temperature.

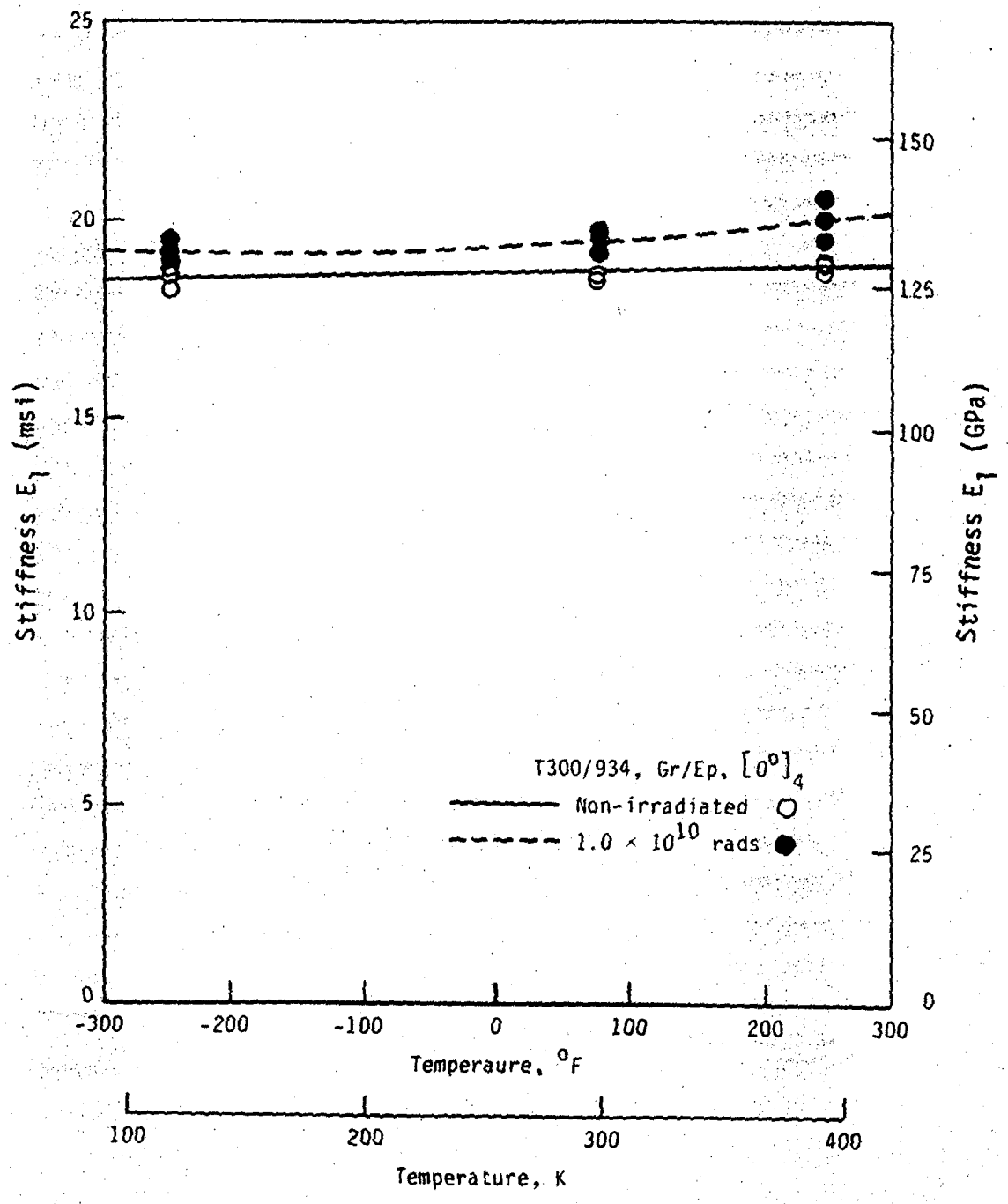

Fig. 43. Non-Irradiated Compared to Irradiated Moduli of Elasticity, E_1, as a Function of Temperature.

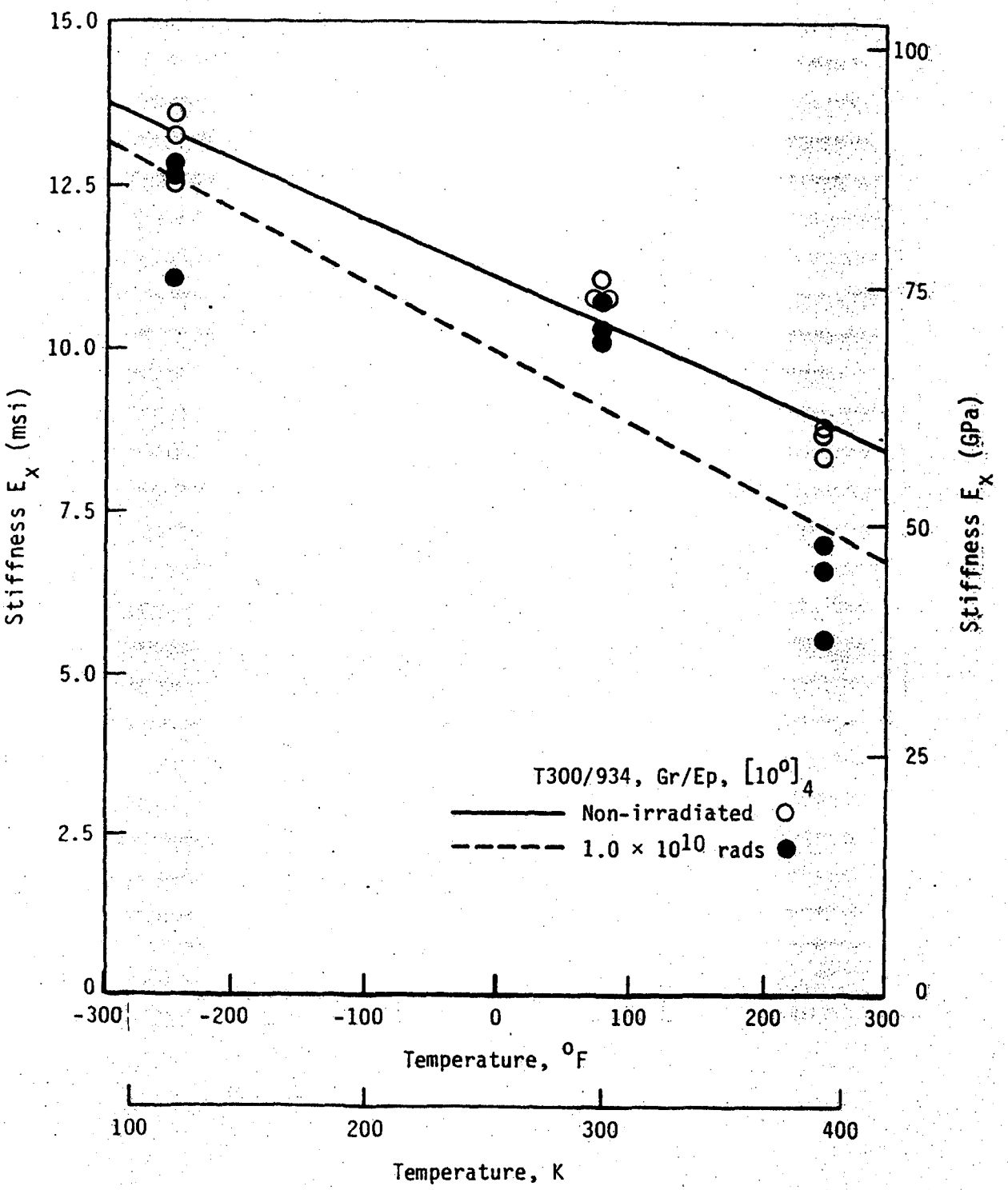

Fig. 44. Non-Irradiated Compared to Irradiated Axial Moduli of the $[10]_4$ Laminate as a Function of Temperature.

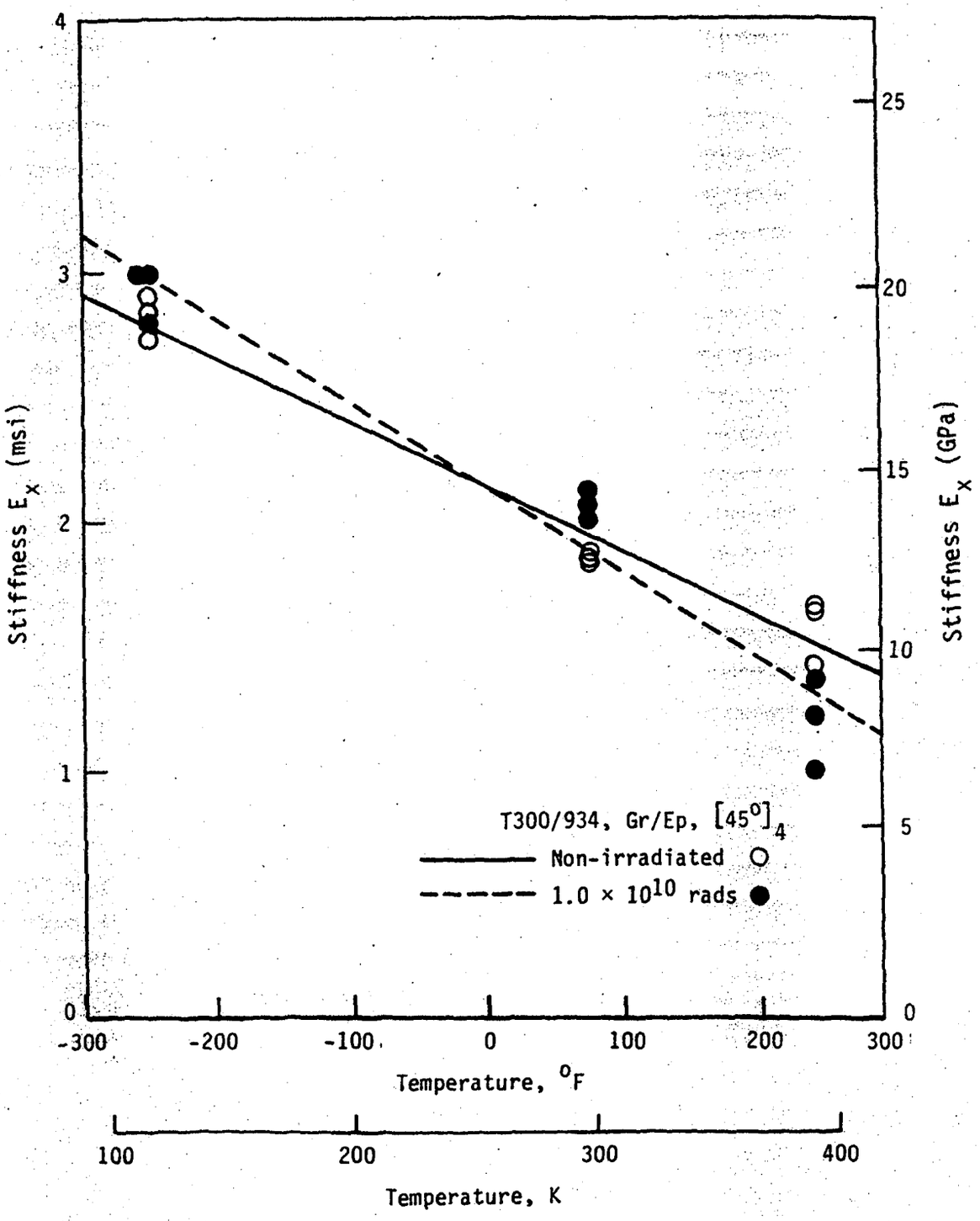

Fig. 45. Non-Irradiated Compared to Irradiated Axial Moduli of the $[45]_4$ Laminate as a Function of Temperature.

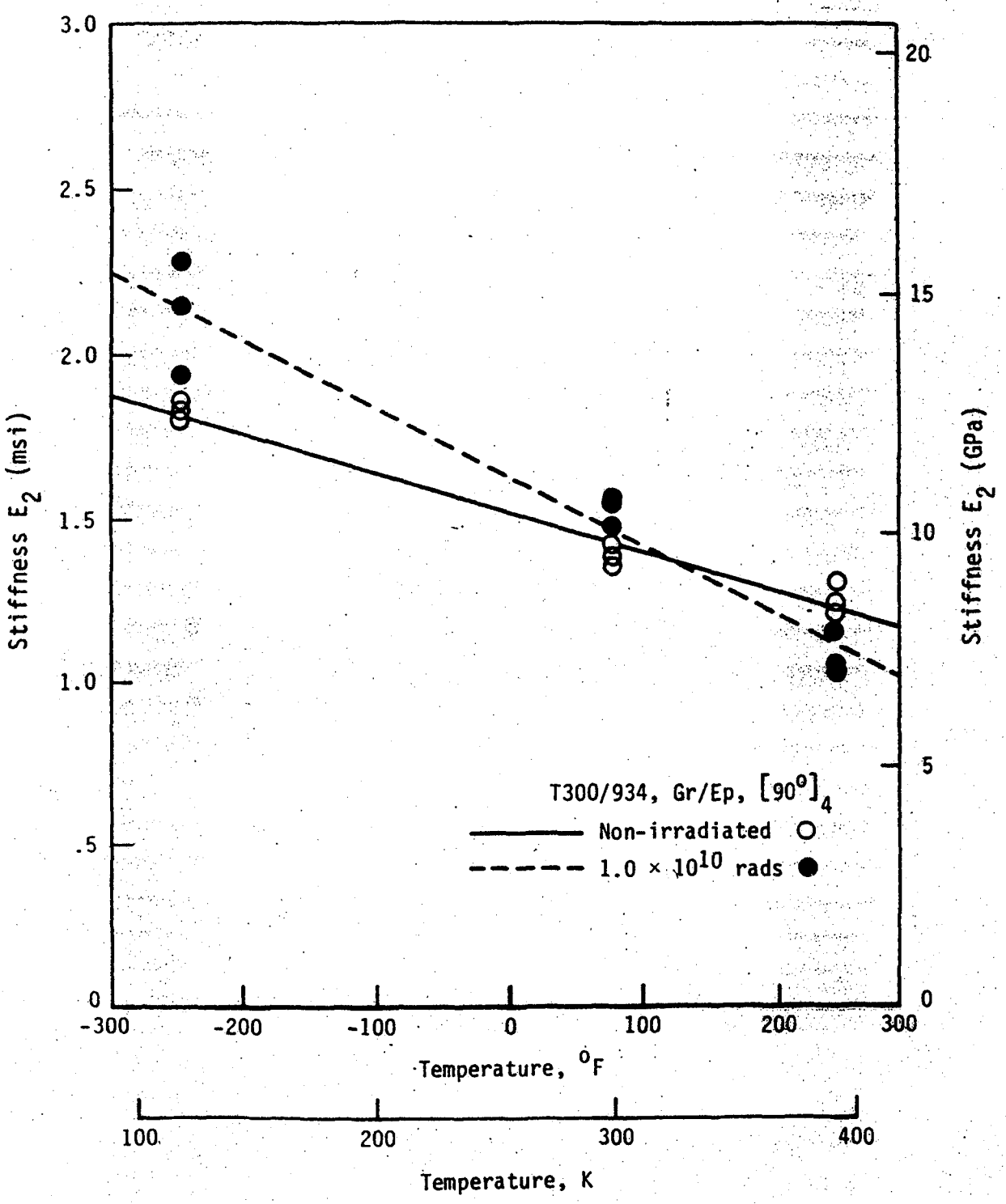

Fig. 46. Non-Irradiated Compared to Irradiated Moduli of Elasticity, E_2, as a Function of Temperature.

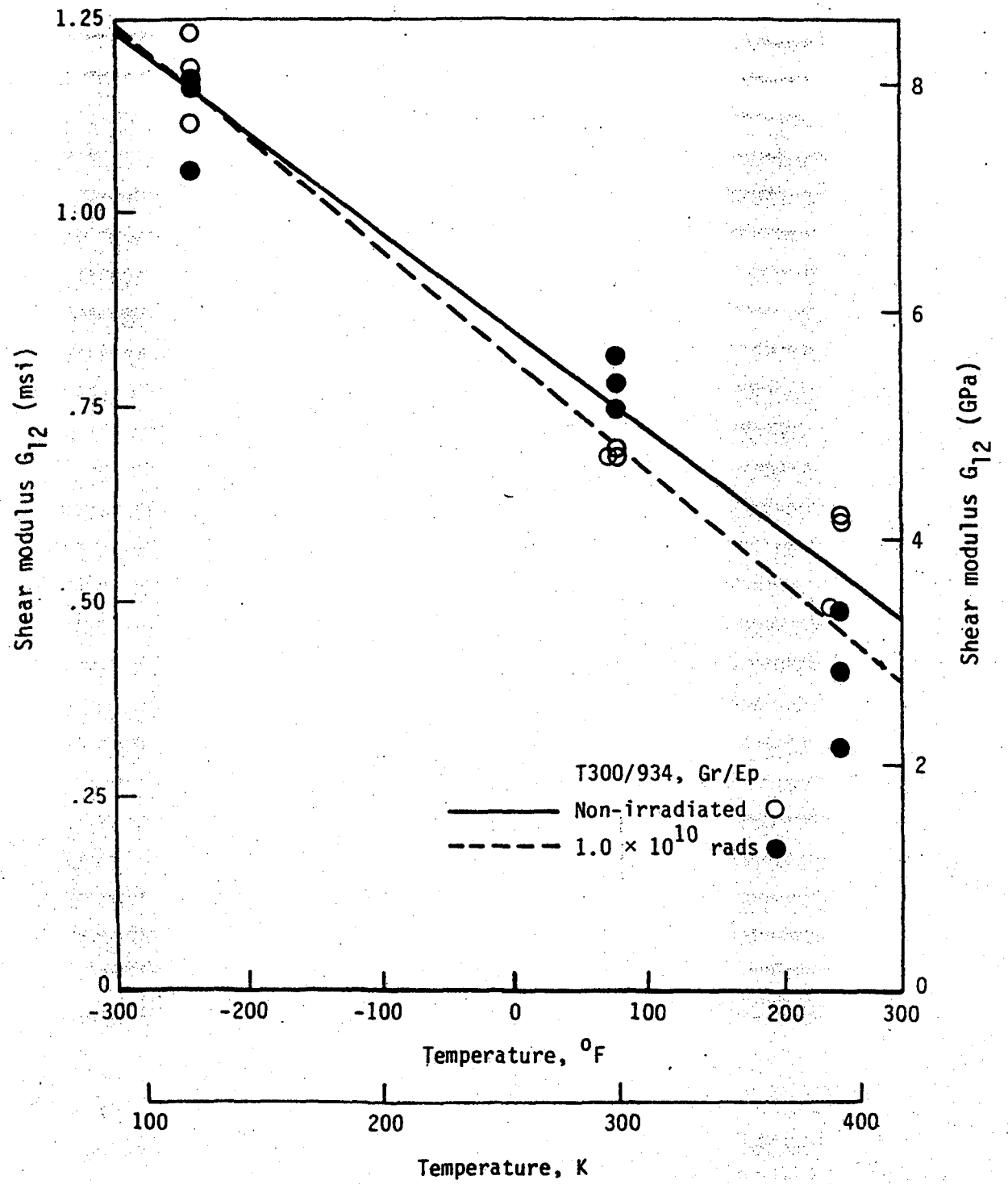

Fig. 47. Non-Irradiated Compared to Irradiated Shear Moduli, G_{12}, as a Function of Temperature.

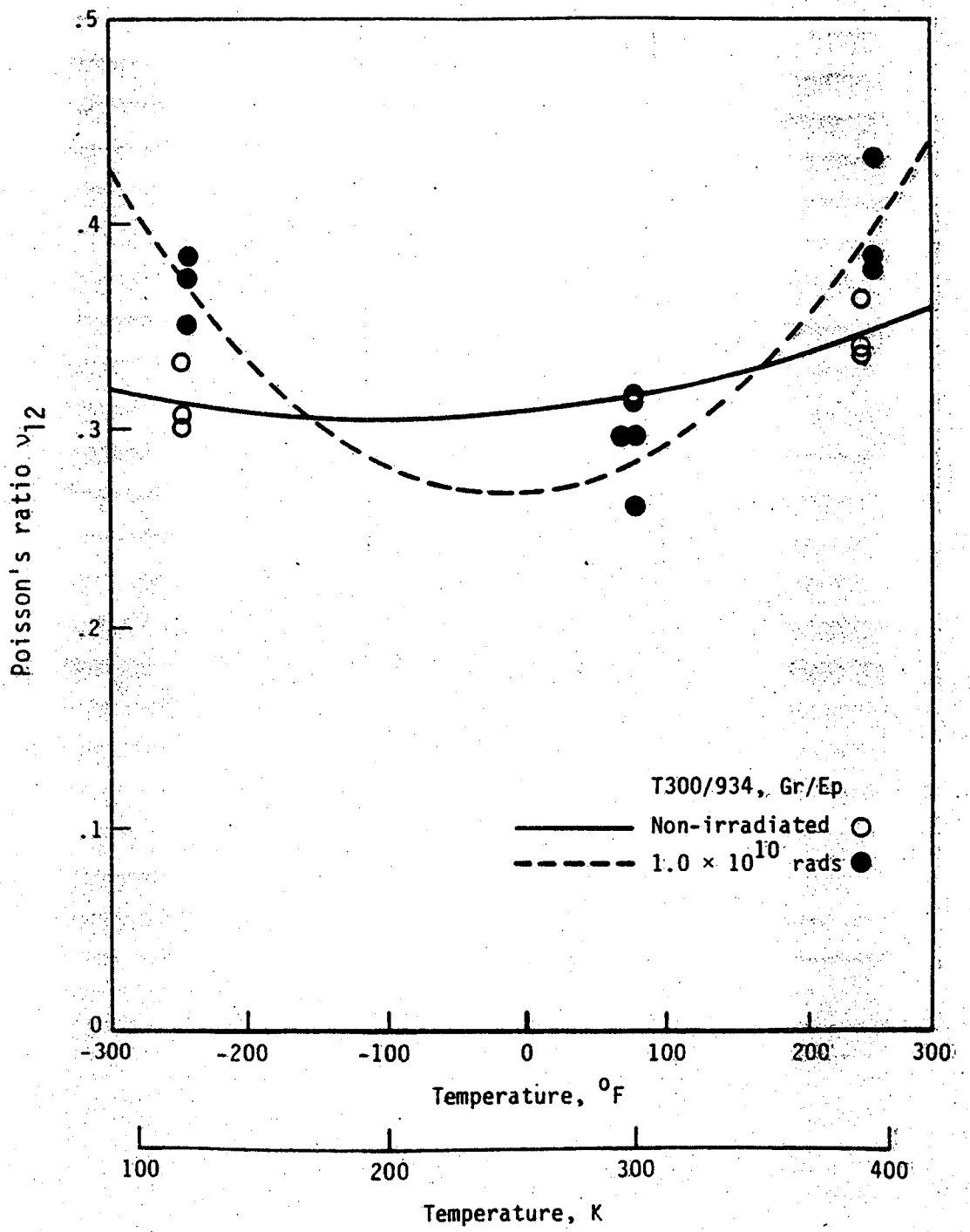

Fig. 48. Non-Irradiated Compared to Irradiated Poisson's Ratio, ν_{12}, as a Function of Temperature.

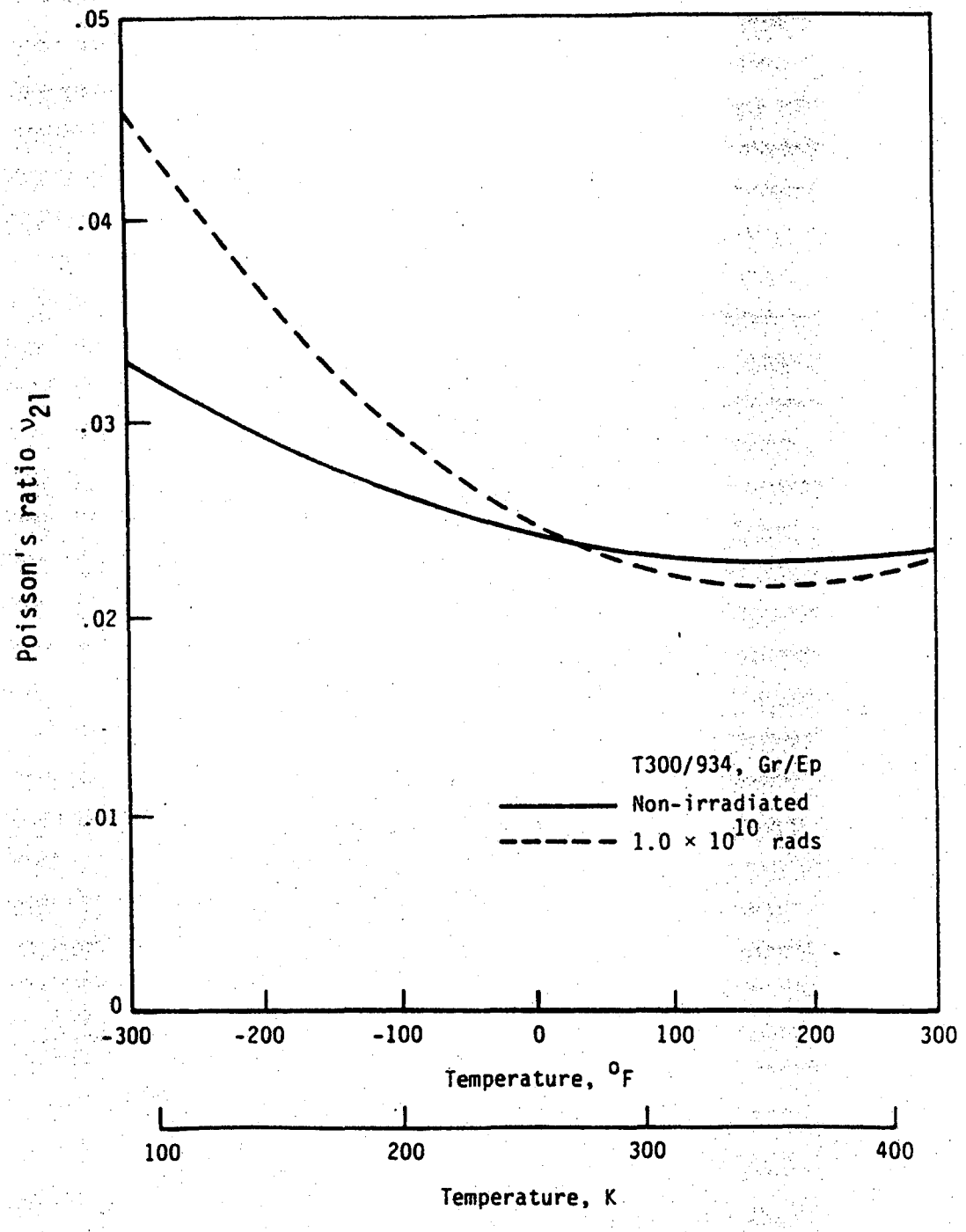

Fig. 49. Calculated, Non-Irradiated Compared to Irradiated Poisson's Ratio, ν_{21}, as a Function of Temperature.

4.1.3 Strength Properties

0°-Laminate: X_T. Figure 50 shows that the ultimate strength of the 0°-laminate for non-irradiated material is highest at room temperature. At -250°F (116K) the average strength drops by 37 percent and at +250°F (394K) the ultimate strength drops by 13 percent. At the lower temperature, the matrix becomes stiffer and more brittle, resulting in higher residual stresses and less-efficient load transfer in regions of stress concentration such as at fiber breaks. At the elevated temperature, the matrix becomes soft and pliable. In this condition, the matrix is too pliable for efficient load transfer around fiber breaks, and again, the strength drops.

Data from the irradiated laminates are presented in Fig. 55. Again, strength is highest at room temperature and decreases by 43 percent at the low test temperature and by 27 percent at the high test temperature. There is a large amount of scatter in the data for both the non-irradiated and irradiated laminates. This is typical of ultimate strength data for composites.

Little difference is noted in the ultimate strength of the non-irradiated compared to irradiated laminates over most of the temperature range. However, a slight decrease in strength for the irradiated material is noted at elevated temperature. Both laminates exhibit brittle behavior at low temperatures (E_1 data, Fig. 43) which results in lower values of ultimate stress. On the other hand, at elevated temperatures, the irradiated material becomes more pliable than the non-irradiated material, which leads to a decrease in ultimate strength. This is probably due to less efficient load transfer at fiber breaks.

10°-Laminate. Results for the ultimate strength of the $[10]_4$ laminate are shown in Fig. 51. Strength is highest at room temperature. Average stress values are 26 percent lower at -250°F (116K) and 40 percent lower at +250°F (394K), when compared to room temperature values.

Data taken from irradiated laminates is added in Fig. 56. Over the entire temperature range, the irradiated strength is either equal to or less than the non-irradiated strength. Irradiated data are roughly equal to the non-irradiated data at -250°F (116K) and drops to a 32 percent decrease at the elevated temperature.

The ultimate strength data obtained from this test were transformed according to Eq. 5 to produce shear strength data. This laminate fails primarily by shear stress. The above results have been included for the sake of completeness.

45°-Laminate. Fig. 52 presents the ultimate strength of the $[45]_4$ laminate as a function of temperature. Strength is highest at room temperature, dropping by 12 percent at the low test temperature and by 28 percent at the high test temperature.

Data for the irradiated laminates is added in Fig. 57. Ultimate stress is roughly equal are both non-irradiated and irradiated laminates at room temperature. However, at -250°F (116K) the irradiated values are 19 percent lower than the non-irradiated values, and at +250°F (394K) the irradiated values are 37 percent lower than the non-irradiated values.

Note that the 45°-off axis specimen was chosen primarily for shear modulus measurements. These results have been included for the sake of completeness.

90°-Laminate: Y_T. Strength data in Fig. 53, for non-irradiated laminate, shows that the ultimate strength of the 90°-material follows the same trends as the 0°-material. The experimental values are highest at room temperature and drop at both higher and lower temperatures. The drop at -250°F (116K) is 51 percent and a 28-percent decrease is observed at +250°F (394K). On the average, the ultimate stress of the irradiated material is lower than that of the non-irradiated data (Fig. 58). Subjecting the composite material to electron radiation at room temperature drops the average strength by 26 percent. This value is lowered by 60 percent at the low test temperature and is also decreased by 16 percent at the high temperature. Again, note that there is a large amount of scatter in the data, this is typical of 90° material.

Data collected from the $[90]_4$ laminates causes one to conclude that the epoxy resin is degraded by irradiation. The matrix is more brittle at low temperatures and more pliable at high temperatures, when compared to non-irradiated material.

Shear Strength, S. Shear strength data for the non-irradiated test condition is presented in Fig. 54. A similar trend, as with the X_T and Y_T data, is also noted here. The largest value is measured at room temperature, a 26-percent decrease is observed at the low temperature, and a 40-percent drop is measured at the elevated temperature. Over the entire temperature range, the irradiated shear strength is either equal to or less than the non-irradiated strength average (Fig. 59). As with

the shear modulus (Fig. 47), the irradiated data are roughly equal to the non-irradiated data at -250°F (116K) and drops to a 32 percent decrease at the elevated temperature. For the irradiated material, a drop of 22 percent is noted at the low temperature, and a drop of 56 percent is noted at +250°F (394K), as compared to room temperature data. This is in addition to a 7 percent decrease in shear strength of irradiated data compared to non-irradiated data at room temperature.

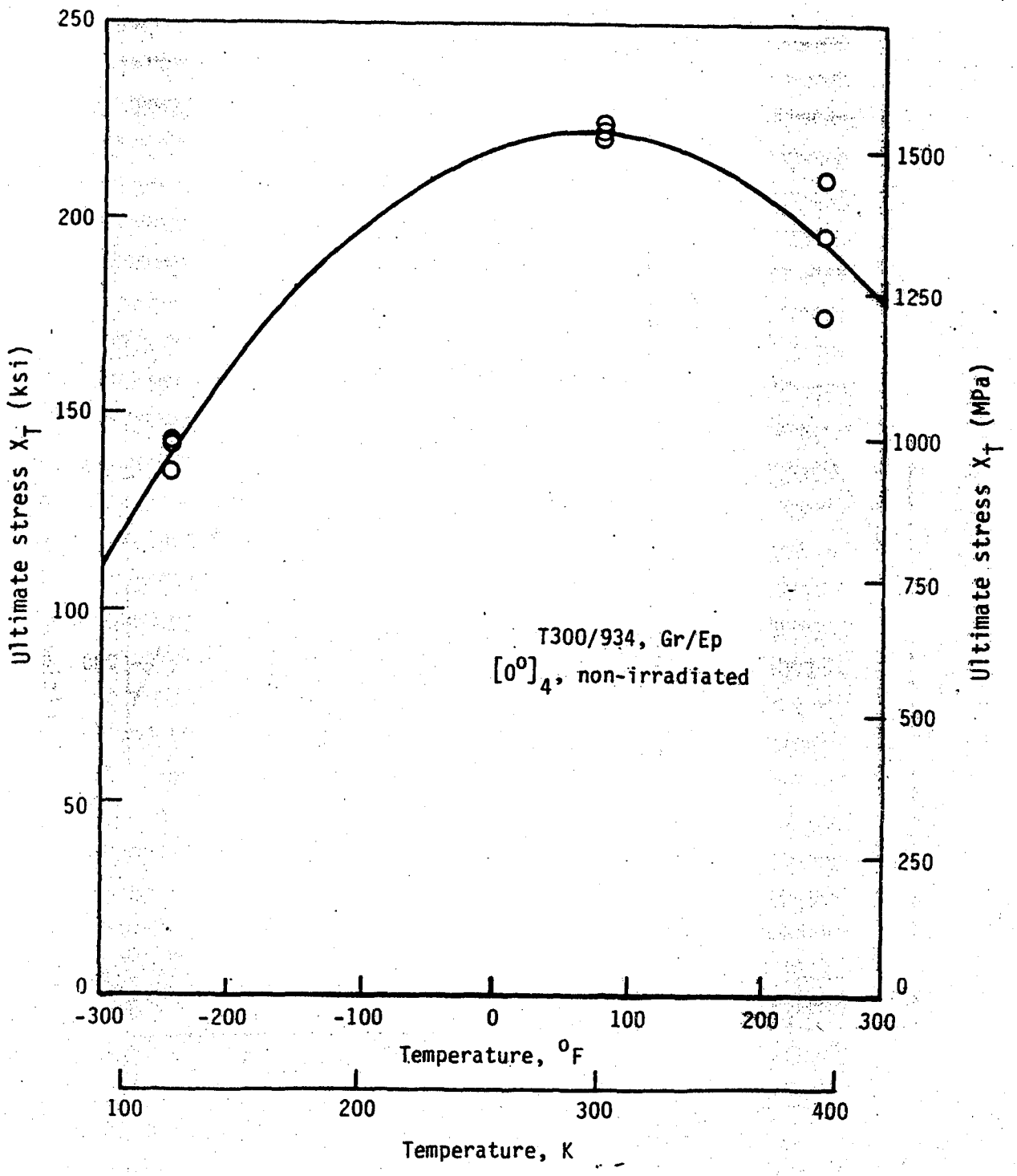

Fig. 50. Non-Irradiated Ultimate Strength, X_T, as a Function of Temperature.

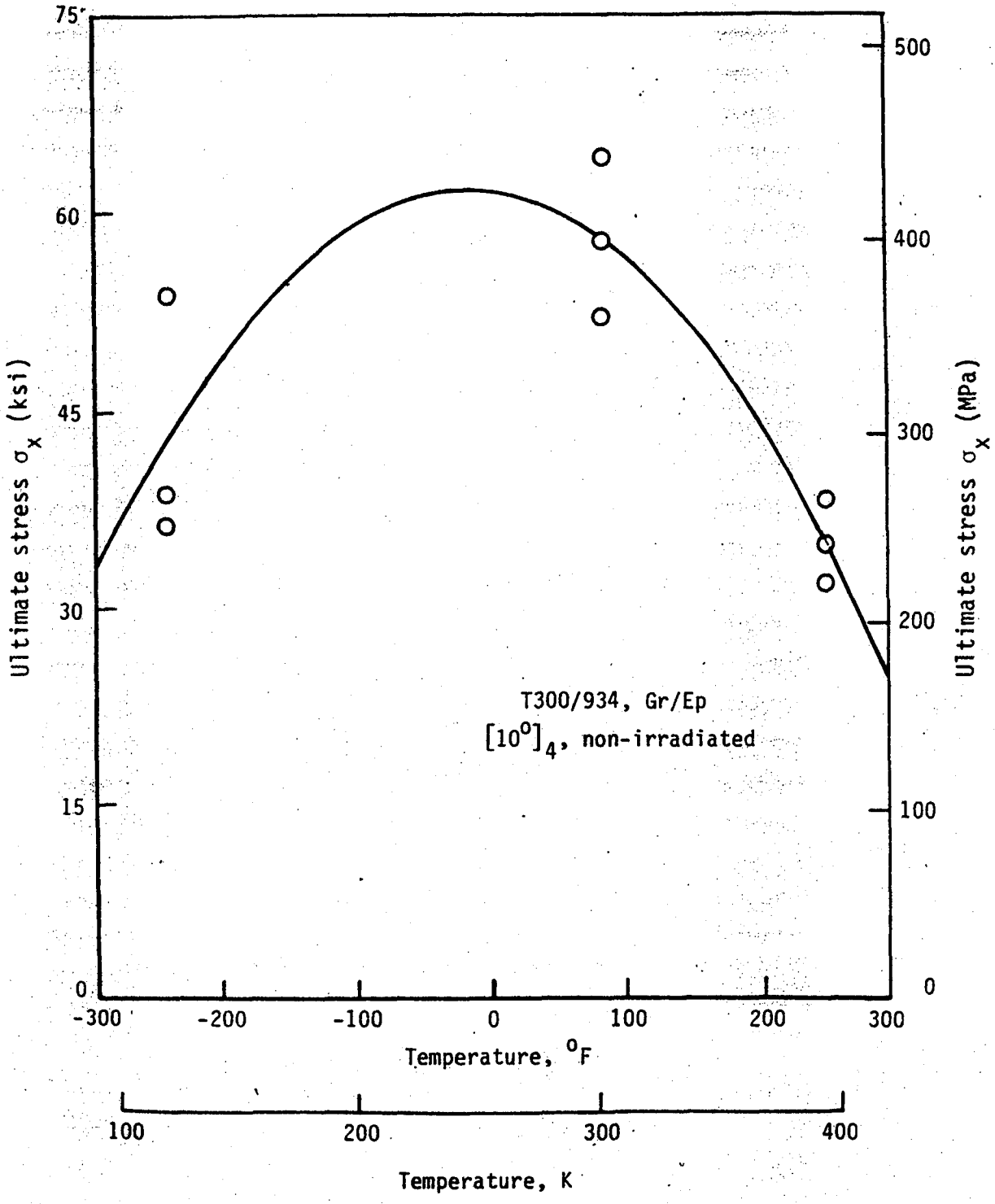

Fig. 51. Non-Irradiated Ultimate Strength of the $[10]_4$ Laminate as a Function of Temperature.

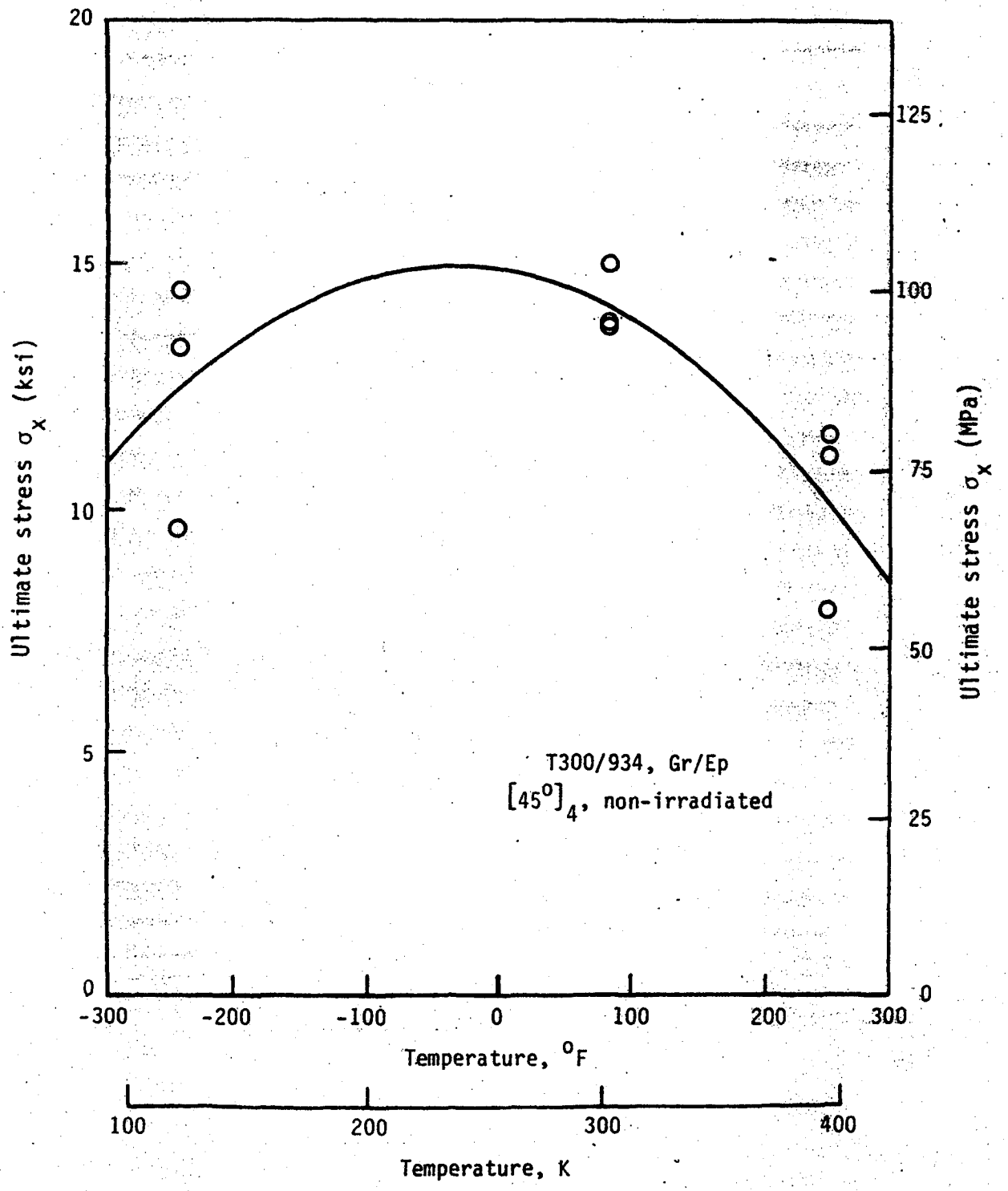

Fig. 52. Non-Irradiated Ultimate Strength of the $[45]_4$ Laminate as a Function of Temperature.

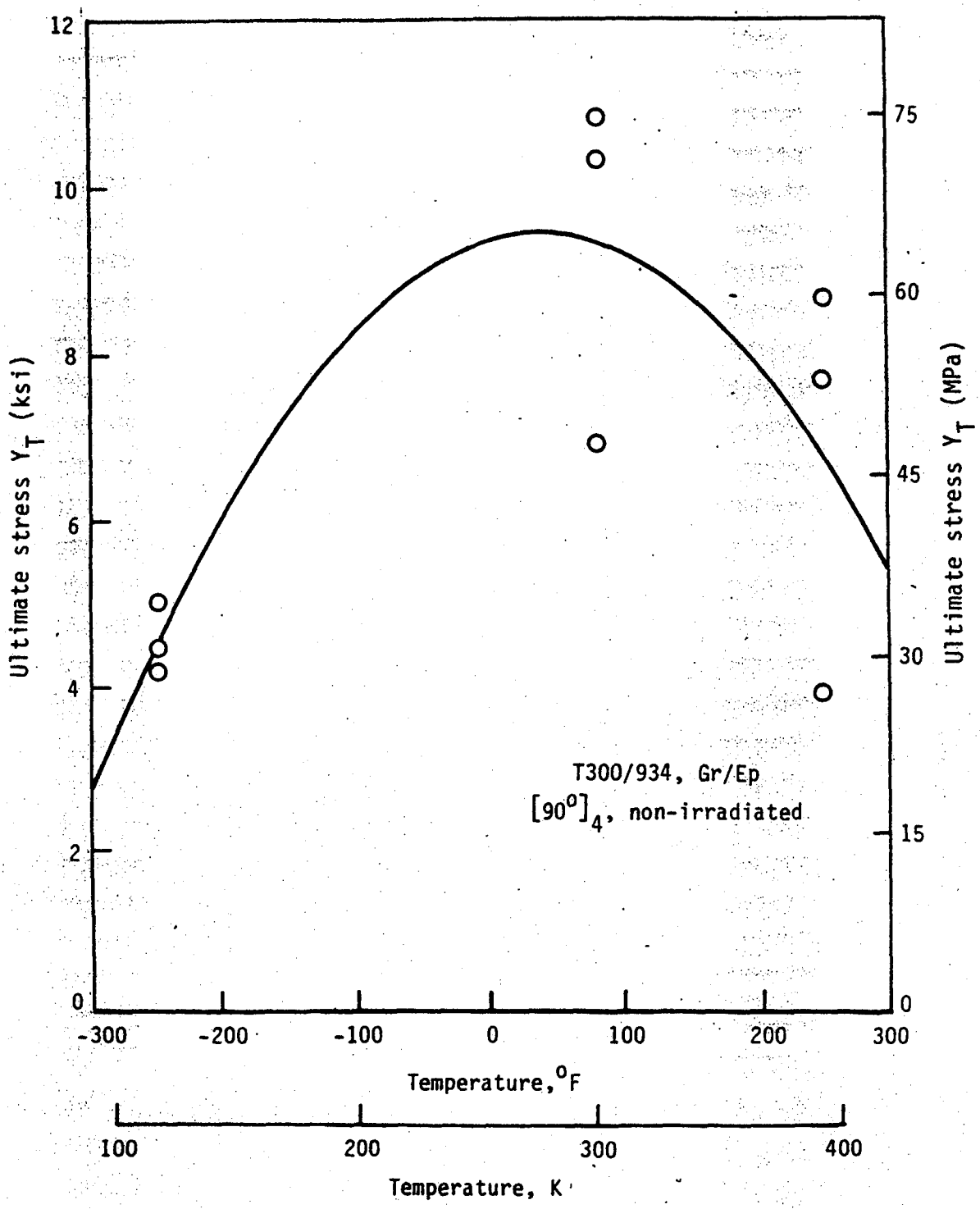

Fig. 53. **Non-Irradiated Ultimate Strength, Y_T, as a Function of Temperature.**

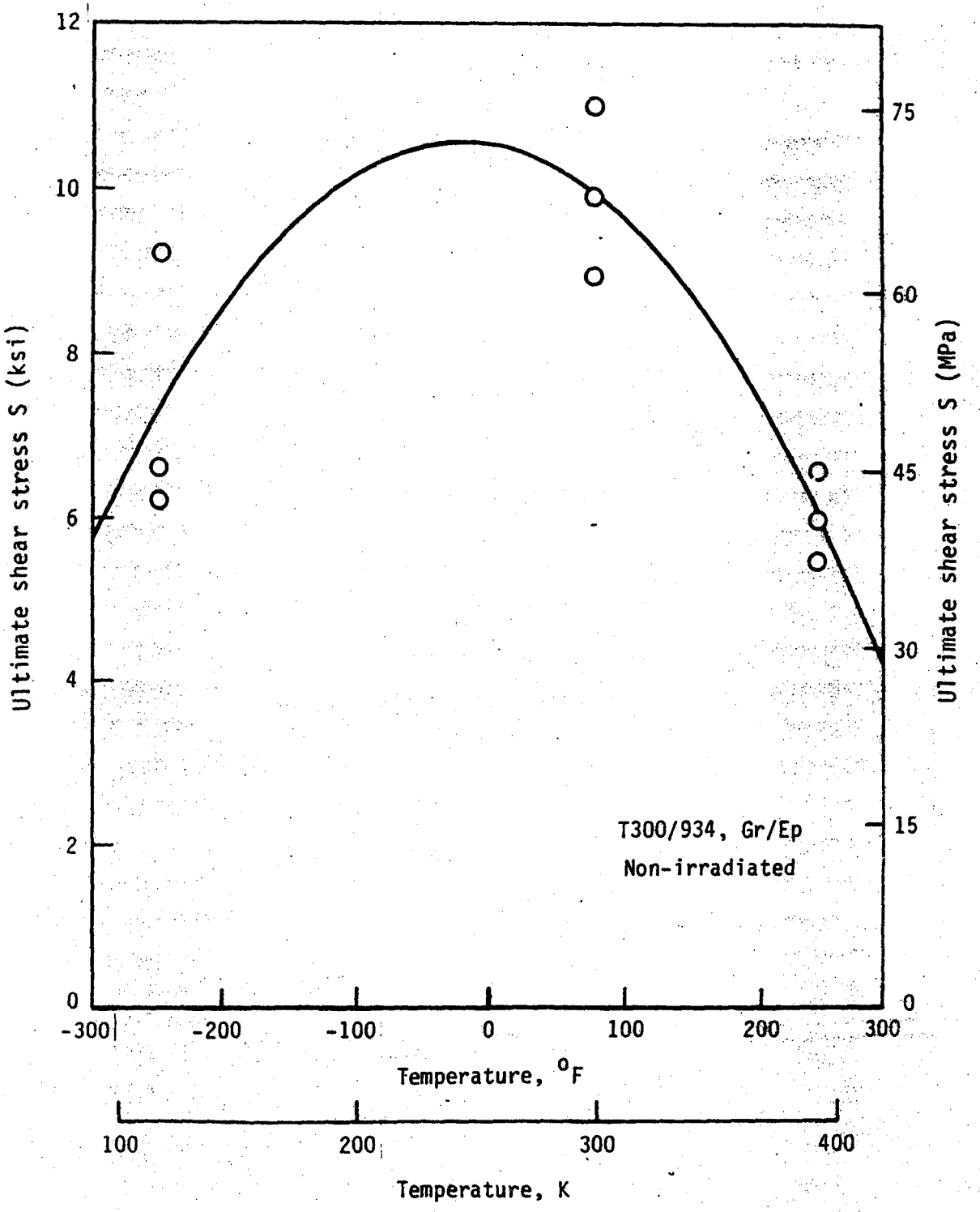

Fig. 54. Non-Irradiated Ultimate Shear Strength, S, as a Function of Temperature.

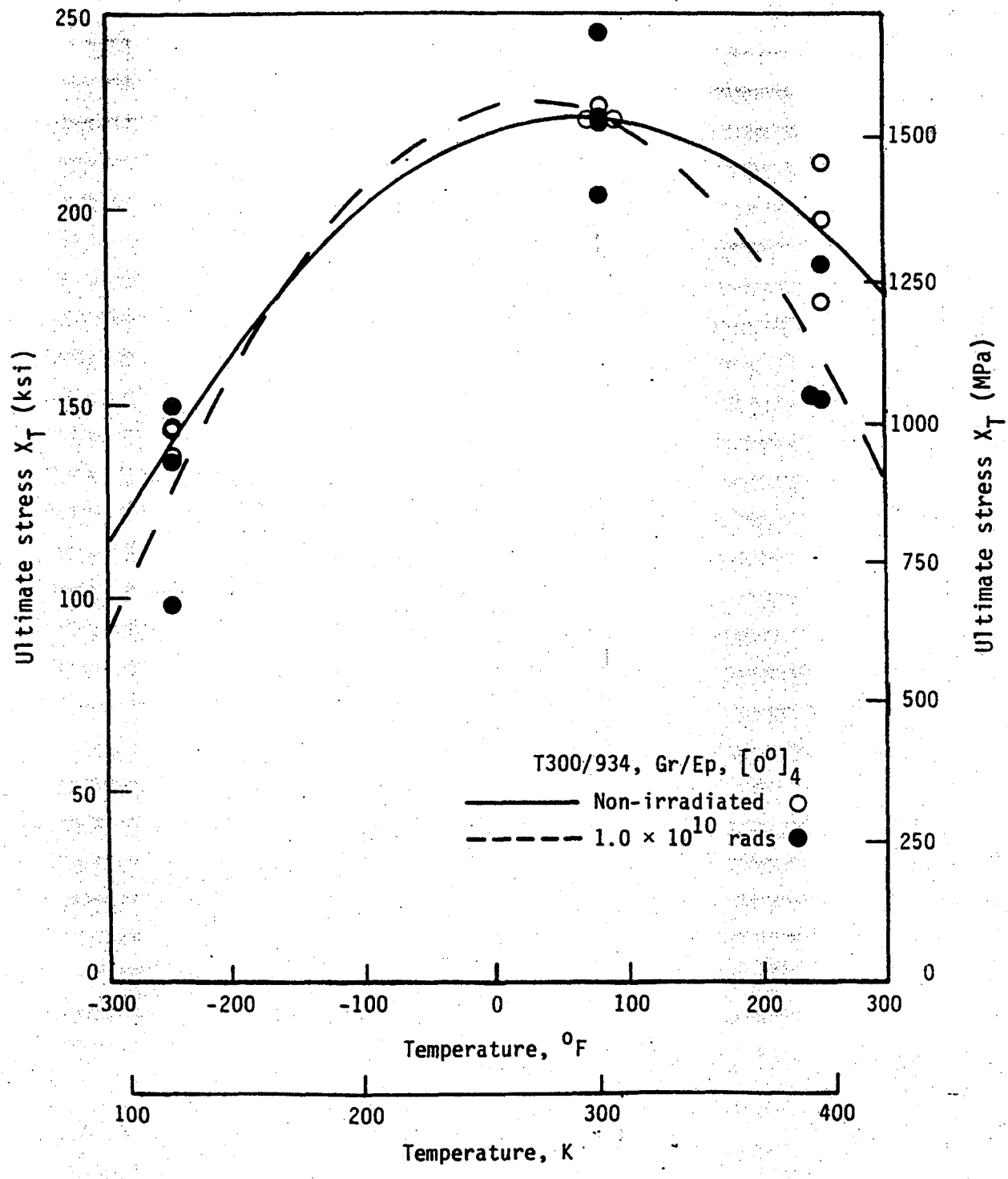

Fig. 55. Non-Irradiated Compared to Irradiated Ultimate Strength, X_T, as a Function of Temperature.

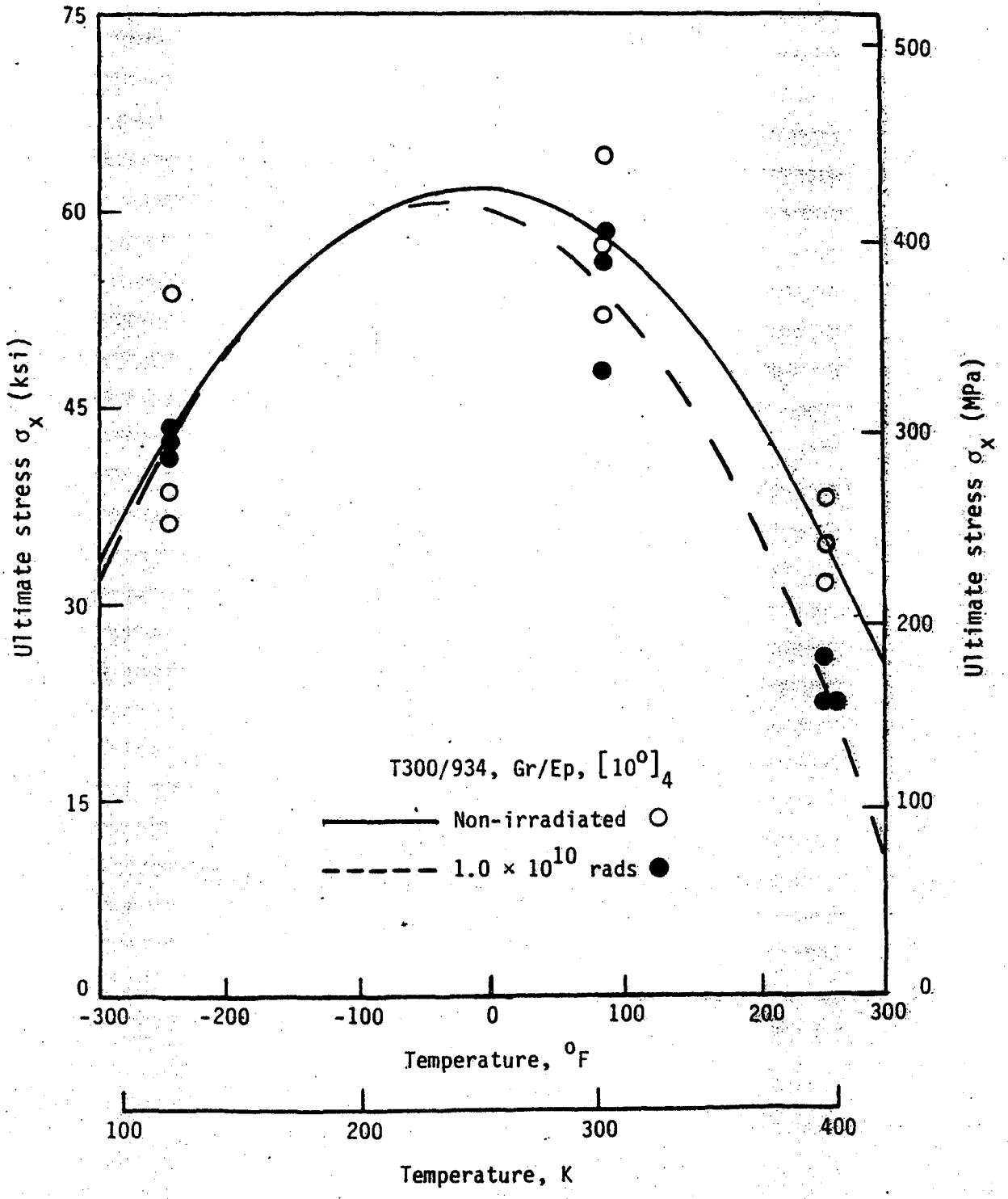

Fig. 56. Non-Irradiated Compared to Irradiated Ultimate Strength of the $[10]_4$ Laminate as a Function of Temperature.

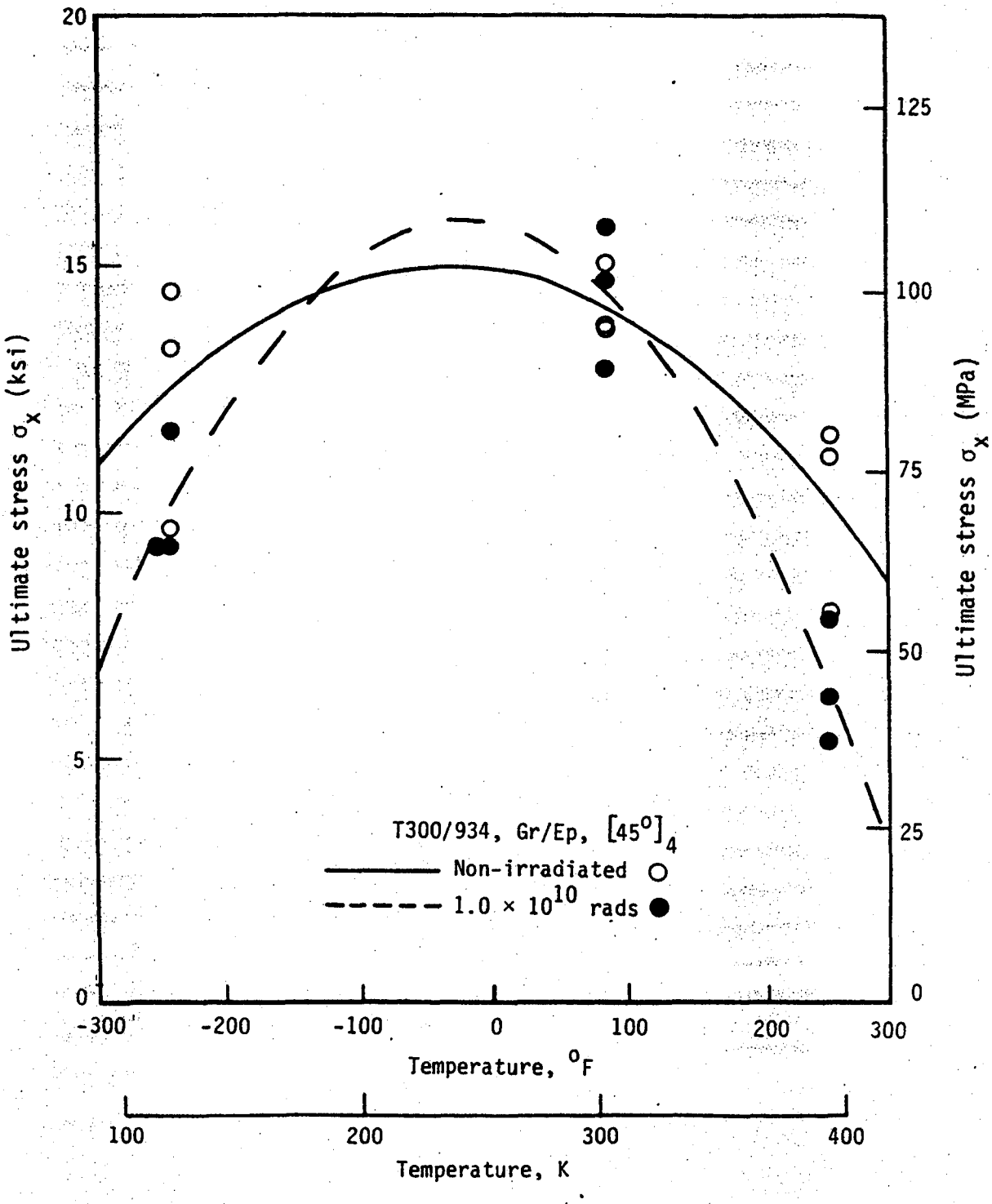

Fig. 57. Non-Irradiated Compared to Irradiated Ultimate Strength of the $[45]_4$ Laminate as a Function of Temperature.

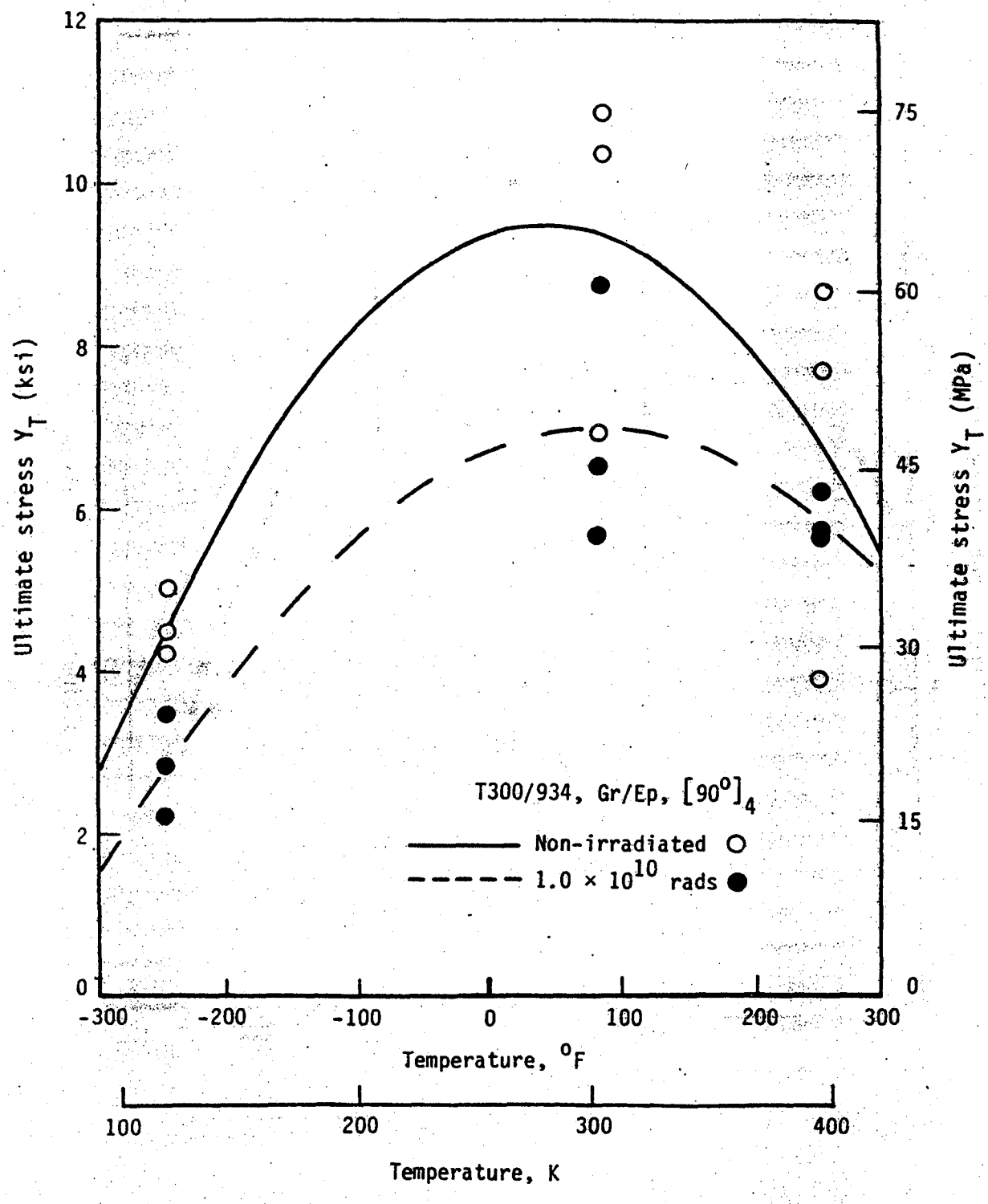

Fig. 58. Non-Irradiated Compared to Irradiated Ultimate Strength, Y_T, as a Function of Temperature.

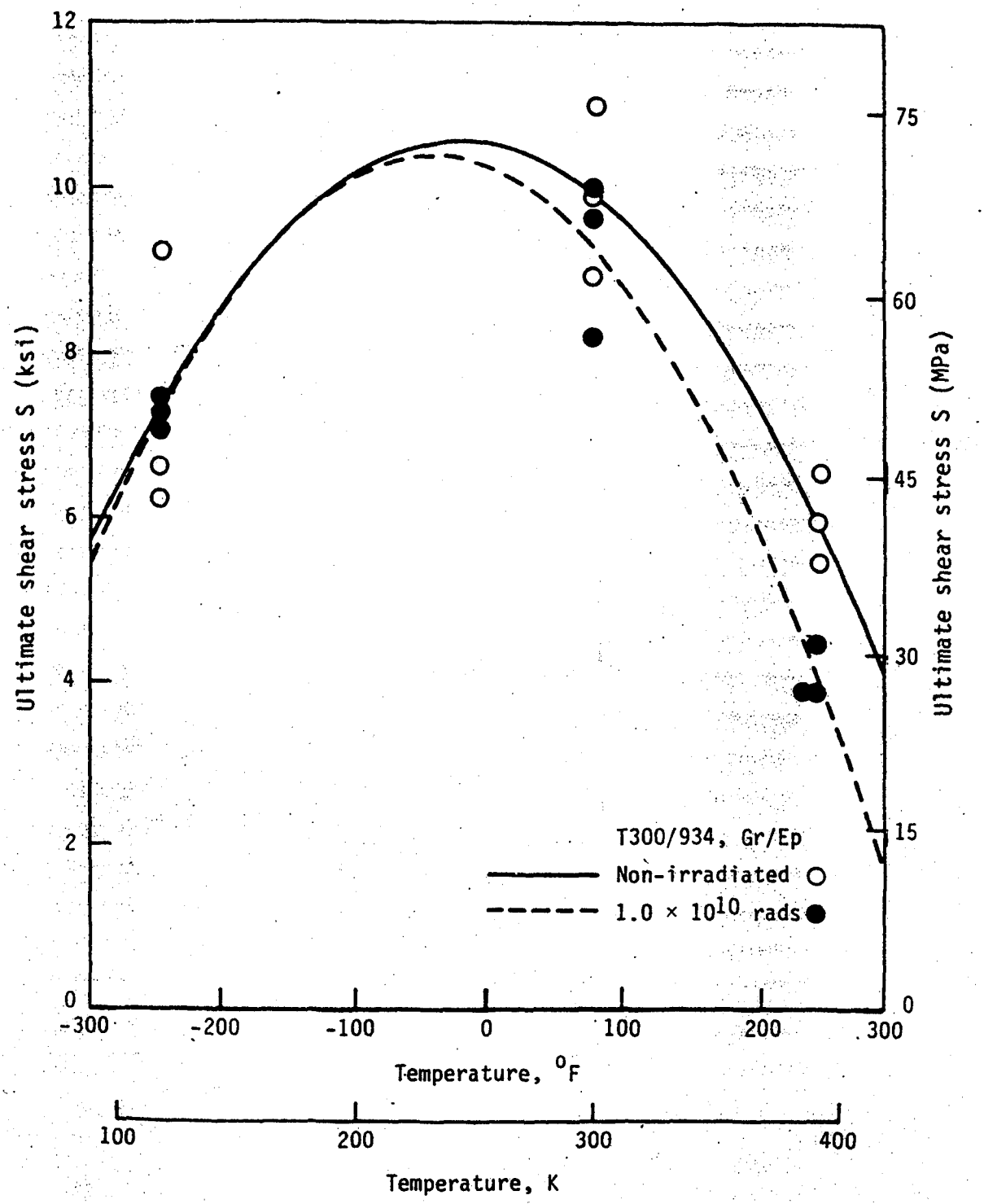

Fig. 59. Non-Irradiated Compared to Irradiated Ultimate Shear Strength, S, as a Function of Temperature.

Table 6

Non-Irradiated Data as a Function of Temperature.

Temperature	Material property	Non-irradiated ksi/msi (MPa/GPa)	Percent change from room temperature
-250°F (116K)	X_T	140.9 (972)	-36.6
	Y_T	4.56 (31)	-51.3
	S	7.34 (51)	-26.0
	E_1	18.62 (128)	- 1.4
	E_2	1.829 (12.6)	+32.9
	ν_{12}	0.3129	n.c.
	G_{12}	1.170 (8.1)	+70.1
Room temperature	X_T	222.1 (1531)	-
	Y_T	9.37 (65)	-
	S	9.92 (68)	-
	E_1	18.88 130	-
	E_2	1.376 (9.5)	-
	ν_{12}	0.3143	-
	G_{12}	0.688 (4.7)	-
+250°F (394K)	X_T	193.7 (1336)	-12.8
	Y_T	6.76 (47)	-27.9
	S	5.97 (41)	-39.8
	E_1	19.03 (131)	+ 1.0
	E_2	1.241 (8.6)	- 9.8
	ν_{12}	0.3447	+ 9.7
	G_{12}	0.563 (3.9)	-18.2

Table 7

Irradiated Data as a Function of Temperature.

Temperature	Material property	1.0×10^{10} rads ksi/msi (MPa/GPa)	Percent change from room temperature
$-250^{o}F$ (116K)	X_T	127.3 (878)	-42.8
	Y_T	2.81 (19)	-59.7
	S	7.25 (50)	-21.6
	E_1	19.16 (132)	n.c.
	E_2	2.123 (14.6)	+40.1
	ν_{12}	0.3682	+30.1
	G_{12}	1.123 (7.7)	+44.5
Room temperature	X_T	222.6 (1535)	-
	Y_T	6.98 (48)	-
	S	9.25 (64)	-
	E_1	19.31 (133)	-
	E_2	1.515 (10.4)	-
	ν_{12}	0.2831	-
	G_{12}	0.777 (5.4)	-
$+250^{o}F$ (394K)	X_T	161.5 (1114)	-27.4
	Y_T	5.88 (41)	-15.8
	S	4.06 (28)	-56.1
	E_1	19.76 (136)	+ 2.3
	E_2	1.064 (7.3)	-29.8
	ν_{12}	0.3970	+40.2
	G_{12}	0.397 (2.7)	-48.9

Table 8

Non-Irradiated Data Compared to Irradiated Data as a Function of Temperature.

Temperature	Material property	Non-irradiated ksi/msi (MPa/GPa)	1.0×10^{10} rads ksi/msi (MPa/GPa)	Percent change
-250°F (116K)	X_T	140.9 (972)	127.3 (878)	- 9.7
	Y_T	4.56 (31)	2.81 (19)	-38.4
	S	7.34 (51)	7.25 (50)	n.c.
	E_1	18.62 (128)	19.16 (132)	+ 2.9
	E_2	1.829 (12.6)	2.123 (14.6)	+16.1
	ν_{12}	0.3129	0.3682	+17.7
	G_{12}	1.170 (8.1)	1.123 (7.7)	- 4.0
Room temperature	X_T	222.1 (1531)	222.6 (1535)	n.c.
	Y_T	9.37 (65)	6.98 (48)	-25.5
	S	9.92 (68)	9.25 (64)	- 6.8
	E_1	18.88 (130)	19.31 (133)	+ 2.2
	E_2	1.376 (9.5)	1.515 (10.4)	+10.1
	ν_{12}	0.3143	0.2831	-11.0
	G_{12}	0.688 (4.7)	0.777 (5.4)	+12.9
+250°F (394K)	X_T	193.7 (1336)	161.5 (1114)	-16.6
	Y_T	6.76 (47)	5.88 (41)	-13.0
	S	5.97 (41)	4.06 (28)	-32.0
	E_1	19.03 (131)	19.76 (136)	+ 3.8
	E_2	1.241 (8.6)	1.064 (7.3)	-14.3
	ν_{12}	0.3447	0.3970	+15.2
	G_{12}	0.563 (3.9)	0.397 (2.7)	-29.5

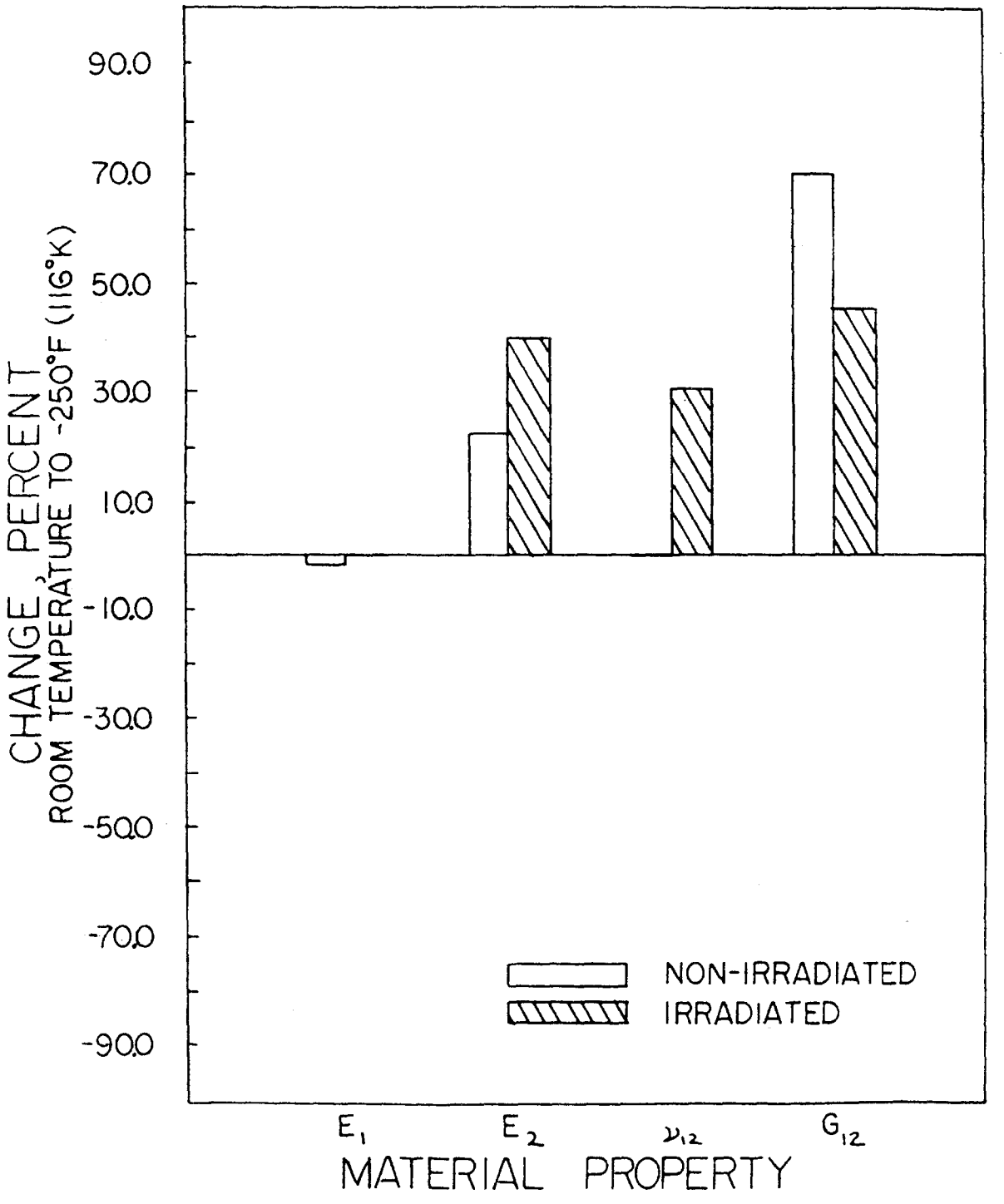

Fig. 60. Bar Chart of Percent Change in Mechanical Properties at -250°F (116K) Compared to Room Temperature.

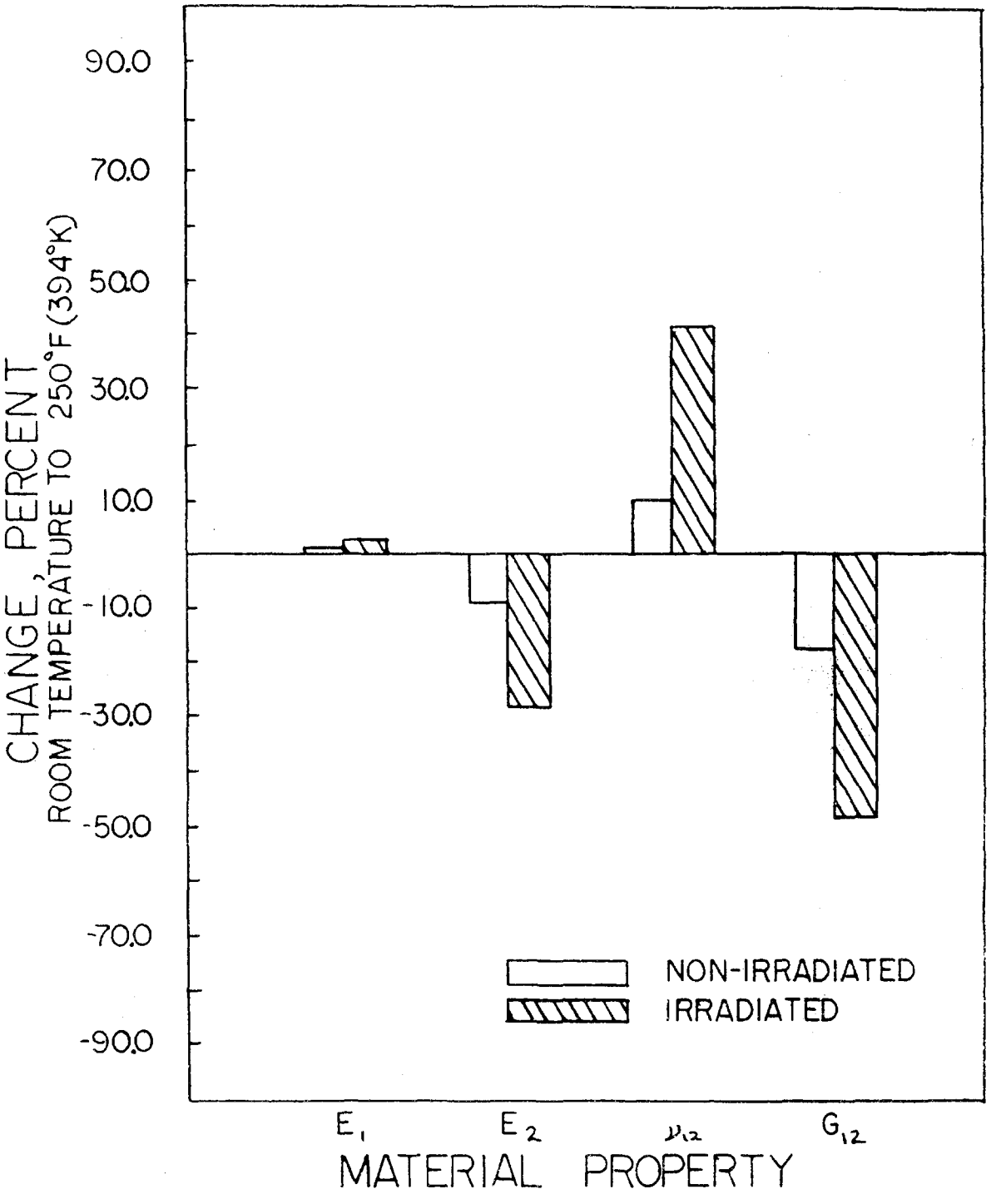

Fig. 61. Bar Chart of Percent Change in Mechanical Properties at +250°F (394K) Compared to Room Temperature.

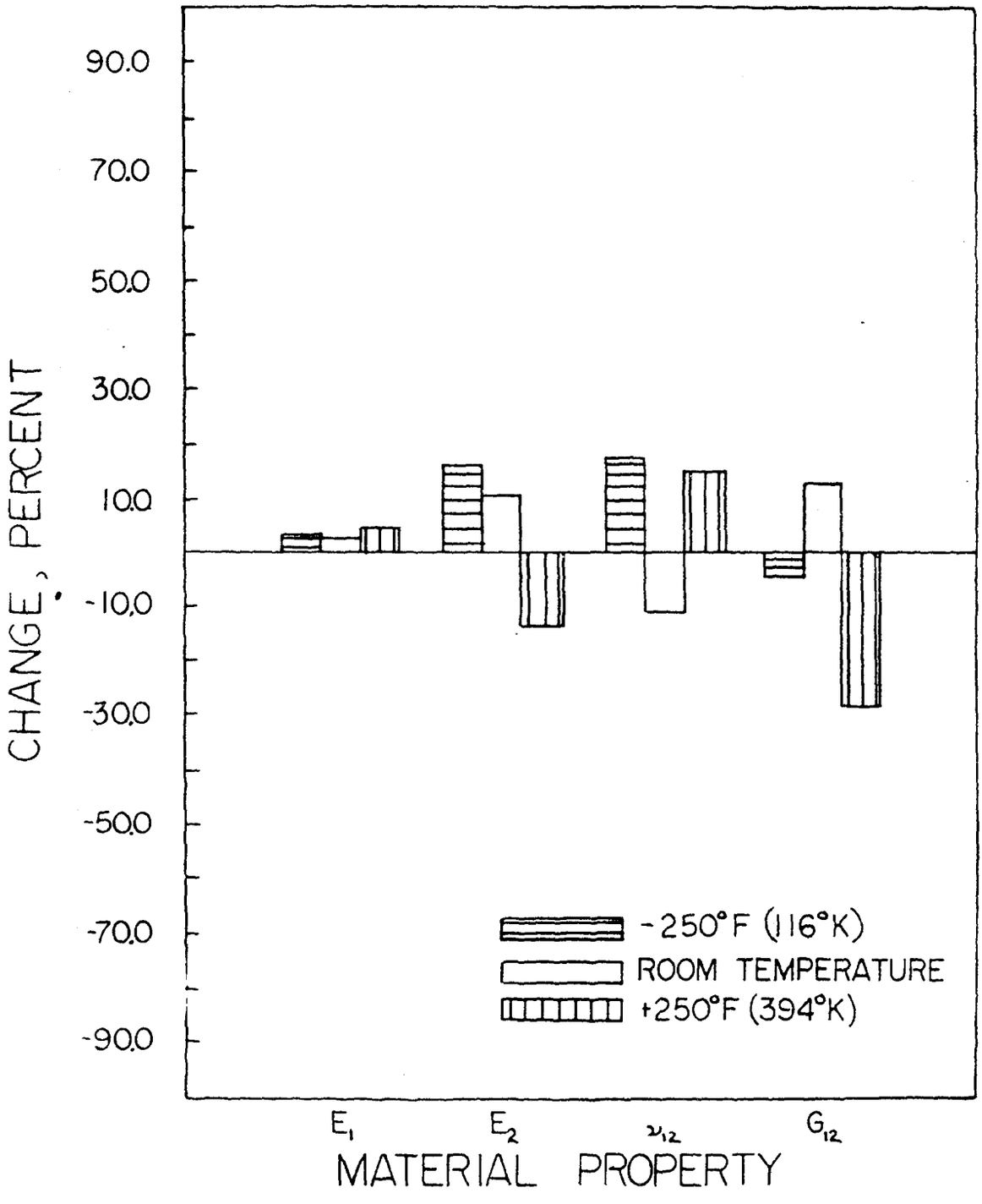

Fig. 62. Bar Chart of Radiation Induced Changes in Mechanical Properties as a Function of Temperature.

Table 9

Polynomial Regression Coefficients for Elastic Properties Temperature Dependence.

Test condition	Material property	C_0 msi (GPa)	C_1 msi (GPa)	C_2 msi (GPa)
Non irradiated	E_1, $[0^o]_4$	1.8814E+01 (1.2972E+02)	8.1333E-04 (5.6079E-03)	2.0915E-07 (1.4421E-06)
	E_x, $[10^o]_4$	1.0980E+01 (7.5707E+01)	-9.0478E-03 (-6.2385E-02)	-
	E_x, $[45^o]_4$	2.1260E+00 (1.4659E+01)	-2.6151E-03 (-1.8031E-02)	-
	E_2, $[90^o]_4$	1.5140E+00 (1.0439E+01)	-1.2025E-03 (-8.2912E-03)	-
1.0×10^{10} rads	E_1, $[0^o]_4$	1.9182E+01 (1.3226E+02)	1.2000E-03 (8.2740E-03)	4.5039E-06 (3.1054E-05)
	E_x, $[10^o]_4$	9.8204E+00 (6.7712E+01)	-1.0972E-02 (-7.5652E-02)	-
	E_x, $[45^o]_4$	2.1208E+00 (1.4623E+01)	-3.3975E-03 (-2.3426E-02)	-
	E_2, $[90^o]_4$	1.6228E+00 (1.1189E+01)	-2.0800E-03 (-1.4342E-02)	-

Table 10

Polynomial Regression Coefficients for Strength Properties Temperature Dependence.

Test condition	Material property	C_0 ksi (MPa)	C_1 ksi (MPa)	C_2 ksi (MPa)
Non irradiated	X_T, $[0^o]_4$	2.1891E+02 (1.5094E+03)	1.0547E-01 (7.2722E-01)	-8.2583E-04 (-5.6941E-03)
	σ_{ult}, $[10^o]_4$	6.1621E+01 (4.2488E+02)	-1.6027E-02 (-1.1051E-01)	-3.6290E-04 (-2.5022E-03)
	σ_{ult}, $[45^o]_4$	1.4937E+01 (1.0299E+02)	-4.4933E-03 -3.0981E-02)	-5.6972E-05 (-3.9282E-04)
	Y_T, $[90^o]_4$	9.4003E+00 (6.4815E+01)	4.4067E-03 (3.0384E-02)	-5.9818E-05 (-4.1245E-04)
1.0×10^{10} rads	X_T, $[0^o]_4$	2.2539E+02 (1.5541E+03)	6.8400E-02 (4.7162E-01)	-1.2958E-03 (-8.9345E-03)
	σ_{ult}, $[10^o]_4$	5.9845E+01 (4.1263E+02)	-3.7353E-02 (-2.5755E-01)	-4.2870E-04 (-2.9559E-03)
	σ_{ult}, $[45^o]_4$	1.5822E+01) (1.0909E+02)	-7.1867E-03 (-4.9552E-02)	-1.2035E-04 (-8.2981E-04)
	Y_T, $[90^o]_4$	6.7293E+00 (4.6399E+01)	6.1467E-03 (4.2381E-02)	-3.8175E-05 (-2.6322E-04)

Table 11

Polynomial Regression Coefficients for Shear Properties and Poisson's Ratio Temperature Dependence.

Test condition	Material property	C_0 ksi/msi (MPa/GPa)	C_1 ksi/msi (MPa/GPa)	C_2 ksi/msi (MPa/GPa)
Non irradiated	S	1.0536E+01 (7.2646E+01)	-2.7400E-03 (-1.8892E-02)	-6.2048E-05 (-4.2782E-04)
	G_{12}	8.4093E-01 (5.7982E+00)	-1.2476E-03 (-8.6022E-03)	-
	ν_{12}	3.0702E-01 (2.1169E+00)	6.3600E-05 (4.3852E-04)	3.4797E-07 (2.3993E-06)
	ν_{21}	2.3940E-02 (1.6507E-01)	-1.6400E-05 (-1.1308E-04)	4.2567E-08 (2.9350E-07)
1.0×10^{10} rads	S	1.0233E+01 (7.0557E+01)	-6.3800E-03 (-4.3990E-02)	-7.3299E-05 (-5.0540E-04)
	G_{12}	8.0407E-01 (5.5441E+00)	-1.3942E-03 (-9.6130E-03)	-
	ν_{12}	2.6659E-01 (1.8381E+00)	5.7467E-05 (3.9623E-04)	1.8562E-06 (1.2798E-05)
	ν_{21}	2.4643E-02 (1.6991E-01)	-3.8800E-05 (-2.6753E-04)	1.0332E-07 (7.1239E-07)

4.2 Effect of Radiation on the Matrix Material

The previous section presented results illustrating that electron irradiation adversely effects the mechanical properties of a graphite-epoxy composite. Now it is important to determine why this has occurred. Literature indicates that ionizing electron radiation alters the polymer matrix material by altering the chemical bonding within the polymer. Studies have shown that electron radiation degrades polymers by changing the crosslinking and scissioning molecular chains within the macromolecules of the polymer [49]. The next step of this study, therefore, has been to determine whether or not the epoxy matrix used in this study has been altered and to what degree. Several techniques have been employed and their results are discussed below.

4.2.1 Dynamic-Mechanical Results

The data presented in Fig. 63 is a plot of damping versus temperature for both the non-irradiated and irradiated $[0]_4$ DMA specimens (section 2.2.2). A decrease in the glass-transition temperature (T_g), for the irradiated sample, from 410°F (483K) to 300°F (422K) is immediately apparent. In addition to this 110°F (61K) drop in the glass-transition temperature, the peak has increased in height and shifted to the left. Such a shift indicates a decrease in the average molecular weight of the polymer, as well as a decrease in crosslink density [26]. It appears that irradiating the graphite-epoxy decreases both its average molecular weight and crosslink density, leading to a substantial decrease in the glass-transition temperature of the epoxy polymer.

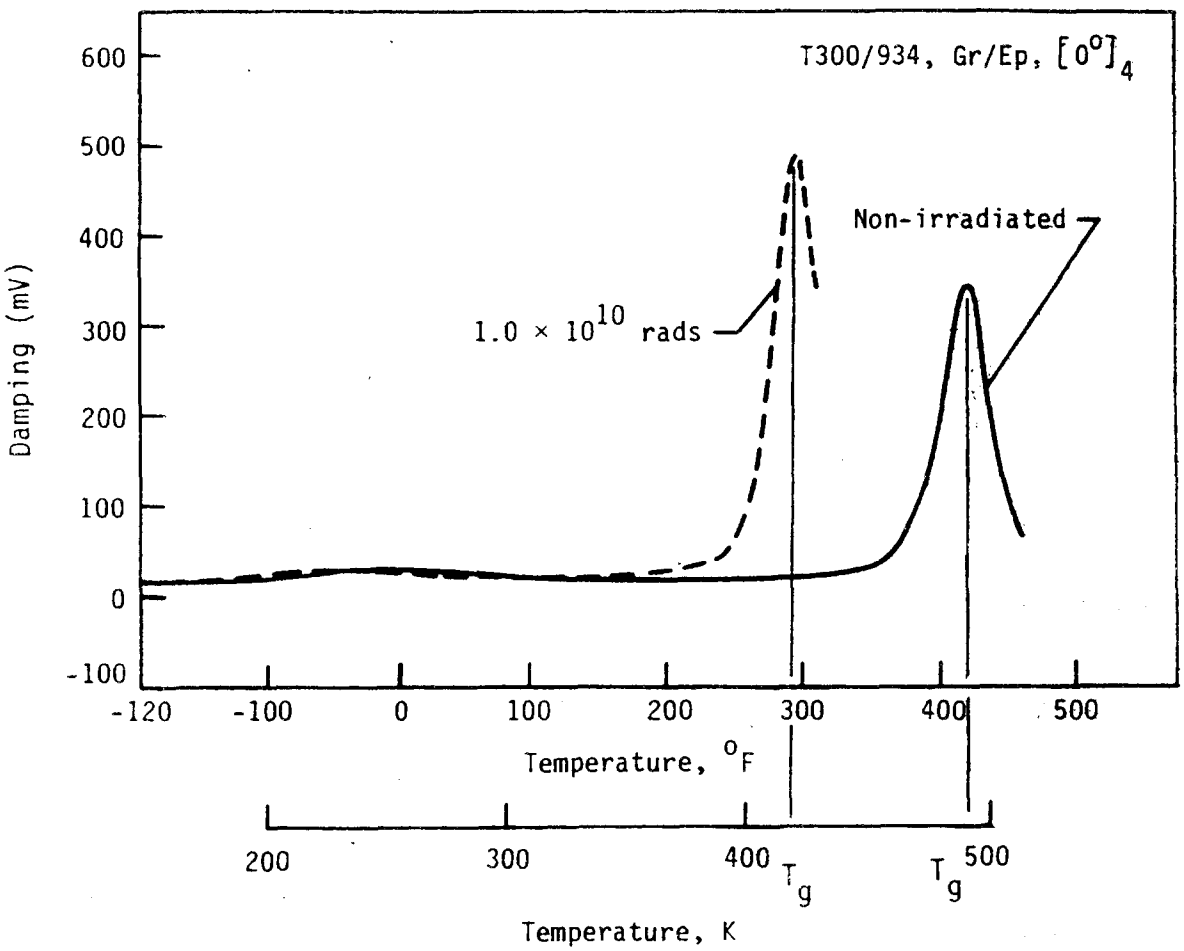

Fig. 63. Damping versus Temperature for Both Non-Irradiated and Irradiated $[0]_4$ DMA Specimens.

Fig. 64 is a plot of dynamic Young's modulus as a function of temperature for the same $[0]_4$ laminates. The dynamic modulus of the non-irradiated material begins to decrease at 350°F (450K). The dynamic modulus of the irradiated material begins to decrease at 250°F (394K). This is a 100°F (56K) change. The irradiated material loses its stiffness at a lower temperature than the non-irradiated material.

Experimental results for non-irradiated and irradiated $[90]_4$ DMA specimens are shown in Figs. 65 and 66. Trends similar to those noted for the $[0]_4$ laminates are noted here for both damping versus temperature and dynamic modulus versus temperature for the $[90]_4$ laminates. The broad peak present in the damping plot (Fig. 65) for the irradiated material is an indication that a large distribution of molecular weights is present in the polymer [26]. Irradiating the graphite-epoxy composite not only produces a decrease in average molecular weight, the distribution of these weights is increased.

4.2.2 Thermomechanical Results

The data shown in Fig. 67 was produced from thermomechanical analysis (TMA) of both non-irradiated and irradiated material. For the non-irradiated laminate, the probe begins penetrating into the composite at 325°F (436K) indicating that the epoxy begins to soften at this temperature. For the irradiated laminate, the weighted probe begins penetrating into the composite at 175°F (352K). This represents a decrease of 150°F (84K) in the softening temperature of the epoxy resin.

However, the most surprising results occur when the irradiated laminate reaches a temperature of 350°F (450K). At this temperature,

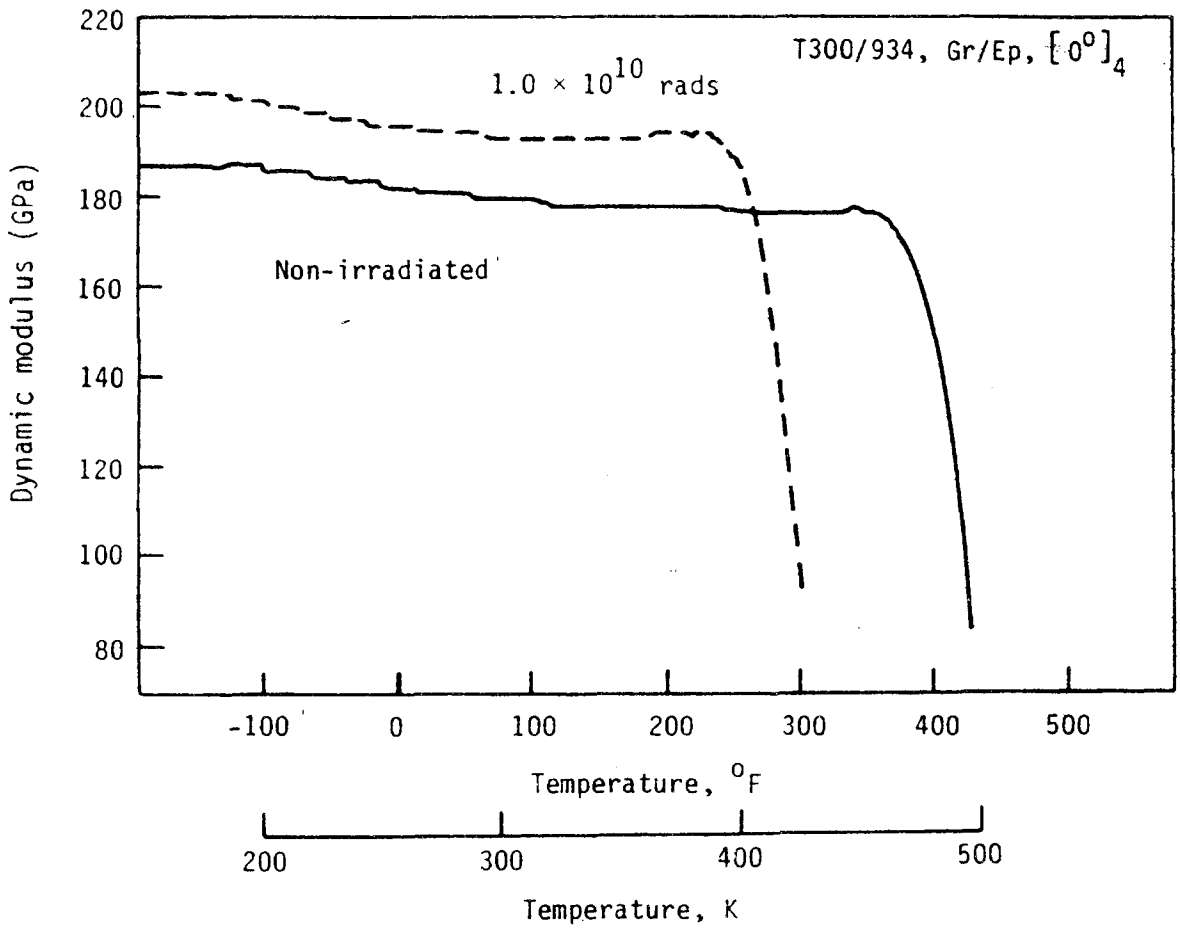

Fig. 64. **Dynamic Young's Modulus versus Temperature for Both Non-Irradiated and Irradiated $[0]_4$ DMA Specimens.**

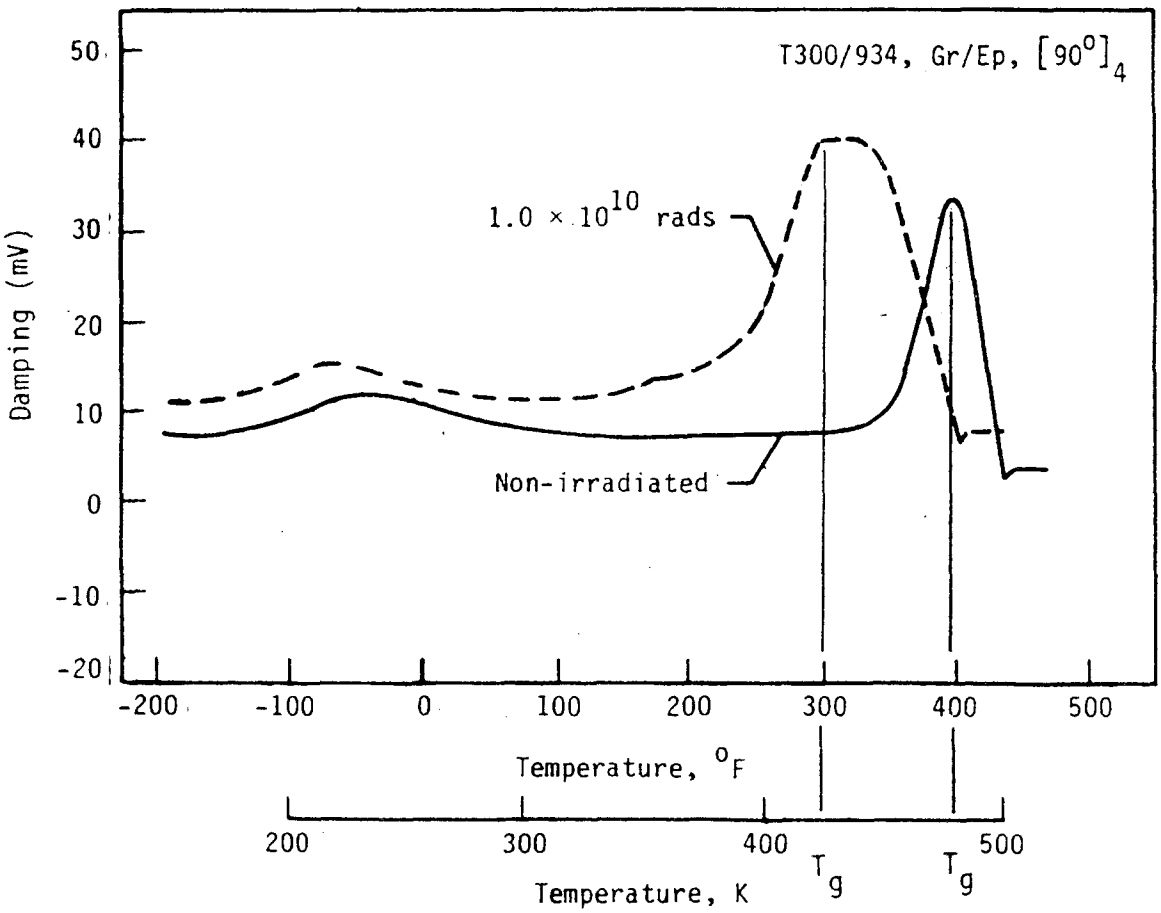

Fig. 65. Damping versus Temperature for Both Non-Irradiated and Irradiated $[90]_4$ DMA Specimens.

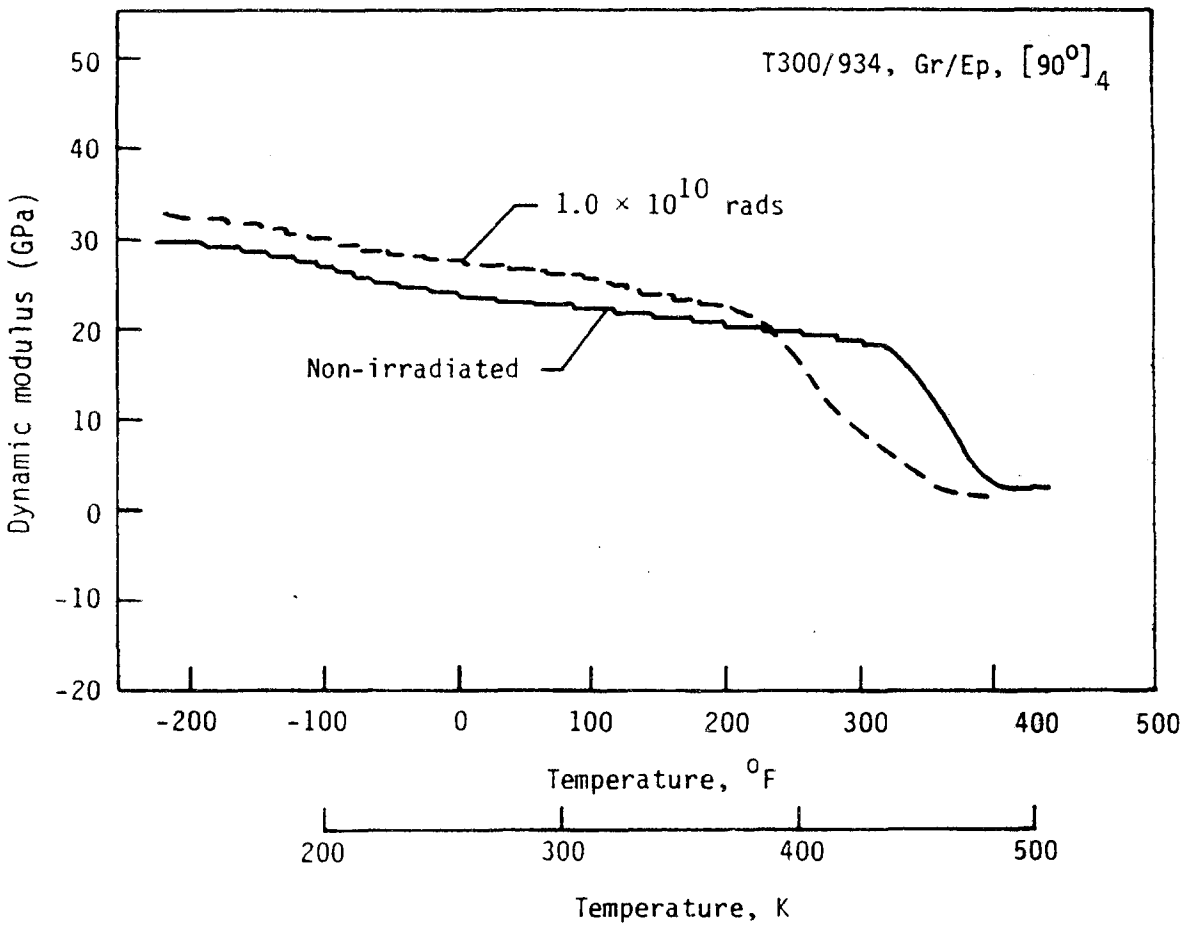

Fig. 66. Dynamic Young's Modulus versus Temperature for Both Non-Irradiated and Irradiated $[90]_4$ DMA Specimens.

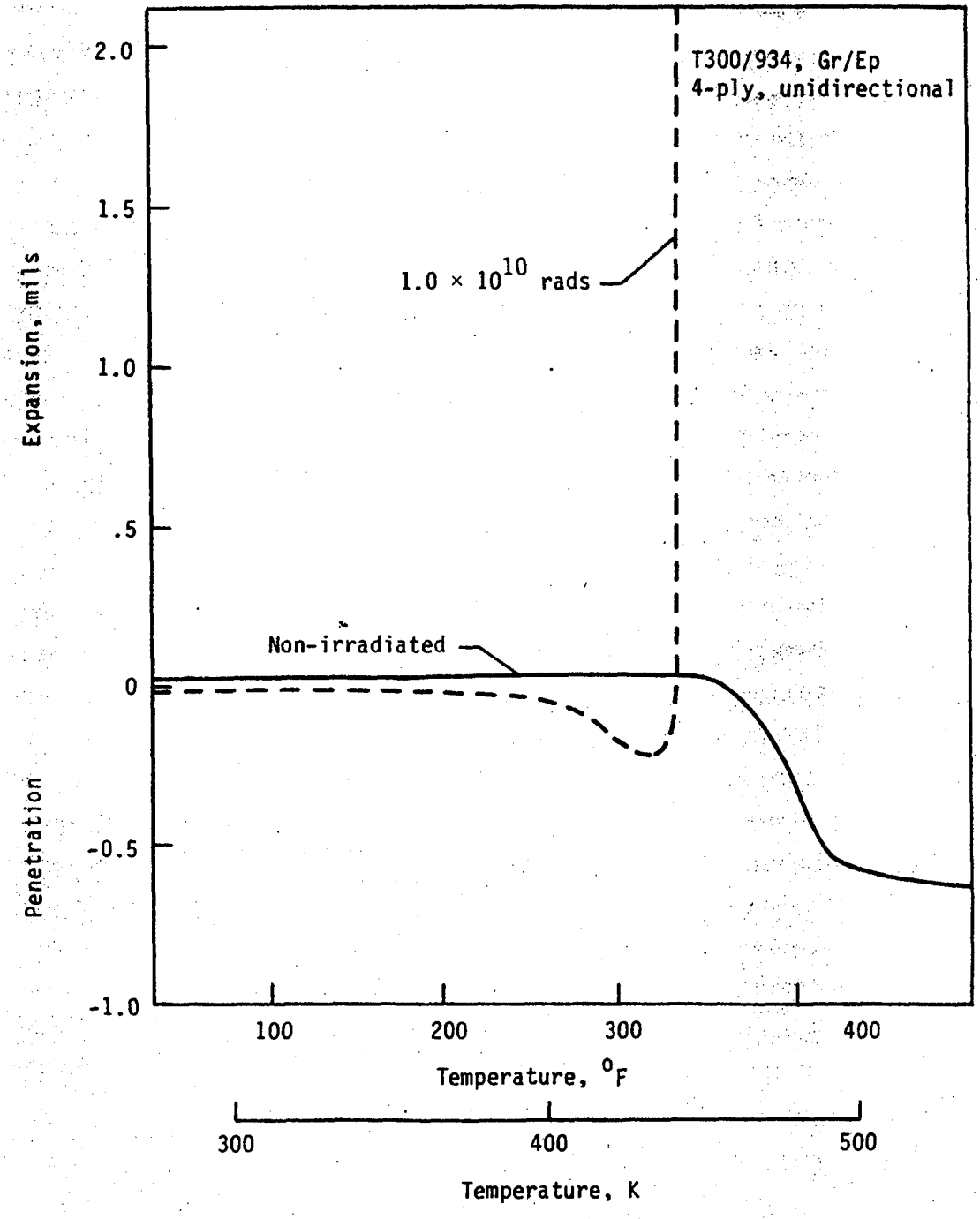

Fig. 67. Thermomechanical Analysis Results for Both Non-Irradiated and Irradiated Specimens.

the probe is pushed out of the graphite-epoxy composite. When the TMA sample was visually inspected, it was discovered that the laminate contained "bubbles" which had caused delaminations that had pushed the probe out of the sample. A photograph of these delaminations is shown in Fig. 68. Apparently, the volatile low molecular weight products, produced by radiation, boil off at this temperature. Gas pockets are formed that cause delaminations as the trapped gas expands.

A summary of radiation induced changes, in the epoxy resin of this composite system, are tabulated in Table 12. Results from dynamic-mechanical analysis (DMA) and thermomechanical analysis (TMA) were used to compile this table.

4.2.3 Degradation Product Analysis

Results from dynamic-mechanical analysis (DMA) of irradiated laminates indicates a decrease in the glass-transition temperature (T_g) by 110°F (61K). Results from thermomechanical analysis (TMA) show that volatile products gasify upon heating to blister and delaminate the composite. Based upon these observations, it appears that electron irradiation chemically alters the structure of the epoxy to provide a lower glass-transition temperature and to generate low boiling point degradation products. Identification of these products was accomplished by extracting them from the irradiated composite material and then characterizing them with infrared spectrophotometry (IR) and mass spectrometry (MS).

Degradation byproducts, produced by irradiation and measured by these two methods, are indeed low molecular weight species. Identifica-

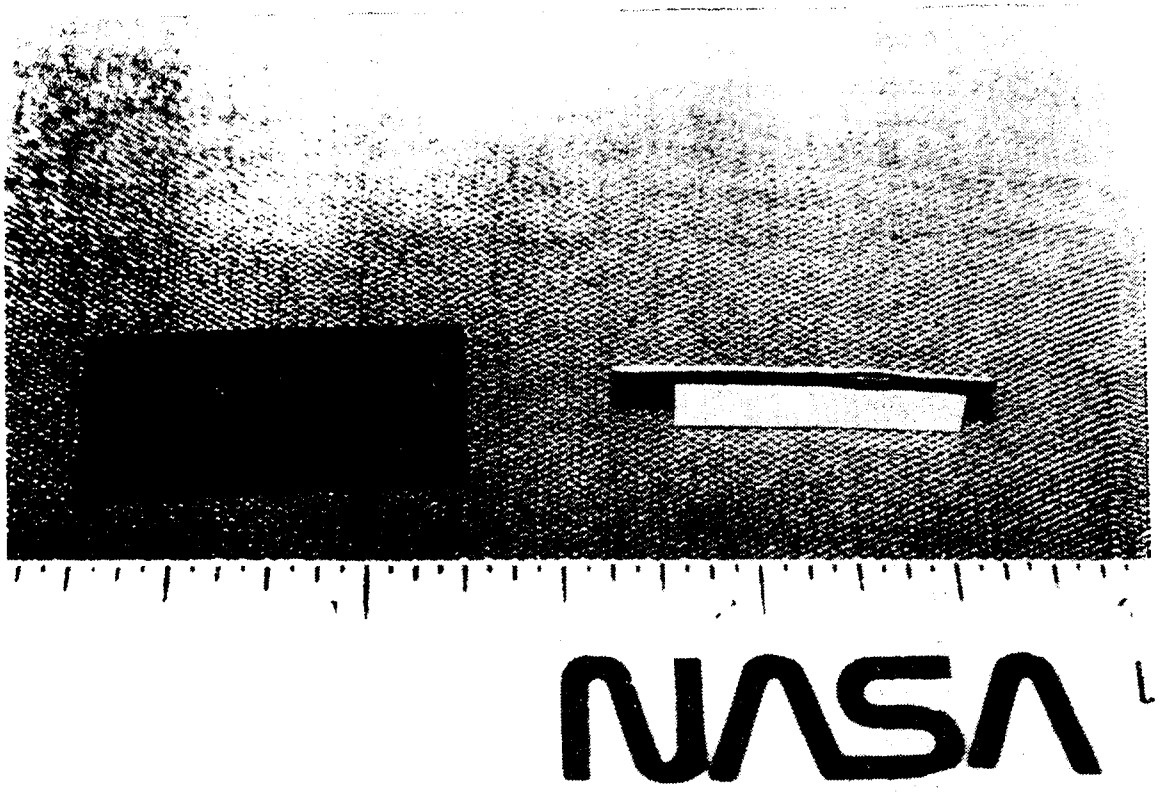

Fig. 68. Photograph of Delaminations Formed in the Irradiated Composites During TMA Tests.

Table 12

Table of Radiation Induced Changes in the Polymeric Matrix

Polymer matrix characterization parameter	Non-irradiated	1.0×10^{10} rads
Beginning of dropoff in dynamic modulus	$350^{o}F$ (450K)	$250^{o}F$ (394K)
Glass transition temperature	$410^{o}F$ (483K)	$300^{o}F$ (422K)
Beginning of plastic behavior	$325^{o}F$ (436K)	$175^{o}F$ (352K)
Temperature at which delamination begins	-	$350^{o}F$ (450K)

tion of these species indicates that the network structure of the epoxy remains basically intact following irradiation. However, small parts of the epoxy are separated from the main molecular structure by chain scisson and crosslink breakage. These products are generally small when compared to the crosslinked network. There are also indications that the majority of these degradation products come from the epoxy processing additives and not from the primary epoxy components (Fig. 69).

Results from the DMA tests can be explained with this knowledge. The formation of low molecular weight degradation products provide a wide distribution of molecular species that are able to absorb energy over an extended temperature range when compared to the non-irradiated material. A wider T_g peak occurs at a lower temperature.

Low molecular weight products will also have a low boiling point. At 350°F (450K) these byproducts gasify, thus explaining the TMA results.

Mechanical results are also explained by these radiation degradation products. Because they are small relative to the epoxy network structure, these products act as plasticizers at high temperatures (thus lowering T_g). Below room temperature, they act as antiplasticizers as they fill the free volume between long molecular segments and "freeze out" to generate a "glass" that effectively embrittles and stiffens the matrix.

4.2.4 Thermal Cycling Results

The optical photographs presented in Fig. 70 were taken during the thermal cycling phase of this investigation. The micrographs were

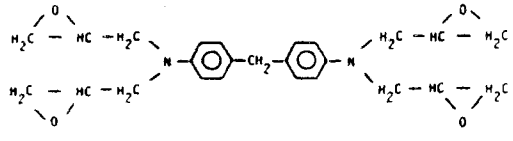

TGDDM, TETRAGLYCIDYL 4,4' - DIAMINO DIPHENYL METHANE

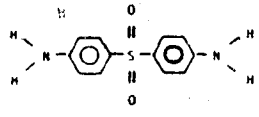

4,4' DIAMINODIPHENYL SULFONE

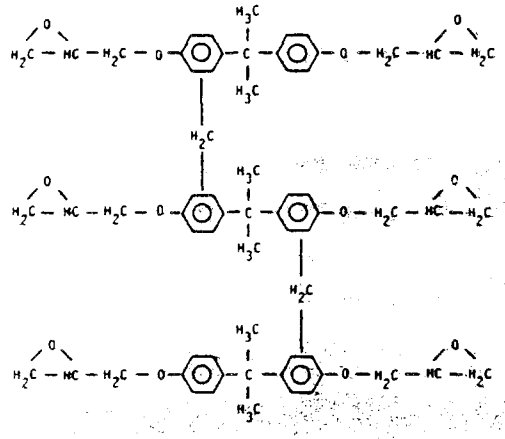

POLYGLYCIDYL ETHER OF BISPHENOL A-NOVALAC

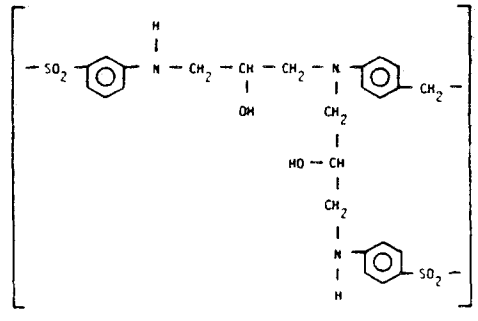

Fig. 69. Basic Chemical Structures of a 350°F-Cure Epoxy Resin.

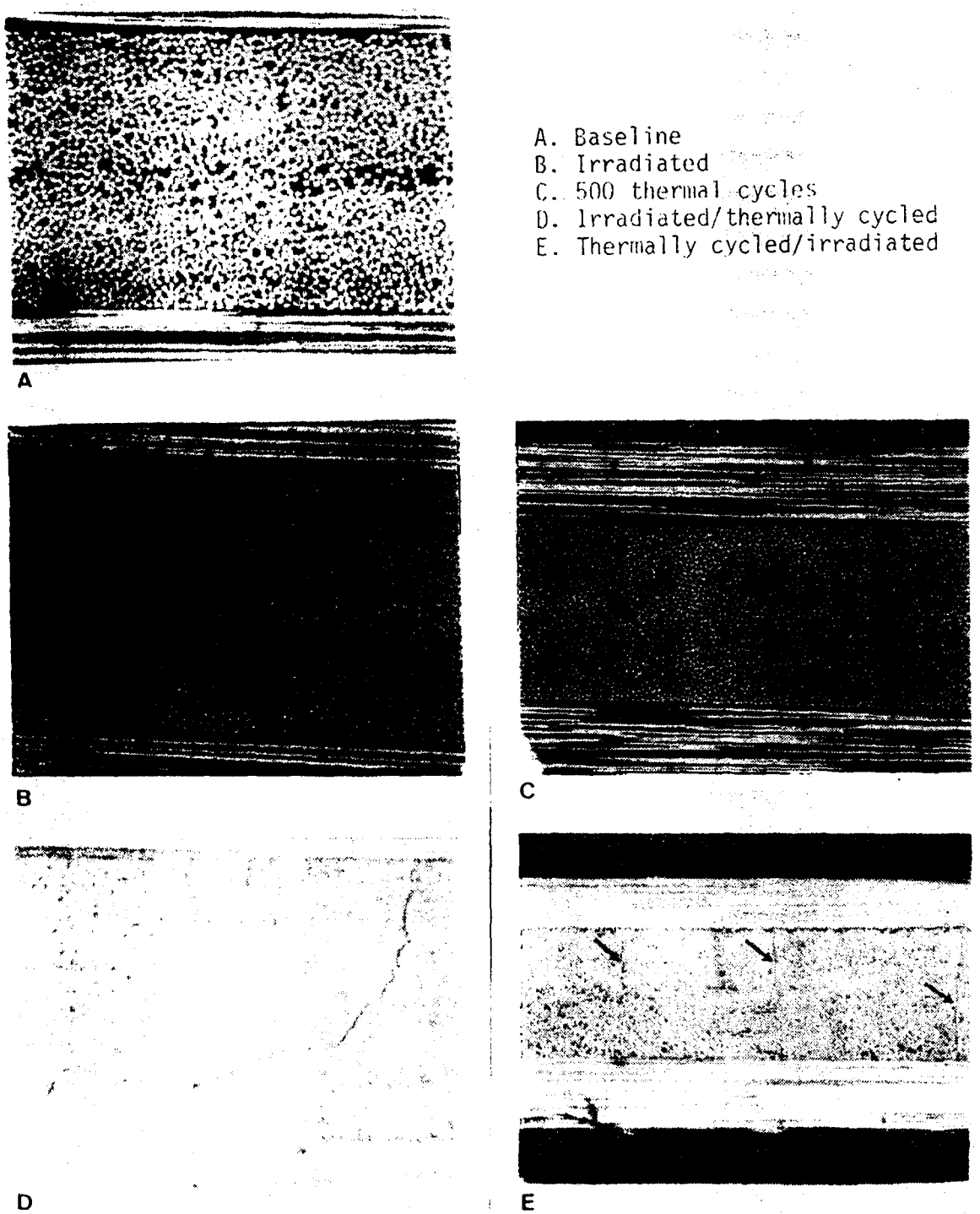

Fig. 70. Optical Photographs of Microcracking Induced by Thermal Cycling.

obtained by photographing the pre-polished edges of the $[0/90]_s$, T300/934 graphite-epoxy, laminate. Each photograph is representative of one of the five exposure conditions employed.

The "as is" or baseline photograph (Fig. 70a) shows no indication of microcracking, thus assuring that no microcracking was present before any of the following exposures.

Following a radiation dose of 1.0×10^{10} rads, inspection of the laminate's polished edge revealed no microcracking (Fig. 70b). Also, for the laminate exposed to 500 thermal cycles (-250°F (116K) to +250°F (394K)), no microcracks were observed (Fig. 70c).

However, a combination of radiation and thermal cycling (±250°F) produced microcracks. The laminate in Fig. 70d was first thermally cycled and then irradiated. Microcracks, as shown, were present in some of the laminates exposed. The laminate in Fig. 70e was first irradiated and then thermally cycled. Microcracks were present in all the laminates exposed.

The X-ray photograph shown in Fig. 71a is from the laminate that was first irradiated and then thermally cycled. The photograph in Fig. 71b is from the laminate that was first thermally cycled and then irradiated. A large amount of microcracking is evident in both cases.

The area to the left of the X-ray photograph in Fig. 71a, which does not contain many microcracks, was masked during irradiation. This area was covered by an aluminum strip which held the laminate to the aluminum back-plate during its radiation exposure. Thus, this area of the laminate did not receive any radiation exposure. Microcracking is present in the irradiated material, but not in the non-irradiated mater-

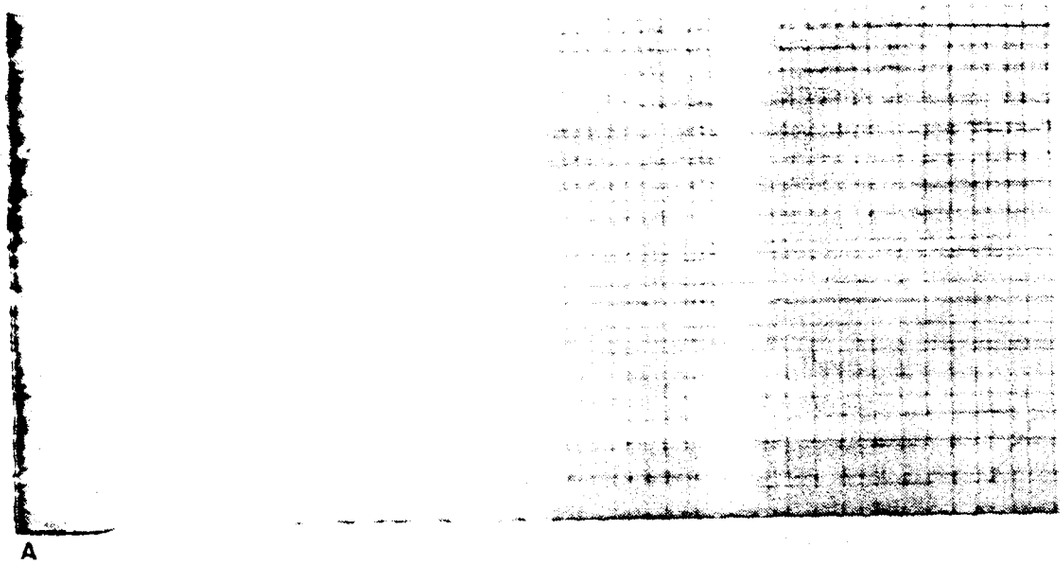

A

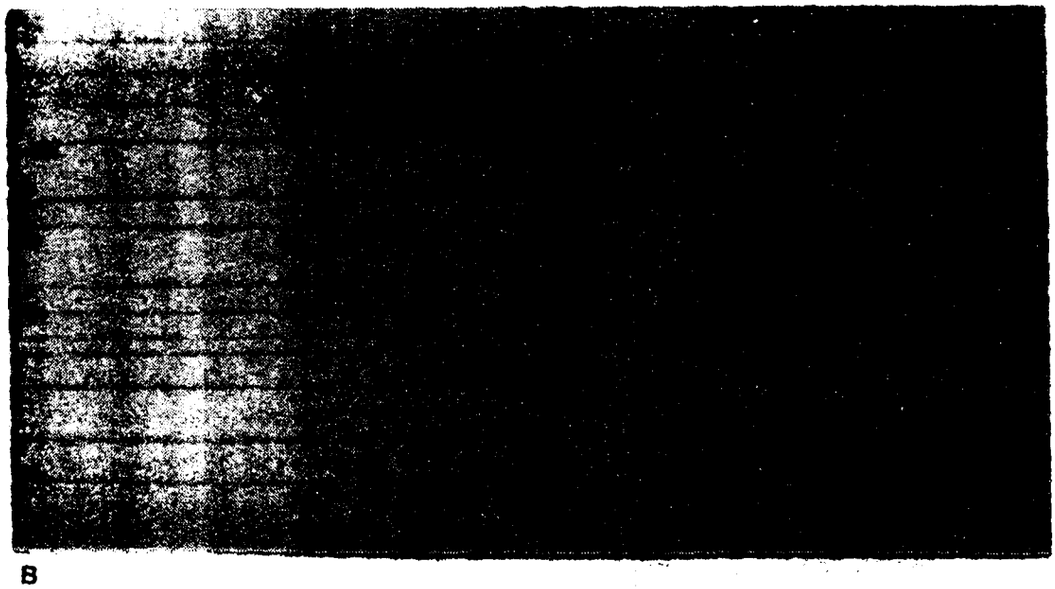

B

Fig. 71. X-Ray Photographs of Microcracking Induced by Thermal Cycling.

ial of the same laminate. This quite strongly illustrates that irradiated graphite-epoxy is susceptible to microcracking, whereas non-irradiated graphite-epoxy is not (for the $[0/90]_S$ laminate).

4.3 Fracture Surfaces of Irradiated Composites

Micrographs taken with a scanning electron microscope (SEM) of the fracture surfaces of the irradiated laminates compared to the non-irradiated laminates are presented in Figs. 72 through 77. Figs. 72 through 74 were taken from the $[10]_4$ laminates and Figs. 75 through 77 were taken from the $[90]_4$ laminates. Fig. 72 and Fig. 75 were taken at a magnification of 375x and all the others were taken at 3,400x. In all microphotographs, the column of fracture surfaces on the left are from non-irradiated laminates, and the column of fracture surfaces on the right are from irradiated laminates. The top row were tested at -250°F (116K). The middle row were tested at room temperature, 80°F (304K). The bottom row were tested at +250°F (394K).

Little difference in fracture surfaces can be noted at 375x (Fig. 72 and Fig. 75). At this magnification, the failure surfaces are, for the most part, very uniform. The only differences present appear to be in the failure patterns of the epoxy matrix.

The microphotographs presented in Figs. 73 and 76 were taken at 3,400x and focused on the matrix. Differences in matrix failure patterns are immediately apparent for each of the exposure conditions. At -250°F (116K), both the non-irradiated and the irradiated laminates exhibit brittle failure in their epoxy matrices. Brittle cleavage planes are noted for both exposure conditions. The cleavage planes in

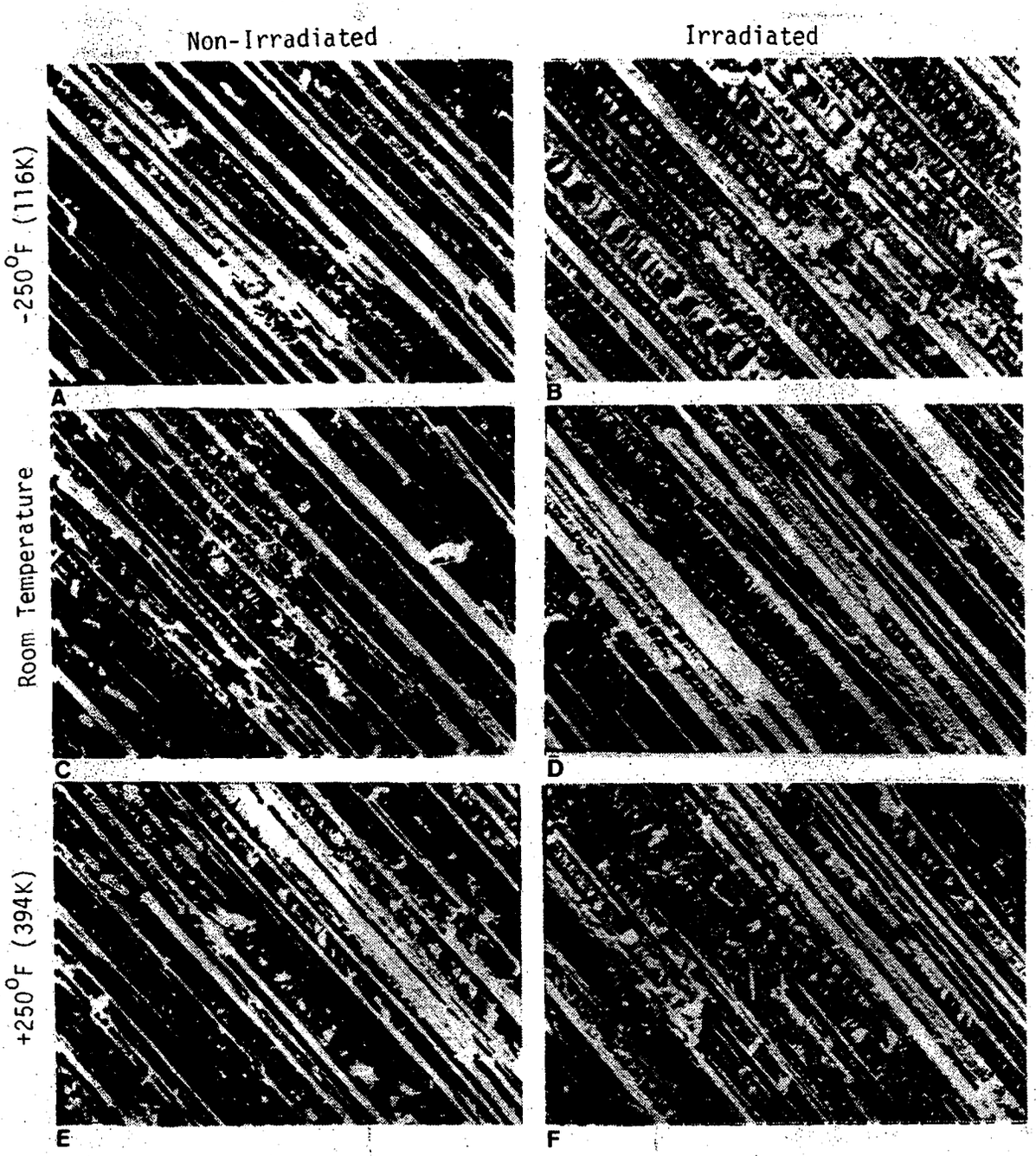

Fig. 72. Electron Micrographs of the Fracture Surfaces of the $[10]_4$ Laminate (375x).

Fig. 73. Electron Micrographs of the Fracture Surfaces of the $[10]_4$ Laminate Concentrating on the Matrix (3,400x).

Fig. 74. Electron Micrographs of the Fracture Surfaces of the $[10]_4$ Laminate Concentrating on the Fibers (3,400x).

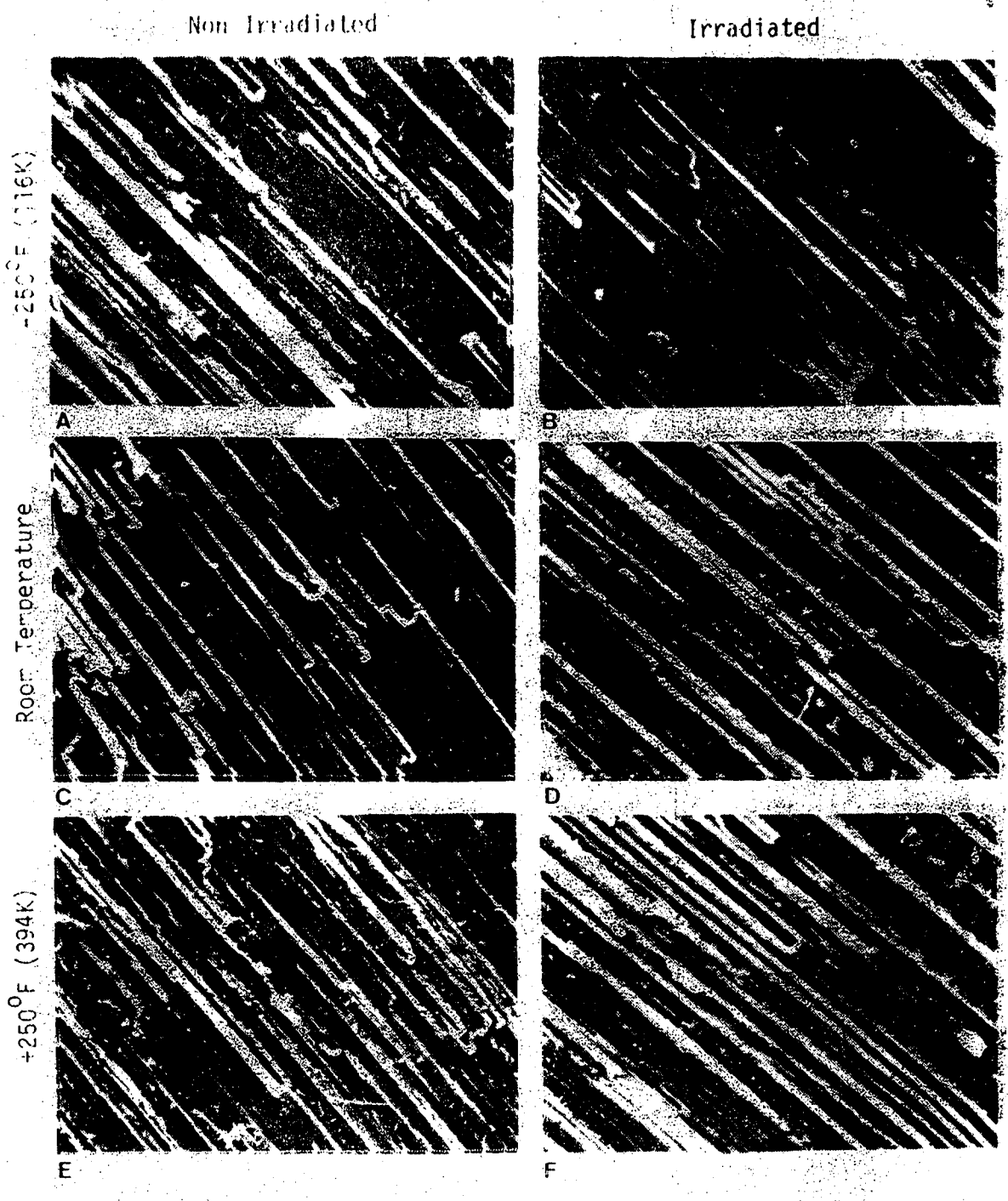

Fig. 75. Electron Micrographs of the Fracture Surfaces of the $[90]_4$ Laminate (375x).

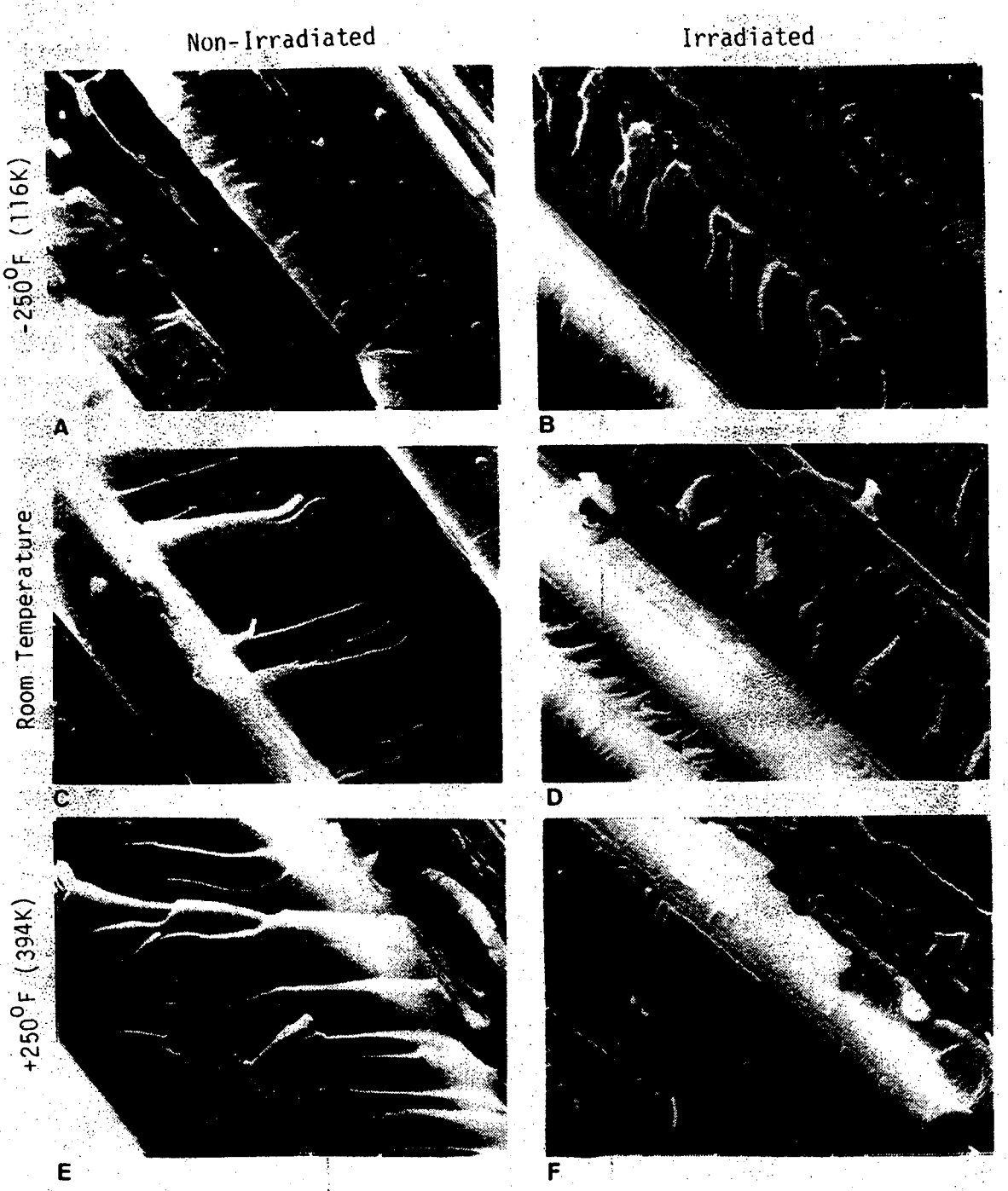

Fig. 76. Electron Micrographs of the Fracture Surfaces of the $[90]_4$ Laminate Concentrating on the Matrix (3,400x).

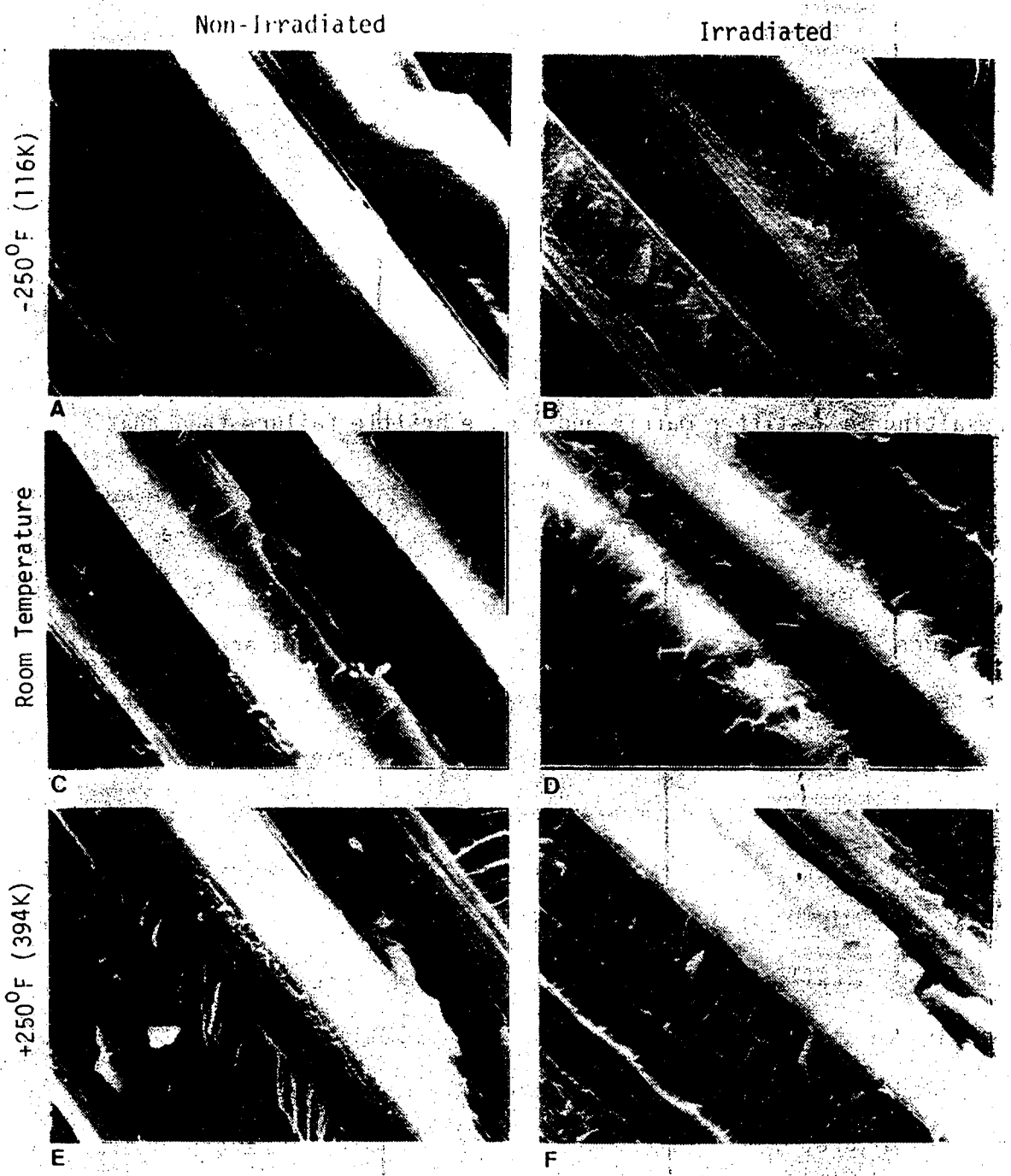

Fig. 77. Electron Micrographs of the Fracture Surfaces of the $[90]_4$ Laminate Concentrating on the Fibers (3,400x).

the irradiated laminate are smaller and more numerous than those observed in the non-irradiated laminate. This is an indication that the irradiated laminate exhibits a more brittle fracture than the non-irradiated composite. Indeed, this is the conclusion that was drawn by observing the stress-strain curves presented earlier. At -250°F (116K), the irradiated composite produces a more brittle failure and a higher modulus of elasticity than the non-irradiated material. In general, at low temperatures, radiation tends to embrittle the epoxy resin matrix resulting in a stiffer matrix and a more brittle failure than that exhibited by the non-irradiated laminate.

The photographs in the middle row of Figs. 73 and 76 were taken from specimens that had been tested at room temperature. At this temperature, the failure patterns exhibited in the matrix are plastic. Instead of failing in brittle cleavage planes, the epoxy stretched and plastically deformed before failing. At room temperature, only slight differences are observed between the non-irradiated and irradiated laminates. The irradiated material exhibits plastic deformation, but it appears "rougher" than the non-irradiated material. This is consistent with mechanical tests which indicate little difference between non-irradiated and irradiated laminates at room temperature.

At +250°F (394K), the plasticity observed in the epoxy matrix, before failure, greatly increases. For the $[10]_4$ laminate (Fig. 73), the irradiated laminate exhibits extreme amounts of plasticity prior to failure. However, this same type of behavior is not noted in the irradiated $[90]_4$ laminate (Fig. 76). This difference in failure mode is probably due to the difference between shear and tension, hydrostatic

stress is known not to influence plastic flow. The stress-strain curves for the $[90]_4$ laminates would seem to indicate this type behavior (Fig. 35). At high temperatures, the irradiated composite produces a more plastic failure and a lower modulus of elasticity than the non-irradiated material. In general, at +250°F (394K), radiation tends to greatly increase the plastic behavior of the epoxy resin matrix resulting in a more pliable matrix and a more plastic failure mode than that exhibited by the non-irradiated laminate.

The photographs presented in Fig. 74 and Fig. 77 were also taken at 3,400x, but focused in on the fibers. Graphite fibers tend to "charge" under the electron beam, making observation slightly difficult. The fibers tend to "white-out" in the photographs due to this phenomenon. Inspection of the fibers, in all photographs, shows little difference as a function of exposure condition. In all cases, the fibers remain relatively inert. Therefore, it can be concluded that the majority of radiation and temperature dependence of the fracture surfaces of this graphite-epoxy composite is due to the matrix and not the fibers. The epoxy matrix is degraded by radiation and influenced by temperature while the fibers remain relatively inert.

V. DISCUSSION

5.1 Degradation of the Elastic and Strength Properties of Graphite-Epoxy Due to Electron Irradiation

Electron radiation degrades the in-plane elastic and strength properties (tensile and shear) of the graphite-epoxy considered in this investigation. This degradation is most strongly exhibited in matrix-dominated laminates where irradiation has chemically altered the epoxy structure of the matrix. The impinging electrons sever atomic bonds in the epoxy structure, causing fragments of the epoxy to "break off". These radiation degradation byproducts are generally small when compared to the crosslink network, and the network structure of the epoxy remains basically intact.

Temperature controls the manner in which the radiation byproducts influence the mechanical behavior of these laminates. At elevated temperatures, the irradiated epoxy matrix becomes soft and pliable; and the modulus of elasticity and ultimate strength, of matrix dominated laminates, decreases (Figs. 46 and 58). At this temperature, lower values of shear modulus and shear strength are also measured, when compared to non-irradiated material (Figs. 47 and 59). The plastic behavior of the epoxy matrix comes about because the low molecular weight products, produced during irradiation, in the presence of a larger molecular structure plasticize that material at elevated temperatures. Lower strengths and stiffnesses as well as a large amount of

plasticity is present in stress-strain behavior at the elevated temperature (Figs. 33, 34, and 35).

At temperatures below room temperature, the epoxy resin becomes stiffer and more brittle following irradiation. The modulus of elasticity of matrix-dominated laminates increases, while the ultimate strength is decreased (Figs. 46 and 58). Because they are small relative to the epoxy network structure, the low molecular weight radiation byproducts fill the free volume between long molecular segments and "freeze out" at low temperatures. A "glass" is generated that effectively embrittles and stiffens the epoxy matrix resulting in lower strengths and higher modulus in matrix dominated laminates.

Small but measurable effects of irradiation are also noted in the fiber-dominated $[0]_4$ laminate. Strength is decreased slightly at high temperatures, although unchanged at and below room temperature; the modulus of elasticity (E_1) is increased slightly over the entire temperature range (Figs. 43 and 55).

Electron irradiation acts to reduce residual stresses in the epoxy matrix of the composite by breaking some of the bonds within the epoxy structure. Lower residual stresses result in straighter fibers giving the irradiated material a higher modulus than the non-irradiated material. The increased plasticity of the irradiated epoxy at high temperatures decreases the matrix's ability to transfer load at fiber breaks, resulting in decreased strength.

5.2 Degradation of the Epoxy Resin Due to Electron Irradiation

The irradiated epoxy resin becomes extremely plastic at elevated temperatures and very brittle at low temperatures. These changes have been attributed to the low-molecular-weight degradation products that are generated within the epoxy when it is exposed to electron radiation.

Dynamic-mechanical analysis (DMA) results show that a large distribution of molecular weights are present in irradiated laminates, and that these degradation byproducts lower the glass-transition temperature (T_g) of the epoxy resin (Fig. 63). A lower glass-transition temperature in an epoxy indicates that the epoxy will lose its crystallinity at a lower temperature. In other words, the epoxy becomes more plastic at lower temperatures, thus supporting the results noted during mechanical testing. Thermomechanical analysis (TMA) results indicate that when the irradiated material is heated, these low molecular weight degradation products vaporize, causing the laminate to blister and delaminate (Fig. 67). This indicates that these byproducts are indeed small when compared to the epoxy network structure, and are able to plasticize the epoxy at high temperatures and embrittle it at low temperatures.

Analysis and characterization of the radiation byproducts, by Infrared Spectrophotometry (IR) and Mass Spectrometry (MS), reveals that the irradiated laminates have a significant quantity of these low molecular weight products trapped within. The network structure of the epoxy remains basically intact. However, small parts of the epoxy have been separated from the main molecular structure by chain scisson and cross-link breakage. Indications are that the majority of these degradation products are generated from the epoxy processing additives and not from

the primary epoxy components. If these processing additives could be replaced or removed, the radiation resistance of the epoxy might be improved.

5.3 Analysis of Failure Surfaces

Inspection of the fracture surfaces of the non-irradiated and irradiated laminates, with the aid of a scanning electron microscope (SEM), shows differences in failure due to radiation and temperature exposure.

At low temperatures, where mechanical results indicate brittle behavior, brittle cleavage planes are observed in the failed epoxy matrix. The cleavage planes in the irradiated laminate are smaller and more numerous than those observed in the non-irradiated laminate, indicating a more brittle fracture.

Mechanical results, especially the stress-strain curves, exhibit significant non-linearity at elevated temperatures. Inspection of the epoxy matrix at high magnifications shows that large amounts of plastic deformation are present.

The experimental results produced in this investigation indicate that the radiation induced degradation is due primarily to changes in the epoxy resin. Microscopic examination of these laminates shows that the matrix fails by different modes that are dependent on the radiation and temperature employed, thus indicating changes in the matrix material. Microscopic examination of the fibers, on the other hand, reveals that they remain inert. Inspection of the fiber-matrix interface does

not clearly indicate whether it plays a role in determining radiation-altered mechanical properties, or not.

Microscopic examination of the fracture surfaces of the laminates tested, supported the differences in mechanical behavior that were measured. By microscopically observing the matrix, changes due to radiation can be noted. The differences in mechanical behavior of the epoxy matrix can be related to differences in mechanical behavior of the composite.

VI. SUMMARY

The following is a summary of the conclusions drawn from the results of this investigation into the effects of the space environment on graphite-epoxy composite materials. It should be noted here that these tests were performed under greatly accelerated conditions; a composite structure may be influenced to a greater or lesser degree during a 10 to 20 year service life.

1) Electron radiation acts to degrade in-plane elastic and strength properties (tensile and shear) of T300/934 graphite-epoxy composite.
   a) This radiation-induced degradation is most evident for matrix-dominated properties.
   b) Temperature controls the manner in which the radiation influences the mechanical behavior. Degradation is severe at both high and low temperatures.
2) The electron radiation degradation is present due to low-molecular- weight products generated during irradiation.
   a) These radiation-induced byproducts plasticize the epoxy matrix at high temperatures, and embrittle it at low temperatures.
   b) The degradation products lower the glass- transition temperature (T_g) of the epoxy.
   c) The degradation products vaporize and cause delaminations at elevated temperatures (above 350°F (450K)).

d) Microcracking is observed in irradiated (but not non-irradiated) laminates during thermal cycling.

3) The fracture behavior of the irradiated laminates is plastic at elevated temperatures and brittle at low temperatures. These differences can be observed with the aid of a scanning electron microscope (SEM).

Recommendations for Future Work

1) A study into the effect of radiation on graphite fibers should be conducted to ascertain whether or not fibers are degraded by electrons.

2) Irradiated laminates should be investigated, at elevated temperatures, by loading and unloading them to fully characterize the plastic (non-linear) behavior that is present.

3) A study should be made to determine whether holding irradiated laminates at high temperatures (<350°F) for long periods of time will "heal" radiation degradation.

4) Another investigation, similar to this one, should be carried out on another resin system, with other processing additives, (or, possibly no additives) to determine if a more radiation-resistant epoxy can be produced.

REFERENCES

1. Zweben, C., "Advanced Composites - A Revolution for the Designer," AIAA 50th Anniversary Annual Meeting and Technical Display, Long Beach, California, May 12-14, 1981.

2. Halstead, C., Schmigle, R., and Welch, D., "Space Shuttle Payload Bay Door Development Certification Test Program," 24th National SAMPE Symposium and Exhibition, San Francisco, California, May 1979.

3. McRoberts, J. J., "Space Telescope," National Aeronautics and Space Administration, Division of Public Affairs, Washington, D.C., NASA-EP-166.

4. Abt, B. and Rieger, H., "High Precision Graphite/Epoxy Antennas for Communications Satellites," Dornier System GmbH, D 7990, Friedrichshafer, Germany.

5. Vaughn, R. L. and Friend, C. A., "The Challenges of Manufacturing Graphite-Epoxy Structural Columns for Space Platforms," 26th National SAMPE Symposium, April 28-30, 1981, pp. 339-349.

6. Hook, W. R., "Space Stations - Historical Review and Current Plans," presented at the ASME Winter Annual Meeting, Phoenix, Arizona, November 14-19, 1982.

7. Tenney, D. R., Sykes, G. F., and Bowles, D. E., "Space Environmental Effects on Materials," presented at AGARD, Environmental Effects on Materials for Space Applications, Toronto, Canada, September 22-24, 1982.

8. Garrett, H. B., "Review of the Near-Earth Spacecraft Environment," SPIE, Vol. 216, Optics in Adverse Environments, 1980, pp. 109-115.

9. Kelley, H. M., Rummler, D. R., and Jackson, L. R., "Research in Structures and Materials for Future Space Transportation Systems - An Overview," J. Spacecraft and Rockets, Vol. 20, No. 1, Jan.-Feb. 1983, pp. 89-96.

10. Delmonte, J., Technology of Carbon and Graphite Fiber Composites, Van Nostrand Reinhold Company, New York, New York, 1980.

11. Haskins, J. F. and Holmes, R. D., "Advanced Composites Design Data for Spacecraft Structural Applications," AFML-TR-79-4208, May 1979.

12. Haskins, J. F., "Advanced Composite Design Data for Spacecraft Structural Applications," presented at the 12th National SASMPE Technical Conference, Seattle, Washington, October 7-9, 1980.

13. Mazzio, V. T., et al., "Composite Data for Spacecraft," AFWL-TR-82-4079, August 1982.

14. Mazzio, V. T. and Juneau, P. W., Jr., "Space Radiation Environmental Effects on Selected Properties of Advanced Composite Materials," American Institute of Aeronautics and Astronautics, 1983.

15. "Inplane Shear Stress-Strain Response of Unidirectional Reinforced Plastics," ASTM-D-3518-76.

16. "Apparent Interlaminar Shear Strength of Parallel Fiber Composites by Short-Beam Method," ASTM-D-2344-76.

17. Naranong, N., "Effect of High Energy Radiation on Mechanical Properties of Graphite Fiber Reinforced Composites," M.S. Thesis, North Carolina State University at Raleigh, 1980.

18. Formes, R. E., et al., "Effects of High Energy Radiation on the Mechanical Properties of Epoxy Graphite Fiber Composites," status report, Jan. 1-Dec. 31, 1981, North Carolina State University at Raleigh, 1981.

19. Wolf, K. W., "Effect of Ionizing Radiation on the Mechanical and Structural Properties of Graphite Fiber Reinforced Composites," Ph.D. Dissertation, North Carolina State University at Raleigh, 1982.

20. Kent, G. M., "X-Ray and ESR Characterization of the Effects of High Energy Radiation of Graphite Fiber Reinforced Composite Materials," M.S. Thesis, North Carolina State University at Raleigh, 1982.

21. Formes, R. E., et al., "Effect of 1.33 MeV Gamma Radiation and 0.5 MeV Electrons of the Mechanical Properties of Graphite Fiber Composites," North Carolina State University at Raleigh, 1982.

22. Wolf, K. W., Memory, J. D., Gilbert, R. D., and Fornes, R. E., "Effects of 0.5 MeV Electrons on the Interlaminar Shear and Flexural Strength Properties of Graphite Fiber Composites," J. Applied Physical, Vol. 54, No. 10, October 1983.

23. "Flexural Properties of Unreinforced and Reinforced Plastics and Electrical Insulating Materials," ASTM-D-790-81.

24. "In-Plane Shear Strength of Reinforced Plastics," ASTM-D-3846-79.

25. Lindenmeyer, P. H. and Fogdall, L. B., "Development of Facilities, Quality-Control Procedures, and Testing Techniques for Irradiation of Spacecraft Composite Materials--Task Report," The Boeing Company, D180-26094-3, November 1983.

26. Murayama, T., "Dynamic Mechanical Analysis of Polymeric Material," Elsexier Scientific Publishing Company, Amsterdam, The Netherlands, 1978.

27. Gramelt, C., "A New Approach for Determining Mechanical Properties of Thermoset Resins During the Cure Cycle," American Laboratory, January 1984.

28. Mauri, R. E. and Crossman, F. W., "Space Radiation Effects on Structural Composites," presented at the AIAA 21st Aerospace Sciences Meeting, Reno, Nevada, January 10-13, 1983.

29. Equsa, S., Kirk, M. A., Birtcher, R. C., Hagiwara, M., and Kawanishi, S., "Irradiation Effects on the Mechanical Properties of Composite Organic Insulators," U.S. Department of Energy, Argonne National Laboratory, Argonne, Illinois, May 1983.

30. Giori, C., Yamauchi, T., Rajan, K., and Mell, R., "Mechanisms of Degradation of Graphite Composites in a Simulated Space Environment," presented at the AIAA 21st Aerospace Sciences Meeting, Reno, Nevada, January 10-13, 1983.

31. Chamis, C. C., and Sinclair, J. H., "Ten-deg Off-axis Test for Shear Properties in Fiber Composites," Experimental Mechanics, Vol. 17, No. 9, p. 339-346, September 1977.

32. Jones, R. M., Mechanics of Composite Materials, Scripta Book Company, Washington, D.C., 1975.

33. Pindera, M. J. and Herakovich, C. T., "An Endochronic Theory for Transversely Isotropic Fiberous Composites," VPI-E-81-27, Virginia Polytechnic Institute and State University, October 1981.

34. Pindera, M. J. and Herakovich, C. T., "An Elastic Potential for the Nonlinear Response of Unidirectional Graphite Composites," Journal of Applied Mechanics, Transactions of the ASME (in press).

35. Curtis, G. J., Milne, J. M., and Reynolds, W. N., "Non-Hookean Behavior of Strong Carbon Fibers," Nature, Volume 220, December 1968, p. 1024.

36. Beetz, C. P., Jr., "Strain-Induced Stiffening of Carbon Fibers," Fibre Science and Technology, Volume 16, 1982.

37. Mansfield, E. H. and Purslow, D., "The Influence of Fiber Waviness on the Moduli of Unidirectional Fiber Reinforced Composites," CP No. 1339, December 1974.

38. Bazant, Z. P., "Effect of Curvature of the Reinforcing Fibers on the Moduli of Elasticity and Strength of Composites," Polymer Mechanics, Volume 4, November 2, 1968, pp. 251-258.

39. Comninou, M. and Yannas, I. V., "Dependence of Stress-Strain Nonlinearity of Connective Tissues on the Geometry of Collagen Fibers," J. of Biomechanics, Volume 9, 1976, pp. 427-433.

40. Bert, C. W., "Micromechanics of the Different Elastic Behavior of Filamentary Composites in Tension and Compression," Mechanics of Bimodulus Materials, AMD Volume 33, ASME, N.Y., 1979, pp. 17-28.

41. VanDreumel, W. H. M., and Kamp, J. L. M., "Non-Hookean Behavior in the Fibre Direction of Carbon-Fibre Composites and the Influence of Fibre Waviness on the Tensile Properties," J. Composite Materials, Volume 11, October 1977, p. 461.

42. Hyer, M. W., Herakovich, C. T., Milkovich, S. M., and Short, J. S., "Temperature Dependence of Mechanical and Thermal Expansion Properties of T300/5208 Graphite-Epoxy," Composites, Volume 14, July 1983, pp. 276-280.

43. Milkovich, S. M. and Herakovich, C. T., "Temperature Dependence of Elastic and Strength Properties of T300/5208 Graphite-Epoxy," VPI-E-83-9, Virginia Polytechnic Institute and State University, Blacksburg, Virginia, 1984.

44. Private communication with W. Slemp, Director of the Space Materials Durability Laboratory, NASA-Langley Research Center, Hampton, Virginia.

45. DuPont Company (Clinical and Instrument Systems Division), 981 Dynamic-Mechanical Analysis System (DMA) Product Bulletin.

46. DuPont Company (Clinical and Instrument Systems Division), 981 Dynamic-Mechanical Analyzer, Instruction Manual.

47. DuPont Company (Clinical and Instrument Systems Division), 942 Thermomechanical Analyzer, Instruction Manual.

48. Adams, D. S., Bowles, D. E., and Herakovich, C. T., "Characteristics of Thermally-Induced Transverse Cracks in Graphite-Epoxy Composite Laminates," VPI-E-83-23, Dept. of Engineering Science and Mechanics, VPI & SU, June 1983.

49. Santos, B., "The Effect of Electron and Proton Radiation on Four Polysulfones," M.S. Thesis, George Washington University, NASA-Langley Research Center, Hampton, Virginia, August 1982.

APPENDIX

Table A1

Table of Individual Test Results for the $[0]_4$ Laminate.

Specimen	Temperature	X_T ksi (MPa)	E_1 msi (GPa)	ν_{12}
Non-irradiated:				
1.	-250°F (116K)	143.8 (992)	18.70 (129)	0.3326
2.		142.8 (985)	18.29 (126)	0.2999
3.		136.2 (939)	18.88 (130)	0.3061
Average		140.9 (972)	18.62 (128)	0.3129
1.	Room temperature	221.2 (1525)	18.74 (129)	0.3161
2.		220.4 (1520)	19.32 (133)	0.3140
3.		224.6 (1549)	18.58 (128)	0.3129
Average		222.1 (1531)	18.88 (130)	0.3143
1.	+250°F (394K)	210.4 (1451)	19.14 (132)	0.3634
2.		195.7 (1349)	19.05 (131)	0.3350
3.		174.9 (1206)	18.90 (130)	0.3356
Average		193.7 (1336)	19.03 (131)	0.3447
1.0×10^{10} rads:				
1.	-250°F (116K)	149.3 (1029)	19.45 (134)	0.3829
2.		134.6 (928)	18.93 (131)	0.3497
3.		98.0 (676)	19.11 (132)	0.3721
Average		127.3 (878)	19.16 (132)	0.3682
1.	Room temperature	221.7 (1529)	19.37 (134)	0.2948
2.		243.8 (1681)	19.52 (135)	0.2941
3.		202.2 (1394)	19.03 (131)	0.2603
Average		222.6 (1535)	19.31 (133)	0.2831
1.	+250°F (394K)	184.5 (1272)	19.77 (136)	0.3768
2.		150.3 (1036)*	19.23 (133)	0.3830
3.		149.7 (1032)*	20.29 (140)	0.4311
Average		161.5 (1114)	19.76 (136)	0.3970

Table A2

Table of Individual Test Results for the $[10]_4$ Laminate.

Specimen	Temperature	$\sigma_{ult}(10^o)$ ksi	(MPa)	S ksi	(MPa)	$E_x(10^o)$ msi	(GPa)
Non-irradiated:							
1.		53.84	(371)	9.21	(63.5)	12.52	(86.3)
2.	-250^oF	38.68	(267)	6.61	(45.6)	13.53	(93.3)
3.	(116K)	36.32	(250)	6.21	(42.8)	13.20	(91.0)
Average		42.95	(296)	7.34	(50.6)	13.08	(90.2)
1.		64.15	(442)	10.97	(75.6)	10.93	(75.4)
2.	Room	57.79	(398)	9.88	(68.1)	10.61	(73.2)
3.	temperature	52.11	(359)	8.91	(61.4)	10.63	(73.3)
Average		58.02	(400)	9.92	(68.4)	10.72	(73.9)
1.		31.83	(219)	5.44	(37.5)	8.19	(56.5)
2.	$+250^oF$	38.22	(264)	6.54	(45.1)	8.52	(58.7)
3.	(394K)	34.75	(240)	5.94	(41.0)	8.52	(58.7)
Average		34.93	(241)	5.97	(41.2)	8.41	(58.0)
1.0×10^{10} rads:							
1.		43.57	(300)	7.45	(51.4)	12.60	(86.9)
2.	-250^oF	41.18	(284)	7.04	(48.5)	11.01	(75.9)
3.	(116K)	42.42	(292)	7.25	(50.0)	12.75	(87.9)
Average		42.39	(292)	7.25	(50.0)	12.12	(83.6)
1.		56.21	(388)	9.61	(66.3)	9.98	(68.8)
2.	Room	58.26	(402)	9.96	(68.7)	10.16	(70.1)
3.	temperature	47.87	(330)	8.19	(56.5)	10.60	(73.1)
Average		54.11	(373)	9.25	(63.8)	10.25	(70.7)
1.		22.63	(156)	3.87	(26.7)	5.37	(37.0)
2.	$+250^oF$	26.02	(179)	4.45	(30.7)	6.44	(44.4)
3.	(394K)	22.49	(155)	3.85	(26.5)	6.84	(47.2)
Average		23.71	(163)	4.06	(28.0)	6.22	(42.9)

Table A3

Table of Individual Test Results for the $[45]_4$ Laminate.

Specimen	Temperature	$\sigma_{ult}(45^{o})$ ksi	(MPa)	$E_x(45^{o})$ msi	(GPa)	G_{12} msi	(GPa)
Non-irradiated:							
1.	-250°F (116K)	14.50	(100.0)	2.892	(19.9)	1.225	(8.4)
2.		13.33	(91.9)	2.725	(18.8)	1.110	(7.7)
3.		9.67	(66.7)	2.825	(19.5)	1.178	(8.1)
Average		12.50	(86.2)	2.814	(19.4)	1.170	(8.1)
1.	Room temperature	15.06	(103.8)	1.823	(12.6)	0.692	(4.8)
2.		13.75	(94.8)	1.806	(12.5)	0.682	(4.7)
3.		13.83	(95.4)	1.819	(12.5)	0.689	(4.8)
Average		14.21	(98.0)	1.816	(12.5)	0.688	(4.8)
1.	+250°F (394K)	11.59	(79.9)	1.381	(9.5)	0.482	(3.3)
2.		11.16	(76.9)	1.617	(11.1)	0.605	(4.2)
3.		8.01	(55.2)	1.618	(11.2)	0.606	(4.2)
Average		10.25	(70.7)	1.539	(10.6)	0.563	(3.9)
1.0×10^{10} rads:							
1.	-250°F (116K)	9.36	(64.5)	2.978	(20.5)	1.165	(8.0)
2.		11.68	(80.5)	2.963	(20.4)	1.156	(8.0)
3.		9.25	(63.8)	2.785	(19.2)	1.051	(7.2)
Average		10.10	(69.6)	2.909	(20.1)	1.123	(7.7)
1.	Room temperature	12.95	(89.3)	2.087	(14.4)	0.810	(5.6)
2.		14.71	(101.4)	2.029	(14.0)	0.776	(5.4)
3.		15.77	(108.7)	1.974	(13.6)	0.744	(5.1)
Average		14.48	(99.8)	2.030	(14.0)	0.777	(5.4)
1.	+250°F (394K)	6.28	(43.3)	1.174	(8.1)	0.407	(2.8)
2.		7.84	(54.1)*	1.326	(9.1)	0.484	(3.3)
3.		5.39	(37.2)	0.956	(6.6)	0.309	(2.1)
Average		6.50	(44.8)	1.152	(7.9)	0.397	(2.7)

Table A4

Table of Individual Test Results for the $[90]_4$ Laminate.

Specimen	Temperature	Y_T ksi	(Y_T MPa)	E_2 msi	(E_2 GPa)	ν_{21}
Non-irradiated:						
1.	-250°F (116K)	4.47	(30.8)	1.824	(12.6)	0.0307
2.		4.19	(28.9)	1.854	(12.8)	
3.		5.02	(34.6)	1.808	(12.5)	
Average		4.56	(31.4)	1.829	(12.6)	
1.	Room temperature	10.34	(71.3)	1.410	(9.7)	0.0187
2.		10.85	(74.8)	1.369	(9.4)	
3.		6.92	(47.7)	1.350	(9.3)	
Average		9.37	(64.6)	1.376	(9.5)	
1.	+250°F (394K)	7.70	(53.1)	1.227	(8.5)	0.0225
2.		8.68	(59.8)	1.199	(8.3)	
3.		3.91	(27.0)	1.296	(8.9)	
Average		6.76	(46.6)	1.241	(8.6)	
10×10^{10} rads:						
1.	-250°F (116K)	2.18	(15.0)	1.939	(13.4)	0.0408
2.		2.80	(19.3)	2.146	(14.8)	
3.		3.44	(23.7)	2.284	(15.7)	
Average		2.81	(19.4)	2.123	(14.6)	
1.	Room temperature	8.73	(60.2)	1.545	(10.7)	0.0222
2.		6.52	(45.0)	1.534	(10.6)	
3.		5.68	(39.2)	1.465	(10.1)	
Average		6.98	(48.1)	1.515	(10.4)	
1.	+250°F (394K)	6.22	(42.9)	1.142	(7.9)	0.0214
2.		5.75	(39.6)	1.037	(7.2)	
3.		5.67	(39.1)	1.014	(7.0)	
Average		5.88	(40.5)	1.064	(7.3)	

VIRGINIA TECH CENTER FOR COMPOSITE MATERIALS AND STRUCTURES

The Center for Composite Materials and Structures is a coordinating organization for research and educational activity at Virginia Tech. The Center was formed in 1982 to encourage and promote continued advances in composite materials and composite structures. Those advances will be made from the base of individual accomplishments of the thirty-four founding members who represent ten different departments in two colleges.

The Center functions by means of an Administrative Board which is elected yearly. The general purposes of the Center include:

- collection and dissemination of information about composites activities at Virginia Tech,
- contact point for other organizations and individuals,
- mechanism for collective educational and research pursuits,
- forum and mechanism for internal interactions at Virginia Tech.

The Center for Composite Materials and Structures is supported by a vigorous program of activity at Virginia Tech that has developed since 1963. Research expenditures for investigations of composite materials and structures total well over five million dollars with yearly expenditures presently approaching two million dollars.

Research is conducted in a wide variety of areas including design and analysis of composite materials and composite structures, chemistry of materials and surfaces, characterization of material properties, development of new material systems, and relations between damage and response of composites. Extensive laboratories are available for mechanical testing, nondestructive testing and evaluation, stress analysis, polymer synthesis and characterization, material surface characterization, component fabrication and other specialties.

Educational activities include eight formal courses offered at the undergraduate and graduate levels dealing with the physics, chemistry, mechanics, and design of composite materials and structures. As of 1982, some 33 Doctoral and 37 Master's students have completed graduate programs and several hundred Bachelor-level students have been trained in various aspects of composite materials and structures. A significant number of graduates are now active in industry and government.

Various Center faculty are internationally recognized for their leadership in composite materials and composite structures through books, lectures, workshops, professional society activities, and research papers.

FOUNDING MEMBERS OF THE CENTER

Aerospace and Ocean Engineering
Raphael T. Haftka
William L. Hallauer, Jr.
Eric R. Johnson

Chemical Engineering
Donald G. Baird

Chemistry
James E. McGrath
Thomas C. Ward
James P. Wightman

Civil Engineering
Raymond H. Plaut

Electrical Engineering
Ioannis M. Besieris
Richard O. Claus

Engineering Science and Mechanics
Hal F. Brinson
John C. Duke, Jr.
Daniel Frederick
Robert A. Heller
Edmund G. Henneke, II
Carl T. Herakovich
Michael W. Hyer
Robert M. Jones
Manohar P. Kamat
Alfred C. Loos
Don H. Morris
Daniel Post
Jununthula N. Reddy
Kenneth L. Reifsnider
Wayne W. Stinchcomb

Industrial Engineering and Operations Research
Joel A. Nachlas

Materials Engineering
David W. Dwight
D. P. H. Hasselman
Charles R. Houska
M. R. Louthan, Jr.

Mathematics
Werner E. Kohler

Mechanical Engineering
Norman S. Eiss, Jr.
Charles E. Knight
S. W. Zewari

Inquiries should be directed to:

Center for Composite Materials & Structures
College of Engineering
Virginia Tech
Blacksburg, VA 24061
Phone: (703) 961-4969

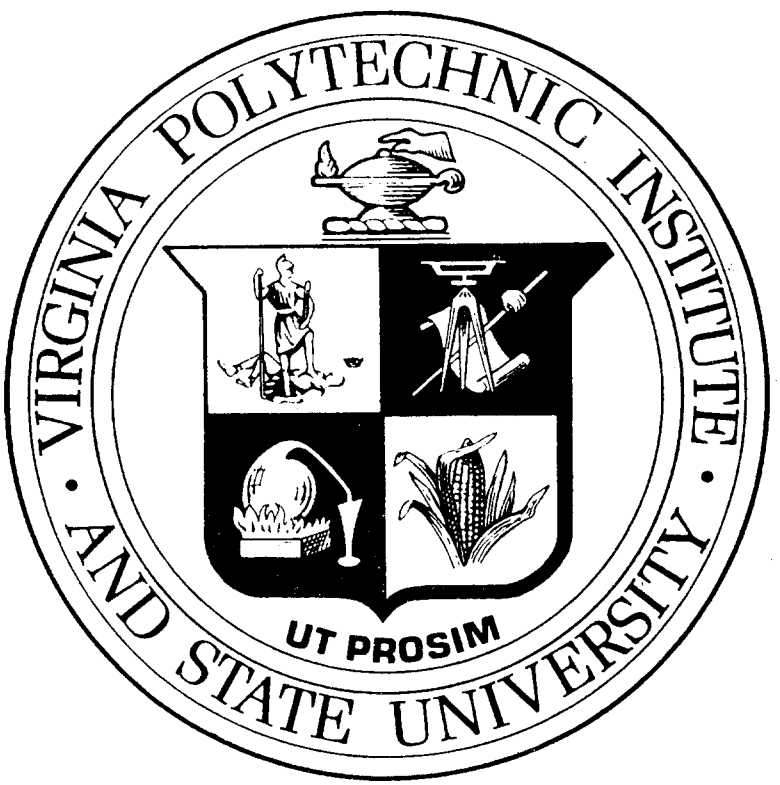
VIRGINIA POLYTECHNIC INSTITUTE
AND STATE UNIVERSITY
UT PROSIM